Linearization-Based Scheduling of Hydropower Systems

Linearization-Based Strategies for Optimal Scheduling of a Hydroelectric Power Plant Under Uncertainty

by

Alexander Tikk, B.Eng

A Thesis
Submitted to the School of Graduate Studies
in Partial Fulfillment of the Requirements
for the Degree
Master of Applied Science

McMaster University

MASTER OF APPLIED SCIENCE (2018)	McMaster University
(Chemical Engineering)	Hamilton, Ontario, Canada

TITLE:	Linearization-Based Strategies for Optimal Scheduling of a Hydroelectric Power Plant Under Uncertainty
AUTHOR:	Alexander Tikk, B.Eng McMaster University, Canada
SUPERVISOR:	Dr. C. L. E. Swartz
NUMBER OF PAGES:	xxii, 151

ABSTRACT

This thesis examines the optimal scheduling of a hydroelectric power plant with cascaded reservoirs each with multiple generating units under uncertainty after testing three linearization methods. These linearization methods are Successive Linear Programming, Piecewise Linear Approximations, and a Hybrid of the two together. There are two goals of this work. The first goal of this work aims to replace the nonconvex mixed-integer nonlinear program (MINLP) with a computationally efficient linearized mixed-integer linear program (MILP) that will be capable of finding a high quality solution, preferably the global optimum. The second goal is to implement a stochastic approach on the linearized method in a pseudo-rolling horizon method which keeps the ending time step fixed. Overall, the Hybrid method proved to be a viable replacement and performs well in the pseudo-rolling horizon tests.

ACKNOWLEDGEMENTS

I'd like to thank Pulkit Mathur for his collaboration, ideas, and feedback. I would also like to express my gratitude to my industry partners at Hatch, Dr. Danielle Zyngier and Dr. François Welt for their knowledge and guidance on my project. Last, but certainly not least, I'd like to thank Dr. Swartz for his expertise and continued support on my thesis.

Table of Contents

List of Figures

List of Tables

Chapter 1

Introduction

This work focuses on optimizing the scheduling of a hydropower plant under uncertainty after testing different linearization methods. The optimization problem is of the type MINLP (Mixed-Integer Nonlinear Programming Problem) due to the nonlinear equations for generator power output and reservoir volume which can be seen later in eqs. (3.2) and (3.15), respectively. Since the generator power output equation is highly nonlinear and nonconvex, this problem is difficult to solve to global optimality, which is why the linearization methods are tested as a replacement. These linearization methods are the SLP (Successive Linear Programming), Hybrid, and PLA (Piecewise Linear Approximation) methods, which will be discussed later in detail. Unfortunately, since the problem is nonconvex, global optimality can not be proven with the linearization methods.

The hydropower plant in this work is comprised of three reservoirs in series each with five, four and three downstream generators, respectively. The first reservoir has four generators of the same type and one larger generator while the second and third reservoirs each have a unique generator type for all generators in that specific reservoir. It is also known that any spill for a particular reservoir is fed to the next downstream reservoir if available. There is also an environmental constraint that requires a small amount of water to continuously leave the second reservoir (into the third) either by spilling or generating power. Since this value is small compared to the minimum flow of an individual generator, it is not uncommon to see the reservoir spill instead of turn on a generator.

The optimization problem requires that the time horizon be discretized into time steps where the variables are optimized and are assumed not to change within each time step. For this work a short-term approach is used on a duration lasting 24 hours separated into hourly time steps in a price following application. This work will also use a price profile that may vary every hour.

A semicontinuous variable is a variable that can either be zero or between some minimum and maximum value (of which both are positive). In this work a minimum flow is required to have a generator be on and we assume the flow is zero if the generator is off. Therefore each generator's individual flow is semicontinuous. Since binary variables are required in the representation of semicontinuous variables, integers must be a part of the optimization. Another instance of binary variables is the presence of spill flows. In this work, for spill flows to occur the reservoir level must be above the sill elevation. This requires a binary variable to indicate whether or not spills are allowed for each reservoir at each time step.

To prevent generators from producing their maximum power for the entire time horizon by emptying all reservoirs, a minimum ending reservoir elevation is introduced in addition to the physical reservoir constraints. This minimum ending elevation is commonly paired with a maximum elevation which creates a target elevation range. This range is often obtained from a long term optimization, but this work will assume that the target elevation is the same as the initial elevation as the focus is to optimize profit using only the incoming water from upstream. By doing so, the total amount of spills and generator discharges will equal the upstream inflow for each reservoir.

This work includes new aspects not seen in the explored literature. The first contribution is the adaptation of linearization methods well established to improve solution quality and computational times. These well established linearization methods are the SLP and PLA methods. The first adaptation is a PLA method that uses two independent variables that uses four weights associated with each rectangular region of feasible space. The next contribution is a completely new linearization method introduced in this work as the Hybrid method, which is a method that combines aspects from the SLP and PLA methods. This new Hybrid method has two types which vary how the piecewise points are updated with each iteration, namely, the fixed grid and adaptive grid methods. The final contribution is the nervousness analysis of generator discharges and a nervousness mitigation strategy with the inclusion of start-up costs.

This thesis is broken down into five chapters. The second chapter contains a short literature review to provide a background of information on related topics such as solving nonlinear problems, short-term hydropower systems, and a contrast of linearization methods, to name a few. The third chapter describes the hydropower problem formulation and linearization methods, and includes a comparison of results for three small base cases and the main daily case. Next is the chapter that introduces the concept of nervousness and includes uncertainty into the optimization problem while also providing a nervousness mitigation strategy and different methods for dealing with uncertainty. Finally, the fifth chapter summarizes the findings of this thesis and provides suggestions for future work.

Chapter 2

Literature Review

A simple way of dealing with a nonlinear optimization problem is to use an SLP methodology, which replaces the nonlinear equations with first order Taylor series approximations [Palacios-Gomez *et al.*, 1982]. This allows the optimization to be linear, but requires a number of iterations to converge to an optimal solution, where each iteration updates the base point and relinearizes to create a new linear optimization subproblem. A sequence of iterations will lead to the global optimum if a minimization problem is convex [Fletcher and de la Maza, 1989; Zhang *et al.*, 1985; Luenberger and Ye, 1984]. If the problem is nonconvex, the iterative process of the SLP will lead to a local solution but this solution is not guaranteed to be the global optimum. Due to this fact, most articles include convex problems to prove global optimality when the SLP is used. Global optimality can be proved for the original nonconvex MINLP by creating underestimators and dividing the optimization problem into subproblems [Ryoo and Sahinidis, 1995; de Castro Amarante e Ribeiro, 2014]. However, depending on the complexity of the nonlinearites, this may be computationally complex.

It is common for SLP implementations to have a trust region to limit the independent variables from being too far from the base point which reduces the amount of error in the approximation [Fletcher and de la Maza, 1989]. A trust region is also useful to converge on the optimum slowly, as opposed to making large changes in each iteration, which may assist in finding the optimum in less iterations overall.

Another way of dealing with nonlinearities is by replacing them with a PLA methodology. This method will calculate the function at discrete points and linearly interpolate between these points to create an estimate of the function. This creates a new variable set that is a special ordered set of type two [Tomlin, 1988]. This means that only two consecutive variables within the set may be nonzero and these variables represent the weights of each discrete point. The weights simulate the linear interpolation between the discrete points, which is why it would be illogical if more than two weights or two non-adjacent weights are non-zero.

When a PLA is implemented in two independent variable dimensions, often the function is approximated by linear interpolation with three points for each region of feasible space [Fu and Scott, 2013]. These three points are one base point and one point to approximate the change in the function value in each dimension. This method separates the rectangular region of discrete points (two values for each independent variable) into two triangles and uses the appropriate one as the approximation based on the values of the independent variables [D'Ambrosio *et al.*, 2010]. However, in this work each region is approximated by linear interpolation with four points for each corner of the rectangular region. The benefit of doing so allows the approximation to be simplified by using half the number of binary variables to designate the active region for both independent variables. However, the downside to such a system is that the optimization is free to decide how to distribute the weights, as long as the weights accurately represent the independent variables. This is the result of one extra degree of freedom for the weights (when considering one individual region), due to the fact that there are four wieghts and three constraints. An additional constraint can be added that would force an accurate ratio between the four weights, but this constraint is bilinear. So including this constraint would remove the benefit of the PLA method which is changing the optimization from an MINLP into an MILP. Thus, not including this constraint may impede the performance of the PLA method used in this work.

A similar approach to the Hybrid method used in this work was completed in de Ladurantaye *et al.* [2009]. However, there are a few limitations that restricted the applications in that work that are expanded on in this work. Firstly, the piecewise approximations in the work by de Ladurantaye *et al.* [2009] are simple as there are no binaries required to indicate which region is active because the rates are placed in decending order due to the concave power equation assumption (which is quadratic). Also, when the piecewise approximations are used for generator flow, there is a constant reservoir head assumed. The head effects are only brought in after the model is changed into a two dimensional SLP which uses a shrinking trust region method. Thus, the piecewise approximations are only used to find an initialization to the iterative SLP. This means that the Hybrid method proposed in this work is different because it utilizes the piecewise approximations in the generator discharge dimension and a successive linearization in the head dimension. Drouin *et al.* [1996] used piecewise linear approximations to estimate the expected revenue (under uncertainty) in future time steps but also used a concave assumption.

The biggest sources of uncertainty for hydropower systems often come from upstream inflows and electricity price (or electricity demand for demand following systems) [Drouin *et al.*, 1996; Pereira and Pinto, 1985]. Considering uncertainity in the optimization can assist in preventing possible infeasibilities in extreme cases and will likely assist in improving the optimal value. There are many examples of uncertainty being simulated with scenario trees and random walk simulations in which some examples can be seen in Pereira [1989]; Fleten and Kristoffersen [2008]; Séguin *et al.* [2017]; Belsnes *et al.* [2016], but this work simulates the uncertainty as random sampling from a normal distribution around a nominal price profile. It has also been shown to be worthwhile to combine a stochastic approach with a rolling horizon implementation [Séguin *et al.*, 2017].

It is common in hydropower to group hydro-generators in with thermal-generators and for these systems to minimize cost while following demand [Rajšl *et al.*, 2011; Hreinsson, 1988]. However, hydropower has become competitive and now there are many case studies for price following hydropower systems. Another aspect that has become interesting when considering price following systems is recirculating water so that it can be used again [Korobeinikov *et al.*, 2010; Guedes *et al.*, 2012]. Pumps run at times with low electricity prices to bring water from lower reservoirs to upper reservoirs to use at times with higher electricity prices, thus allowing a greater profit to be achieved. Later in this work the presence of generator start-up costs are included, which can be estimated based on many factors [Osburn, 2014; Fleten and Kristoffersen, 2008]. However, only a rough estimate is used based on the maximum power output of each generator in this work.

Chapter 3

Linearization Methods

3.1 Hydropower Scheduling Problem

3.1.1 Setup

The hydroelectric generating system considered in this work is comprised of multiple reservoirs in series, each with a varying number of associated downstream generators. The spill from each reservoir and its generators' discharges (flow through the individual generator to produce power) all flow into the next reservoir such that no water is wasted within the system. The object of this work is to find the schedule that maximizes the profit obtained by selling produced electricity. There is no specified demand or minimum power requirement at any time and there is no limit on how much electricity that can be sold. There is no cost in the system currently considered, however there will be a cost associated to turn on all generators later in this work.

3.1.2 MINLP Description

The original formulation of this hydroelectric generation scheduling is of the type MINLP. The nonlinearities are caused by the generator power equation (which is dependent on reservoir head and generator discharge) and the reservoir storage equation (which has a relationship with reservoir level). The integer requirement is due to the generator statuses and the spill statuses, which are both binary variables as each generator must be on or off and spill is either possible or impossible dependent on if the sill level is greater or less than the reservoir level. One may also consider the discharge through generators to be a semicontinuous variable as it should be zero when the generator is off or above some minimum value in order to start producing electricity. The material balances are linear, and the other equations simply define boundaries for each variable based on the physical system.

3.1.3 Discretization

In order to solve this optimization problem, the time horizon must be partitioned into discrete time periods. Hourly time steps have been chosen for the daily time horizon considered in this work. The inclusion of discrete time periods introduces restrictions and minor issues related to the accuracy of the model, but these are well within the realm of error of such systems. One such example is forcing all decisions to only change after the hour has passed, and one can not include information that may change more often than every hour. For example, energy prices may change every fifteen minutes in some markets.

One error that is introduced is that the head effects may change within an hour time step as the level increases or decreases due to the inflow being unequal to the outflow for that time step. Since the power production assumes the head is constant for the duration of each inidividual time step (being the same as it was at the beginning of the time step), the power calculations will be slightly incorrect. The only way to accomodate this error would be to integrate the power over the hour horizon as the level changes, but this is an unnecessary complexity considering the amount of error that is introduced (which is very little since the reservoir levels do not change much over the daily horizon).

3.1.4 MINLP Optimization Formulation

All equations apply for all elements of every set included unless otherwise indicated. The equations, parameters, and variables that are contained in the formulations for this work are explained; Appendix A provides a summary of all symbols used.

The purpose of this problem is to maximize profit for the time horizon considered by determining the flows of each generator at each time step and the spill flows of each reservoir at each time step. In this chapter it is assumed that there is no start-up cost associated with any of the generators, meaning that the profit is simply equal to the revenue. The revenue (REV) is the sum of all the power produced ($P_{i,j,t}$) in each reservoir (index i) and each generator (index j) across all time steps (index t) multiplied by the appropriate energy selling price at the time it was produced (EP_t).

$$REV = \sum_{t \in T} EP_t \sum_{i \in I} \sum_{j \in J} P_{i,j,t} \tag{3.1}$$

The power produced for a particular generator is dependent on the head ($H_{i,t}$) in the associated reservoir and the flow through the specified generator ($F_{i,j,t}$) as seen in eq. (3.2). The power produced is also dependent on coefficients determined for each generator ($GC_{i,j,gs}$) and if the generator is on given by the binary variable ($S_{i,j,t}$).

$$\begin{aligned} P_{i,j,t} = & \left(GC_{i,j,a_1} + GC_{i,j,a_2} H_{i,t} + GC_{i,j,a_3} \left(H_{i,t}\right)^2\right) S_{i,j,t} + \\ & \left(GC_{i,j,b_1} + GC_{i,j,b_2} H_{i,t} + GC_{i,j,b_3} \left(H_{i,t}\right)^2\right) F_{i,j,t} + \\ & \left(GC_{i,j,c_1} + GC_{i,j,c_2} H_{i,t} + GC_{i,j,c_3} \left(H_{i,t}\right)^2\right) \left(F_{i,j,t}\right)^2 + \\ & \left(GC_{i,j,d_1} + GC_{i,j,d_2} H_{i,t} + GC_{i,j,d_3} \left(H_{i,t}\right)^2\right) \left(F_{i,j,t}\right)^3 \end{aligned} \tag{3.2}$$

The next five equations define the limits placed on the continuous variables contained in the formulation, namely, the level ($L_{i,t}$), volume ($V_{i,t}$) and spill flow ($FS_{i,t}$) of each reservoir, and the flow ($F_{i,j,t}$) and power ($P_{i,j,t}$) of each generator. Spill is only allowed to occur when the binary spill status ($SS_{i,t}$) is 1, which only happens if the level in that reservoir is above the associated sill elevation (described later). Similarly, a generator can only produce power when the generator is on, which requires the flow for that generator to be between some lower and upper limit, $F_{i,j,Min}$ and $F_{i,j,Max}$, respectively. If a generator is off, it does not allow water to pass through the generator.

$$L_{i,Min} \leq L_{i,t} \leq L_{i,Max} \tag{3.3}$$

$$V_{i,Min} \leq V_{i,t} \leq V_{i,Max} \tag{3.4}$$

$$0 \leq FS_{i,t} \leq FS_{i,Max} SS_{i,t} \tag{3.5}$$

$$F_{i,j,Min} S_{i,j,t} \leq F_{i,j,t} \leq F_{i,j,Max} S_{i,j,t} \tag{3.6}$$

$$0 \leq P_{i,j,t} \leq P_{i,j,Max} S_{i,j,t} \tag{3.7}$$

The next equation simplifies the mass (water) balances by summing up all the inidividual generator flows for each reservoir into the total reservoir flow (excluding spill) as $FT_{i,t}$.

$$FT_{i,t} = \sum_{j \in J} F_{i,j,t} \tag{3.8}$$

In addition to the limits of each generator, there is also an environmental constraint in which each reservoir must achieve a minimum flow ($FT_{i,Min}$) (which comprises both generator flow and spill flow) for all time steps.

$$FT_{i,Min} \leq FT_{i,t} + FS_{i,t} \tag{3.9}$$

The head for each reservoir is defined to be the level of that reservoir minus the associated downstream elevation ($L_{i,Down}$), which is assumed constant in this work.

$$H_{i,t} = L_{i,t} - L_{i,Down} \tag{3.10}$$

The next four equations mathematically describe the mass (water) balance for this formulation. Each reservoir has an associated inflow ($F_{i,t,In}$) at each time step and the flows leaving a reservoir enter the next downstream reservoir (including the spill flow). The amount of time of each time step is given by Δt and the final volume for each reservoir is given by $V_{i,Final}$. Please note that this formulation starts at time step $t = 0$ and ends at time step $t = T_{End}$, but the final volume and level are enforced at the end of the last time step so that the effects of all discharges and spills that occur in the last time step are included in these constraints.

$$V_{i,t+1} = V_{i,t} + \Delta t\,(F_{i,t,In} - FT_{i,t} - FS_{i,t}) \qquad \forall i = 1, t \neq T_{End} \tag{3.11}$$

$$V_{i,t+1} = V_{i,t} + \Delta t\,(F_{i,t,In} + FT_{i-1,t} - FT_{i,t} + FS_{i-1,t} - FS_{i,t}) \qquad \forall i \neq 1, t \neq T_{End} \tag{3.12}$$

$$V_{i,Final} = V_{i,t} + \Delta t\,(F_{i,t,In} - FT_{i,t} - FS_{i,t}) \qquad \forall i = 1, t = T_{End} \tag{3.13}$$

$$V_{i,Final} = V_{i,t} + \Delta t\,(F_{i,t,In} + FT_{i-1,t} - FT_{i,t} + FS_{i-1,t} - FS_{i,t}) \qquad \forall i \neq 1, t = T_{End} \tag{3.14}$$

The volume in each reservoir has a particular relationship to the level mathematically described by eq. (3.15) given by the reservoir coefficients ($RC_{i,rs}$). To prevent the reservoirs from emptying at the end of time horizon, the final level and volume are required to be the same as the initial conditions ($L_{i,Init}$ for level and $V_{i,Init}$ for volume).

$$V_{i,t} = RC_{i,C0} + RC_{i,C1}\left[L_{i,t} - RC_{i,C2}\right]^{RC_{i,C3}} \tag{3.15}$$

$$L_{i,Final} = L_{i,t} = L_{i,Init} \qquad \forall t = 0 \tag{3.16}$$

$$V_{i,Final} = V_{i,t} = V_{i,Init} = RC_{i,C0} + RC_{i,C1}\left[L_{i,Init} - RC_{i,C2}\right]^{RC_{i,C3}} \qquad \forall t = 0 \tag{3.17}$$

To remove some nonuniqueness from the formulation, we require each reservoir to sort the generator flows into descending order for generators of the same type ($j = \{1,2,3,4\}$). This is accomplished by forcing the first generator to have more or equal flow than the second, the second more or equal than the third, and the third more or equal than the fourth. This unnecessary constraint does not limit any of the generators to be on or off, nor does it remove any of the physically feasible space.

$$F_{i,1,t} \geq F_{i,2,t} \geq F_{i,3,t} \geq F_{i,4,t} \tag{3.18}$$

The next two equations enforce the spill to only occur when above the sill elevation ($L_{i,Sill}$). The spill amount is considered a decision variable, but is limited to zero if the current level of a reservoir is below the sill elevation. A problem with this formulation is that it may cause the scenario to be infeasible. For example, if a large inflow occurs at a particular time step, and the generators cannot discharge the entire amount, and if the level is below the sill elevation, then there can be no spill until the next time step, possibly causing a violation of the maximum level/volume. This problem is ultimately a result of the time discretization and is dependent on an extreme situation occuring, and is unlikely to happen in general practice.

$$L_{i,t} \geq L_{i,Min} + \left[L_{i,Sill} - L_{i,Min}\right] SS_{i,t} \tag{3.19}$$

$$L_{i,t} \leq L_{i,Sill} + \left[L_{i,Max} - L_{i,Sill}\right] SS_{i,t} \tag{3.20}$$

3.2 SLP Method

The SLP method removes the nonlinearities in the original model by replacing the storage and power equations with first order Taylor series approximations. This method then solves for the optimum iteratively after updating the base points to have the values of the previous solution. Since this is just an approximation, a trust region is added to mitigate the error by enforcing each generator's discharge to be within a certain range of the base point (indicated as the trust region). This trust region shrinks after each iteration making the solution progress towards a local optimum. There is no guarantee that the final solution will be a global optimum, but it can often be improved by starting with a large trust region, shrinking the trust region slowly, and giving the method a good initialization point. One benefit to the SLP is that it is computationally efficient, meaning a quality feasible solution can be obtained in much less time than the MINLP, even though it may not be the global optimum.

To illustrate the SLP method, fig. 3.1 is included as an example of a function, $f(x)$, of one variable, x. The black dot demonstrates the current base point and the light grey line is used as an approximation in place of the dark grey line which is the true nonlinear function. Two dotted lines are also included which represent the trust region, meaning the value of x in this example must be within these bounds for this iteration.

3.2.1 SLP New/Modified Model Equations

The first order Taylor series approximation for the power equation (eq. (3.2)) would be as it appears in eq. (3.21), but there are corrections that need to be made to accurately depict the binary effects of the generator status. Since the power must be zero when the generator is off, the linearization point values must be set to zero when

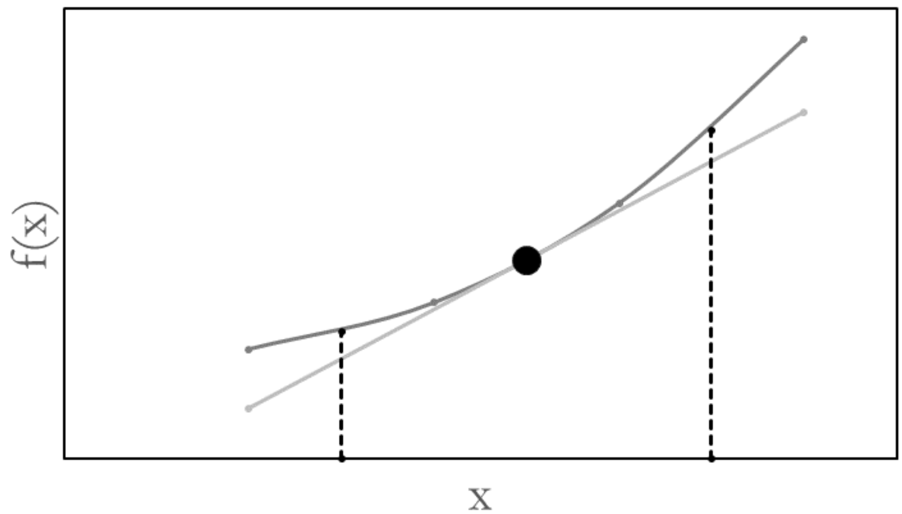

Figure 3.1: An illustration of one iteration of the SLP (Successive Linear Programming) method.

the generator is off, which can easily be achieved by multiplying the linearization point terms by the generator status. However, the head would also contribute a nonzero value even when the generator is off, which is why it is replaced by $PH_{i,j,t}$. By doing so, every term in the linearized power equation becomes zero when the generator is off, but accurately depicts the first order Taylor series approximation when the generator is on. This does not need to be done for the flow since it already must be zero when the generator is off. To be clear, eq. (3.21) is not included in the model and is simply to show the transition from the original first order Taylor series approximation to the modified true version in eq. (3.22).

$$P_{i,j,t} = CF_{i,j,t}\left(F_{i,j,t} - F_{i,j,t,S}\right) + CH_{i,j,t}\left(H_{i,t} - H_{i,t,S}\right) + P_{i,j,t,S} \tag{3.21}$$

$$P_{i,j,t} = CF_{i,j,t}\left(F_{i,j,t} - F_{i,j,t,S}S_{i,j,t}\right) + CH_{i,j,t}\left(PH_{i,j,t} - H_{i,t,S}S_{i,j,t}\right) + P_{i,j,t,S}S_{i,j,t} \tag{3.22}$$

$CF_{i,j,t}$ and $CH_{i,j,t}$ are the Taylor series coefficients and $F_{i,j,t,S}$, $H_{i,t,S}$, and $P_{i,j,t,S}$ are the base points for the power equation which are all explained and defined in the next section.

The combination of constraints in eq. (3.23) are necessary to force the variable $PH_{i,j,t}$ to be zero when generator j in reservoir i at time step t is off and to be the value of the head of reservoir i at time step t when the generator is on. This allows the head to accurately change the power without affecting the power produced when the generator is off (which must be zero). Note from eq. (3.10) that $L_{i,Max} - L_{i,Down}$ is the maximum value for the head.

$$\begin{aligned} 0 \leq PH_{i,j,t} &\leq (L_{i,Max} - L_{i,Down})\, S_{i,j,t} \\ H_{i,t} - (1 - S_{i,j,t})\,(L_{i,Max} - L_{i,Down}) \leq PH_{i,j,t} &\leq H_{i,t} \end{aligned} \tag{3.23}$$

The following equation replaces the volume to level relation (eq. (3.15)) with a first order Taylor series approximation, with the coefficient $CL_{i,t}$ and base points $L_{i,t,S}$ and $V_{i,t,S}$ being defined and explained in the next section.

$$V_{i,t} = CL_{i,t}\,(L_{i,t} - L_{i,t,S}) + V_{i,t,S} \tag{3.24}$$

To ensure that the Taylor series approximations are sufficiently accurate, a trust region limits the deviation of each individual generator's flow from its linearization point.

$$\begin{aligned} F_{i,j,t} - F_{i,j,t,S} &\leq TR \\ F_{i,j,t,S} - F_{i,j,t} &\leq TR \end{aligned} \tag{3.25}$$

3.2.2 SLP Iteration Equations

The SLP formulation uses an iterative approach, and thus needs to change its linearization point values with each iteration. The first step is to initialize the linearization points for reservoir level, generator discharge, generator power, reservoir volume, and reservoir head ($L_{i,t,S}, F_{i,j,t,S}, P_{i,j,t,S}, V_{i,t,S}$, and $H_{i,t,S}$, respectively). Clearly a better initialization will assist in finding the location of the optimum of the overall problem sooner. In all subsequent iterations, the linearization points are obtained from the previous solution. In a similar fashion, the trust region is initialized with $TR = TR_{Init}$ then reduced after each iteration by using $TR = TR_{Factor}TR$ (using the most updated value for TR in the right half of the equation for the new value of TR in the left side of the equation). After defining the linearization points, the coefficients of flow ($CF_{i,j,t}$), head ($CH_{i,j,t}$), and level ($CL_{i,t}$) are calculated to be used in the first order Taylor series approximations used in the previous section. It is assumed that $RC_{i,C3} \neq 0$ for all reservoirs.

$$\begin{aligned}
CF_{i,j,t} = &\left(GC_{i,j,b_1} + GC_{i,j,b_2}H_{i,t,S} + GC_{i,j,b_3}\left(H_{i,t,S}\right)^2\right) + \\
&2\left(GC_{i,j,c_1} + GC_{i,j,c_2}H_{i,t,S} + GC_{i,j,c_3}\left(H_{i,t,S}\right)^2\right)F_{i,j,t,S} + \\
&3\left(GC_{i,j,d_1} + GC_{i,j,d_2}H_{i,t,S} + GC_{i,j,d_3}\left(H_{i,t,S}\right)^2\right)\left(F_{i,j,t,S}\right)^2 \qquad (3.26)
\end{aligned}$$

$$\begin{aligned}
CH_{i,j,t} = &\left(GC_{i,j,a_2} + 2GC_{i,j,a_3}H_{i,t,S}\right) + \\
&\left(GC_{i,j,b_2} + 2GC_{i,j,b_3}H_{i,t,S}\right)F_{i,j,t,S} + \\
&\left(GC_{i,j,c_2} + 2GC_{i,j,c_3}H_{i,t,S}\right)\left(F_{i,j,t,S}\right)^2 + \\
&\left(GC_{i,j,d_2} + 2GC_{i,j,d_3}H_{i,t,S}\right)\left(F_{i,j,t,S}\right)^3 \qquad (3.27)
\end{aligned}$$

$$CL_{i,t} = RC_{i,C1}RC_{i,C3}\left[L_{i,t,S} - RC_{i,C2}\right]^{RC_{i,C3}-1} \qquad (3.28)$$

The linearization points for power and volume are calculated with the true nonlinear equations using the other updated linearization points.

$$\begin{aligned}
P_{i,j,t,S} = &\left(GC_{i,j,a_1} + GC_{i,j,a_2}H_{i,t,S} + GC_{i,j,a_3}\left(H_{i,t,S}\right)^2\right) + \\
&\left(GC_{i,j,b_1} + GC_{i,j,b_2}H_{i,t,S} + GC_{i,j,b_3}\left(H_{i,t,S}\right)^2\right)F_{i,j,t,S} + \\
&\left(GC_{i,j,c_1} + GC_{i,j,c_2}H_{i,t,S} + GC_{i,j,c_3}\left(H_{i,t,S}\right)^2\right)\left(F_{i,j,t,S}\right)^2 + \\
&\left(GC_{i,j,d_1} + GC_{i,j,d_2}H_{i,t,S} + GC_{i,j,d_3}\left(H_{i,t,S}\right)^2\right)\left(F_{i,j,t,S}\right)^3 \qquad (3.29)
\end{aligned}$$

$$V_{i,t,S} = RC_{i,C0} + RC_{i,C1}\left[L_{i,t,S} - RC_{i,C2}\right]^{RC_{i,C3}} \qquad (3.30)$$

The individual generator error ($EF_{i,j,t}$) and total error (ET) are calculated after each iteration with the following equations:

$$EF_{i,j,t} = |F_{i,j,t} - F_{i,j,t,S}| \tag{3.31}$$

$$ET = \sum_{i \in I} \sum_{j \in J} \sum_{t \in T} EF_{i,j,t} \tag{3.32}$$

The optimization problem is solved maximizing the value of REV and if the value of ET is less than some tolerance, the solution is returned. If not, then the linearization points are updated, the linearization equations are recalculated, the trust region shrinks, and the optimization problem is solved again.

3.3 General One Dimension PLA Formulation

Please note that sections 3.3 and 3.5 are completely separate from the hydropower formulations. In this section, the general PLA formulation in one dimension will be described. An illustration of the PLA in one dimension can be seen in an example of a function, $f(x)$, in fig. 3.2. The function, $f(x)$, is seen in black which is approximated by the grey linear segments after calculating the function at the discrete grey points. The independent variable, x, has lower and upper bounds of x_L and x_U.

$$x \in [x_L, x_U] \tag{3.33}$$

There are $N + 1$ equidistant discrete points that separate the feasible space that will be labelled $\tilde{x}_i$.

$$i \in I = \{0, 1, ...N\} \tag{3.34}$$

$$\tilde{x}_i = x_L + (x_U - x_L)\frac{i}{N} \tag{3.35}$$

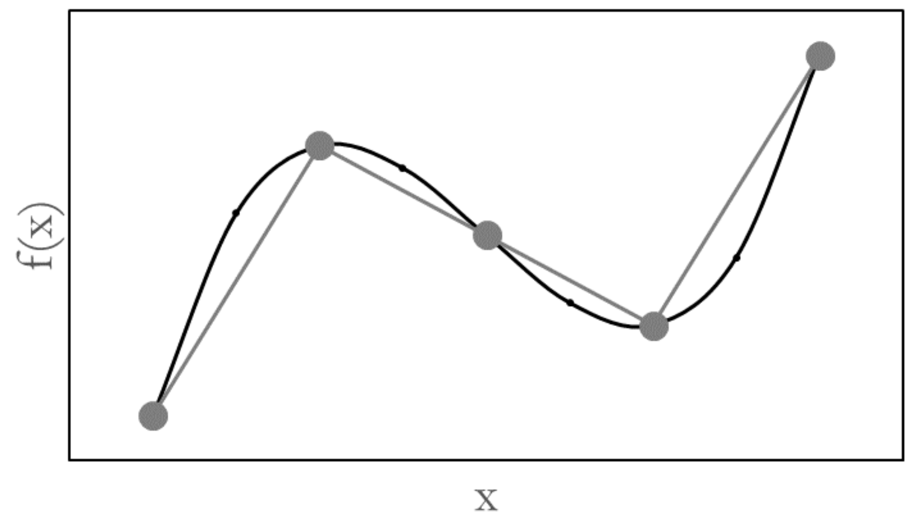

Figure 3.2: An illustration of the PLA (Piecewise Linear Approximation) method in one dimension.

A_i is a binary variable indicating if $x \in [\tilde{x}_{i-1}, \tilde{x}_i]$ and only one A_i value can be non-zero (one).

$$A_i \in \{0, 1\} \tag{3.36}$$

$$\sum_{i \in I} A_i = 1 \tag{3.37}$$

In the general case, A_0 would indicate the region less than x_L, thus it is set to zero.

$$A_i = 0 \qquad \forall i = 0 \tag{3.38}$$

α_i are weights that linearly interpolate between discrete points on the unknown function $f(x)$ to approximate as $\tilde{f}(x)$.

$$\alpha_i \in [0,1] \tag{3.39}$$

$$\sum_{i \in I} \alpha_i = 1 \tag{3.40}$$

$$x = \sum_{i \in I} \tilde{x}_i \alpha_i \tag{3.41}$$

$$\tilde{f}(x) = \sum_{i \in I} f(\tilde{x}_i) \alpha_i \tag{3.42}$$

Next, we must ensure that only two adjacent weights are nonzero to make an accurate estimation. Since the last point is at the upper bound, there is no feasible region greater than this value. This means that the weight at that point, α_N, is only allowed to be nonzero when the last region, A_N is active (equal to one).

$$\alpha_i \leq A_i + A_{i+1} \qquad \forall i \neq N \tag{3.43}$$

$$\alpha_i \leq A_i \qquad \forall i = N \tag{3.44}$$

This formulation is based on the foundation of linear interpolation between two points. For $x \in [\tilde{x}_i, \tilde{x}_{i+1}]$, eqs. (3.40) to (3.42) simplify and we can write them out as:

$$1 = \alpha_i + \alpha_{i+1}$$

$$\alpha_{i+1} = 1 - \alpha_i \tag{3.45}$$

$$\begin{aligned} x &= \alpha_i \tilde{x}_i + \alpha_{i+1} \tilde{x}_{i+1} \\ &= \alpha_i \tilde{x}_i + (1-\alpha_i) \tilde{x}_{i+1} \qquad \alpha_i \in [0,1] \end{aligned} \tag{3.46}$$

$$\begin{aligned} \tilde{f}(x) &= \alpha_i f(\tilde{x}_i) + \alpha_{i+1} f(\tilde{x}_{i+1}) \\ &= \alpha_i f(\tilde{x}_i) + (1-\alpha_i) f(\tilde{x}_{i+1}) \qquad \alpha_i \in [0,1] \end{aligned} \tag{3.47}$$

Equation (3.46) can be rearranged for α_i as follows:

$$\alpha_i = \frac{\tilde{x}_{i+1} - x}{\tilde{x}_{i+1} - \tilde{x}_i} \tag{3.48}$$

In words, the summations in eqs. (3.40) to (3.42) reduce to describe one linear segment of the feasible space as all other weights (α_i values) must be zero due to the binary variable set A_i.

3.4 Hybrid (SLP-PLA) Method

3.4.1 Hybrid Description

As the name suggests, the Hybrid method uses a combination of aspects from both the SLP and PLA methods. The generator power in this method is approximated using piecewise linear segments for the generator discharge and a first order Taylor series approximation for the reservoir head. The reservoir storage equation is also a first order Taylor series approximation as it was in the SLP method.

The most beneficial part of this method is that it can accurately approximate the major aspect of the nonlinearity (the generator discharge) while still including the effects of head on the power. This is because the PLA approach is more accurate when compared to one iteration of the SLP, however, the PLA method lacks because its approximations are not updated in an iterative process. This is the idea behind the Hybrid method, which is to update the PLA linear segments in an iterative process to be more accurate in each iteration while converging on the optimum.

The nonlinear effects of head are not as important as the generator discharge in this work because the reservoirs are large compared to the inflow, meaning the reservoir levels do not change much, and only the short term time horizon is considered. This may not be the case if monthly, seasonal, or yearly time horizons are considered. Thus, in this work, the SLP approach is sufficient for reservoir head, but not generator discharge. This method also does not guarantee to find the global optimum, although it obtains a high quality solution.

3.4.2 Hybrid New/Modified Iteration Equations

There are two slightly different Hybrid methods used in this work. One uses a fixed grid for the piecewise flow points (updating the necessary linearization parameters with each iteration) and the other uses an adaptive grid for the piecewise flow points.

Fixed PLA Grid

As the name suggests, the piecewise flow points ($\tilde{F}_{i,j,t,n}$) do not change from iteration to iteration for the Hybrid fixed grid (Hybrid FG) method. The minimum flow for each generator is used as the first piecewise point and the maximum flow is used for the last point ($n = 1$ and $n = N_F$, respectively), noting that the piecewise flow point is zero when $n = 0$. The other flow points are calculated at evenly distributed points (given by the index n, which varies from 0 to N_F) between the first and last points defined above, with the following equations:

$$\begin{aligned} &\tilde{F}_{i,j,t,n} = 0 && \forall n = 0 \\ &\tilde{F}_{i,j,t,n} = \tilde{F}_{i,j,t,1} + \left(\tilde{F}_{i,j,t,N_F} - \tilde{F}_{i,j,t,1}\right) \frac{n-1}{N_F - 1} && \forall n \neq 0 \end{aligned} \tag{3.49}$$

Instead of making a coefficient for the flow variable as in the SLP formulation, the power is calculated at discrete flow points using the current head linearization point for the Hybrid formulation as follows:

$$\begin{aligned}
\tilde{P}_{i,j,t,n} &= 0 && \forall n = 0 \\
\tilde{P}_{i,j,t,n} &= \left(GC_{i,j,a_1} + GC_{i,j,a_2} H_{i,t,S} + GC_{i,j,a_3} \left(H_{i,t,S}\right)^2\right) + \\
&\quad \left(GC_{i,j,b_1} + GC_{i,j,b_2} H_{i,t,S} + GC_{i,j,b_3} \left(H_{i,t,S}\right)^2\right) \tilde{F}_{i,j,t,n} + \\
&\quad \left(GC_{i,j,c_1} + GC_{i,j,c_2} H_{i,t,S} + GC_{i,j,c_3} \left(H_{i,t,S}\right)^2\right) \left(\tilde{F}_{i,j,t,n}\right)^2 + \\
&\quad \left(GC_{i,j,d_1} + GC_{i,j,d_2} H_{i,t,S} + GC_{i,j,d_3} \left(H_{i,t,S}\right)^2\right) \left(\tilde{F}_{i,j,t,n}\right)^3 && \forall n \neq 0 \quad (3.50)
\end{aligned}$$

A note regarding this method is that since the flow points are only dependent on the generator and span the entire feasible space, they will be the same for any time step index (t). Thus, the time step index can be dropped from the piecewise flow points for this method, changing it from $\tilde{F}_{i,j,t,n}$ to $\tilde{F}_{i,j,n}$. However, the adaptive grid method (described in the next section), will require this index to be present, which is why it is left in for clarity.

Adaptive PLA Grid

For the Hybrid adaptive grid (Hybrid AG) method, the flow points are defined based on surrounding the current linearization point ($F_{i,j,t,S}$) using the trust region value to determine how far apart the points are placed. However, they should be checked if the values are above or below the feasible region, as this would waste linearization segments on infeasible space. If the lower bound is below the minimum flow required to generate power, it is simply set to the minimum flow.

$$\begin{aligned}
&\text{If} && \left(F_{i,j,t,S} - TR > F_{i,j,Min}\right): \\
&\downarrow && \quad \tilde{F}_{i,j,t,n} = F_{i,j,t,S} - TR && \forall n = 1 \\
&\text{Else:} \\
& && \quad \tilde{F}_{i,j,t,n} = F_{i,j,Min} && \forall n = 1 \quad (3.51)
\end{aligned}$$

If the upper bound would be above the maximum flow or below the minimum flow, it is set to the maximum flow. Thus, if the trust region is completely below the minimum flow, it resets the points to include the entire feasible region. This is done because it is not possible for the flow to be nonzero due to the trust region boundaries. Otherwise the flow points would be made up of all zeros, which would introduce nonuniqueness into the formulation.

$$\begin{aligned}
&\text{If} \quad (F_{i,j,t,S} + TR < F_{i,j,Max}) \text{ AND } (F_{i,j,t,S} + TR > F_{i,j,Min}): \\
&\downarrow \qquad \tilde{F}_{i,j,t,n} = F_{i,j,t,S} + TR \qquad \forall n = N_F \\
&\text{Else}: \\
&\qquad \tilde{F}_{i,j,t,n} = F_{i,j,Max} \qquad \forall n = N_F
\end{aligned} \tag{3.52}$$

The other piecewise flow points are then calculated as before using eq. (3.49). For modelling simplicity, the flow points at $n = 0$ are kept at zero flow even if it is outside the trust region.

3.4.3 Hybrid New/Modified Model Equations

The equations in this section replace eq. (3.22) in the SLP formulation (still leaving out eqs. (3.2) and (3.15) from the MINLP formulation). After approximating the power produced at certain flow points, the optimization uses variable weights ($Y_{i,j,t,n}$) to calculate the optimal overall flow and power for each generator.

$$F_{i,j,t} = \sum_{n \in N} \left[\tilde{F}_{i,j,t,n} Y_{i,j,t,n} \right] \tag{3.53}$$

$$P_{i,j,t} = \sum_{n \in N} \left[\tilde{P}_{i,j,t,n} Y_{i,j,t,n} \right] + CH_{i,j,t} \left(PH_{i,j,t} - H_{i,t,S} S_{i,j,t} \right) \tag{3.54}$$

Equations (3.55) to (3.60) all result from the piecewise approximation. The $Z_{i,j,t,n}$ binary variables create partitions that represent part of the feasible space for each generator. Alternative to the one dimensional PLA method, $Z_{i,j,t,n}$ must be zero when $n = 1$ because this region represents flow between zero and the minimum for each generator. If $Z_{i,j,t,n} = 1$ when $n = 0$, this means that the generator is off and there is zero flow through the generator at that time. The other $Z_{i,j,t,n}$ variables ensure that only two consecutive weights are nonzero (and thus approximates the power between the two adjacent points using linear interpolation).

$$0 \leq Y_{i,j,t,n} \leq 1 \tag{3.55}$$

$$Z_{i,j,t,n} = 0 \qquad \forall n = 1 \tag{3.56}$$

$$Y_{i,j,t,n} \leq Z_{i,j,t,n} + Z_{i,j,t,n+1} \qquad \forall n \neq N_F \tag{3.57}$$

$$Y_{i,j,t,n} \leq Z_{i,j,t,n} \qquad \forall n = N_F \tag{3.58}$$

$$\sum_{n \in N} Z_{i,j,t,n} = 1 \tag{3.59}$$

$$\sum_{n \in N} Y_{i,j,t,n} = 1 \tag{3.60}$$

3.5 General Two Dimension PLA Formulation

The descriptions in this section refer to and expand on the General One Dimension PLA Formulation outlined in section 3.3.

3.5.1 Main Additions

Similar bounds and constraints can be made for the second independent variable, y.

$$y \in [y_L, y_U] \tag{3.61}$$

We shall replace N in the single dimension PLA case with N_x for the x dimension. Similarly, N_y will be used for the y dimension and similar to $\tilde{x}_i$, the discrete points in the y dimension shall be labelled $\tilde{y}_j$.

$$j \in J = \{0, 1, ...N_y\} \tag{3.62}$$

$$\tilde{y}_j = y_L + (y_U - y_L)\frac{j}{N_y} \tag{3.63}$$

B_j and β_j shall be the parallels to A_i and α_i for the y dimension, having similar constraints.

$$B_j \in \{0, 1\} \tag{3.64}$$

$$\sum_{j \in J} B_j = 1 \tag{3.65}$$

$$B_j = 0 \qquad \forall j = 0 \tag{3.66}$$

$$\beta_j \in [0, 1] \tag{3.67}$$

$$\sum_{J \in J} \beta_j = 1 \tag{3.68}$$

$$y = \sum_{j \in J} \tilde{y}_j \beta_j \tag{3.69}$$

$$\beta_j \leq B_j + B_{j+1} \qquad \forall j \neq N_y \tag{3.70}$$

$$\beta_j \leq B_j \qquad \forall j = N_y \tag{3.71}$$

3.5.2 Three Point Method

The three point method explained here is a basic expansion into the two dimension formulation. What is seen here is a simplifed modification (only slightly changed) to show the connection of how one might use the one dimensional method and expand it into two dimensions.

Everything expands as expected, except for the approximation of the unknown function. The same summation seen in eq. (3.42) cannot be used since the unknown function is also dependent on y. We want to implement a linear approximation in both dimensions, which will result in a plane that connects three points of the unknown function. These points are the base point for the region (which lies at the lower bound of that region for both independent variables) and the points at the upper bound of the region for each independent variable (while keeping the other independent variable constant at the lower bound of the region). The linear approximation resulting from this plane is shown later in eq. (3.85) as the foundation for one region.

Since a generic region will be considered here (made of grey dashed lines as seen in fig. 3.3), α and β may be used to represent the proximity away from the base point, $f(\tilde{x}, \tilde{y})$, (towards the discrete point in the same dimension), and δx and δy are used to simulate the difference between adjacent discrete points in each independent variable. α and β must still be between zero and one. It is desired to create a function for a plane which will be the approximation used ($\tilde{f}(x, y)$) that includes the points $f(\tilde{x}, \tilde{y})$, $f(\tilde{x} + \delta x, \tilde{y})$, and $f(\tilde{x}, \tilde{y} + \delta y)$. With the introduction of a coefficient for each of x and y (C_x and C_y) and a constant term (C_z), the approximation can be written as follows:

$$\tilde{f}(x, y) = C_x x + C_y y + C_z \tag{3.72}$$

Since it must coincide with the three points described previously, we can enforce the following three equalities:

$$f(\tilde{x}, \tilde{y}) = C_x \tilde{x} + C_y \tilde{y} + C_z \tag{3.73}$$

$$f(\tilde{x} + \delta x, \tilde{y}) = C_x(\tilde{x} + \delta x) + C_y \tilde{y} + C_z \tag{3.74}$$

$$f(\tilde{x}, \tilde{y} + \delta y) = C_x \tilde{x} + C_y(\tilde{y} + \delta y) + C_z \tag{3.75}$$

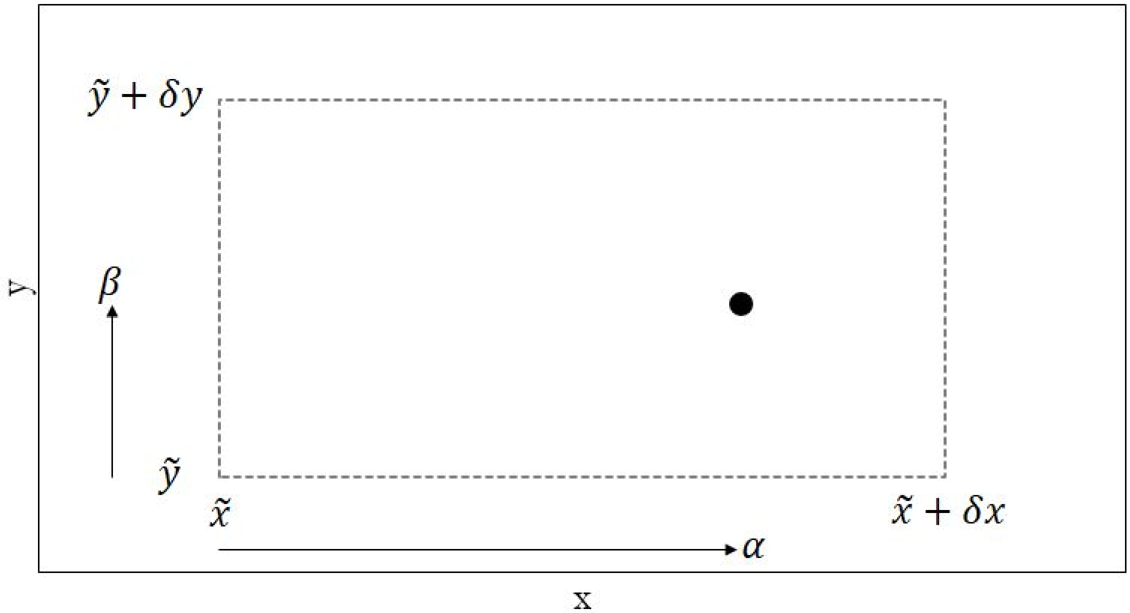

Figure 3.3: An illustration of one generic region of the two dimension PLA (Piecewise Linear Approximation) method.

Manipulating these equations, we can determine values for C_x, C_y, and C_z.

$$C_x \delta x = f(\tilde{x}+\delta x, \tilde{y}) - f(\tilde{x}, \tilde{y}) \qquad \text{(3.74 minus 3.73)}$$

$$C_x = \frac{f(\tilde{x}+\delta x, \tilde{y}) - f(\tilde{x}, \tilde{y})}{\delta x} \tag{3.76}$$

$$C_y \delta y = f(\tilde{x}, \tilde{y}+\delta y) - f(\tilde{x}, \tilde{y}) \qquad \text{(3.75 minus 3.73)}$$

$$C_y = \frac{f(\tilde{x}, \tilde{y}+\delta y) - f(\tilde{x}, \tilde{y})}{\delta y} \tag{3.77}$$

Substituting eqs. (3.76) and (3.77) into eq. (3.73) yields:

$$f(\tilde{x}, \tilde{y}) = \frac{f(\tilde{x}+\delta x, \tilde{y}) - f(\tilde{x}, \tilde{y})}{\delta x}\tilde{x} + \frac{f(\tilde{x}, \tilde{y}+\delta y) - f(\tilde{x}, \tilde{y})}{\delta y}\tilde{y} + C_z$$

$$C_z = f(\tilde{x}, \tilde{y}) - \frac{f(\tilde{x}+\delta x, \tilde{y}) - f(\tilde{x}, \tilde{y})}{\delta x}\tilde{x} - \frac{f(\tilde{x}, \tilde{y}+\delta y) - f(\tilde{x}, \tilde{y})}{\delta y}\tilde{y} \tag{3.78}$$

Substituting the values of C_x, C_y, and C_z into eq. (3.72) yields the approximation that is only a function of x, y, and known constants.

$$
\begin{aligned}
\tilde{f}(x,y) = {} & \frac{f(\tilde{x}+\delta x,\tilde{y})-f(\tilde{x},\tilde{y})}{\delta x}x + \frac{f(\tilde{x},\tilde{y}+\delta y)-f(\tilde{x},\tilde{y})}{\delta y}y + \\
& + f(\tilde{x},\tilde{y}) - \frac{f(\tilde{x}+\delta x,\tilde{y})-f(\tilde{x},\tilde{y})}{\delta x}\tilde{x} + \\
& - \frac{f(\tilde{x},\tilde{y}+\delta y)-f(\tilde{x},\tilde{y})}{\delta y}\tilde{y} \\
\tilde{f}(x,y) = {} & f(\tilde{x},\tilde{y}) + \left[\frac{f(\tilde{x}+\delta x,\tilde{y})-f(\tilde{x},\tilde{y})}{\delta x}\right](x-\tilde{x}) + \\
& + \left[\frac{f(\tilde{x},\tilde{y}+\delta y)-f(\tilde{x},\tilde{y})}{\delta y}\right](y-\tilde{y}) \qquad (3.79)
\end{aligned}
$$

The α and β values can be defined as the proximity of the independent variables to their respective upper bounds with the following equations:

$$\alpha = \frac{x-\tilde{x}}{\delta x} \qquad x \in [\tilde{x}, \tilde{x}+\delta x] \qquad (3.80)$$

$$\beta = \frac{y-\tilde{y}}{\delta y} \qquad y \in [\tilde{y}, \tilde{y}+\delta y] \qquad (3.81)$$

The previous two equations can also be written as:

$$x = \tilde{x} + \alpha \times \delta x \qquad \alpha \in [0,1] \qquad (3.82)$$

$$y = \tilde{y} + \beta \times \delta y \qquad \beta \in [0,1] \qquad (3.83)$$

Using the definitions for α and β, we can substitute these into eq. (3.79) to simplify the equation.

$$
\begin{aligned}
\tilde{f}(x,y) = {} & f(\tilde{x},\tilde{y}) + \left[f(\tilde{x}+\delta x,\tilde{y}) - f(\tilde{x},\tilde{y})\right]\alpha + \\
& + \left[f(\tilde{x},\tilde{y}+\delta y) - f(\tilde{x},\tilde{y})\right]\beta \qquad (3.84)
\end{aligned}
$$

Finally, after reorganizing we end with the accurate approximation for one region:

$$\tilde{f}(x,y) = (1-\alpha-\beta)f(\tilde{x},\tilde{y}) + \alpha f(\tilde{x}+\delta x,\tilde{y}) + \beta f(\tilde{x},\tilde{y}+\delta y) \qquad (3.85)$$

A couple examples of this approximation may include the following:

$$\tilde{f}(x,y) = f(\tilde{x},\tilde{y})$$
$$\forall\alpha = 0, \beta = 0 \leftrightarrow x = \tilde{x}, y = \tilde{y} \tag{3.86}$$
$$\tilde{f}(x,y) = \frac{1}{2}f(\tilde{x}+\delta x,\tilde{y}) + \frac{1}{2}f(\tilde{x},\tilde{y}+\delta y)$$
$$\forall\alpha = \frac{1}{2}, \beta = \frac{1}{2} \leftrightarrow x = \tilde{x} + \frac{1}{2}\delta x, y = \tilde{y} + \frac{1}{2}\delta y \tag{3.87}$$
$$\tilde{f}(x,y) = -f(\tilde{x},\tilde{y}) + f(\tilde{x}+\delta x,\tilde{y}) + f(\tilde{x},\tilde{y}+\delta y)$$
$$\forall\alpha = 1, \beta = 1 \leftrightarrow x = \tilde{x} + \delta x, y = \tilde{y} + \delta y \tag{3.88}$$

It is worth noting that the previous equation is a terrible approximation as the true value of the unknown function is $f(\tilde{x}+\delta x,\tilde{y}+\delta y)$ and not the combination of three other function evaluations. The approximation worsens as x and y both approach their respective upper bound of the rectangular region meaning we desire the following for an accurate approximation (which is unlikely to occur in nonlinear functions):

$$f(\tilde{x}+\delta x,\tilde{y}+\delta y) \cong -f(\tilde{x},\tilde{y}) + f(\tilde{x}+\delta x,\tilde{y}) + f(\tilde{x},\tilde{y}+\delta y)$$

From a generic active region, eq. (3.85) can be expanded into the following equation. Please note that due to constraints, α_i and β_j can be replaced with $1-\alpha_{i+1}$ and $1-\beta_{j+1}$, respectively, yielding the same as in eq. (3.85).

$$\tilde{f}(x,y) = (\alpha_i + \beta_j - 1)f(\tilde{x}_i,\tilde{y}_j) + \alpha_{i+1}f(\tilde{x}_{i+1},\tilde{y}_j) + \beta_{j+1}f(\tilde{x}_i,\tilde{y}_{j+1}) \tag{3.89}$$

Since the previous equation is only accurate for one specfic region, "big-M" constraints are introduced to ensure the inactive regions have no effect on the approximation (where M is an arbitrarily large positive value). Thus, the unknown function approximation is forced to be accurate for the active region and has unrestricting constraints on other regions.

$$\begin{aligned}\tilde{f}(x,y) \leq (\alpha_i + \beta_j - 1) f(\tilde{x}_i, \tilde{y}_j) + \alpha_{i+1} f(\tilde{x}_{i+1}, \tilde{y}_j) + \\ + \beta_{j+1} f(\tilde{x}_i, \tilde{y}_{j+1}) + M(2 - A_{i+1} - B_{j+1}) \\ \tilde{f}(x,y) \geq (\alpha_i + \beta_j - 1) f(\tilde{x}_i, \tilde{y}_j) + \alpha_{i+1} f(\tilde{x}_{i+1}, \tilde{y}_j) + \\ + \beta_{j+1} f(\tilde{x}_i, \tilde{y}_{j+1}) - M(2 - A_{i+1} - B_{j+1}) \\ \forall i \neq N_x, j \neq N_y \end{aligned} \tag{3.90}$$

Also, since the regions A_i and B_j must be zero when $i = 0$ and $j = 0$, respectively, it may be easier to understand eq. (3.91) rather than eq. (3.90) (as it is the same constraint with all variables just shifted by one index value). Equation (3.90) is written to show the base point of each region, $f(\tilde{x}_i, \tilde{y}_j)$, as the focus and eq. (3.91) is written to show the region, A_i,B_j, as the focus. One may notice that by using this method the point that is associated with the upper bound of both independent variables, $f(\tilde{x}_{N_x}, \tilde{y}_{N_y})$, is never used.

$$\begin{aligned}\tilde{f}(x,y) \leq (\alpha_{i-1} + \beta_{j-1} - 1) f(\tilde{x}_{i-1}, \tilde{y}_{j-1}) + \alpha_i f(\tilde{x}_i, \tilde{y}_{j-1}) + \\ + \beta_j f(\tilde{x}_{i-1}, \tilde{y}_j) + M(2 - A_i - B_j) \\ \tilde{f}(x,y) \geq (\alpha_{i-1} + \beta_{j-1} - 1) f(\tilde{x}_{i-1}, \tilde{y}_{j-1}) + \alpha_i f(\tilde{x}_i, \tilde{y}_{j-1}) + \\ + \beta_j f(\tilde{x}_{i-1}, \tilde{y}_j) - M(2 - A_i - B_j) \\ \forall i \neq 0, j \neq 0 \end{aligned} \tag{3.91}$$

It is worth noting that in addition to the previous equation (either eq. (3.90) or eq. (3.91)), all of eqs. (3.33) to (3.44) and eqs. (3.61) to (3.71) (ie. the equations restricting x, y, α_i, β_j, A_i, and B_j) are included in this formulation with the exception of eq. (3.42), which is the unknown function approximation in one dimension.

3.5.3 Triangle and Rectangular Methods

In the work done by D'Ambrosio *et al.* [2010], they also explain two additional methods to the one explained previously. The three point method used previously has rectangular regions and uses three points in an "L"-shape to approximate the unknown function. The triangle method separates these rectangular regions into two equal triangles (one an upper left and the other a lower right) and has a binary variable to indicate which is used. For each region, the x and y values used in the approximation must be contained in the active region and introduces some equations to show how this can be done (please refer to the article for more information).

For the rectangular method, the value $f(\tilde{x}_i, \tilde{y}_{j+1})$ in eq. (3.90) (used to simulate the change in the unknown function in the y dimension) may replaced with $f(\tilde{x}_{i+1}, \tilde{y}_{j+1})$ if $f(\tilde{x}_i, \tilde{y}_{j+1}) - f(\tilde{x}_i, \tilde{y}_j) > f(\tilde{x}_{i+1}, \tilde{y}_{j+1}) - f(\tilde{x}_{i+1}, \tilde{y}_j)$ for a minimization problem. The reverse is true for a maximization problem. Additionally, this replacement also affects the coefficient of the base point if it occurs. The purpose of this method is to utilize the most optimal change in the y dimension, which is based purely on the difference of the unknown function at the discrete points described by the inequaity above (keeping x constant either at $x = \tilde{x}_i$ or $x = \tilde{x}_{i+1}$). In other words, the numerically lesser difference (or higher absolute negative difference) will be used in a minimization problem.

Mathematically, this can be defined as follows, with eq. (3.92) replacing eq. (3.90). The $\beta_j - 1$ part of the first coefficient (for the base point) is now built into the $\Delta_{i,j}$ function. This is shown explicitly in eq. (3.94) after realizing that $\beta_j = 1 - \beta_{j+1}$ for the active region.

$$\tilde{f}(x,y) \leq \alpha_i f(\tilde{x}_i,\tilde{y}_j) + \alpha_{i+1} f(\tilde{x}_{i+1},\tilde{y}_j) + \beta_{j+1}\Delta_{i,j} + M(2 - A_{i+1} - B_{j+1})$$
$$\tilde{f}(x,y) \geq \alpha_i f(\tilde{x}_i,\tilde{y}_j) + \alpha_{i+1} f(\tilde{x}_{i+1},\tilde{y}_j) + \beta_{j+1}\Delta_{i,j} - M(2 - A_{i+1} - B_{j+1})$$
$$\forall i \neq N_x, j \neq N_y \tag{3.92}$$

$$\Delta_{i,j} = \min\{f(\tilde{x}_i,\tilde{y}_{j+1}) - f(\tilde{x}_i,\tilde{y}_j), f(\tilde{x}_{i+1},\tilde{y}_{j+1}) - f(\tilde{x}_{i+1},\tilde{y}_j)\} \tag{3.93}$$

$$\begin{aligned}(\beta_j - 1)f(\tilde{x}_i,\tilde{y}_j) + \beta_{j+1} f(\tilde{x}_i,\tilde{y}_{j+1}) &= \\ &= -\beta_{j+1} f(\tilde{x}_i,\tilde{y}_j) + \beta_{j+1} f(\tilde{x}_i,\tilde{y}_{j+1}) \\ &= \beta_{j+1}(f(\tilde{x}_i,\tilde{y}_{j+1}) - f(\tilde{x}_i,\tilde{y}_j)) \\ &= \beta_{j+1}\Delta_{i,j}\end{aligned} \tag{3.94}$$

Of course, this assumes that $\Delta_{i,j} = f(\tilde{x}_i,\tilde{y}_{j+1}) - f(\tilde{x}_i,\tilde{y}_j)$ and not the alternative. However, the alternative would have to use $f(\tilde{x}_{i+1},\tilde{y}_j)$ instead of $f(\tilde{x}_i,\tilde{y}_j)$ and $f(\tilde{x}_{i+1},\tilde{y}_{j+1})$ instead of $f(\tilde{x}_i,\tilde{y}_{j+1})$, which leads to the same conclusion. These equations also imply that β_j is actually not used for the active region, which is correct because it is accounted for in the $\Delta_{i,j}$ function, as stated previously.

3.5.4 Four Point Method

The four point method proposed here is different from the literature examined. The first adaptation is that the weights are made to be indexed for both independent variables (and thus only one weight variable set is needed). To be especially clear, all equations will be rewritten or adapted as necessary so that the method described in this section may stand on its own mathematical formulation (though many similarities will appear).

$$x \in [x_L, x_U] \tag{3.95}$$

$$y \in [y_L, y_U] \tag{3.96}$$

$$i \in I = \{0, 1, ...N_x\} \tag{3.97}$$

$$j \in J = \{0, 1, ...N_y\} \tag{3.98}$$

$$\tilde{x}_i = x_L + (x_U - x_L)\frac{i}{N_x} \tag{3.99}$$

$$\tilde{y}_j = y_L + (y_U - y_L)\frac{j}{N_y} \tag{3.100}$$

$$\alpha_{i,j} \in [0, 1] \tag{3.101}$$

The difference is that since the weights are dependent on both dimensions, the overall sum must be one for all weights.

$$\sum_{i \in I} \sum_{j \in J} \alpha_{i,j} = 1 \tag{3.102}$$

Another difference is that since the weights are in both dimensions, calculating each independent variable is not dependent on the other index of the weights. Thus, the summation across the opposite dimension is done on the weights before multiplying by the discrete point values. This can be compared with the original method of having one independent variable if one thinks "$\alpha_i = \sum_{j \in J} \alpha_{i,j}$" and vice-versa for the other independent variable dimension (this is shown for comparison and is not used as an actual equation).

$$x = \sum_{i \in I} \tilde{x}_i \sum_{j \in J} \alpha_{i,j} \tag{3.103}$$

$$y = \sum_{j \in J} \tilde{y}_j \sum_{i \in I} \alpha_{i,j} \tag{3.104}$$

The unknown function approximation is simple because it has a discrete point associated with each dimension. Geometrically, this is equivalent to the convex summation of four points which forms an irregular tetrahedron (assuming the four points do not lie within the same plane).

$$\tilde{f}(x, y) = \sum_{i \in I} \sum_{j \in J} f(\tilde{x}_i, \tilde{y}_j)\alpha_{i,j} \tag{3.105}$$

Two Binary Variables

Next the binary variables must be introduced. One may either make a binary variable for each independent variable or one binary variable for both indices. The two binary variable method is shown here and the one binary variable method is shown in the next section. First, the constraints on the binary variables are shown to be explicitly clear.

$$A_i \in \{0, 1\} \tag{3.106}$$

$$B_j \in \{0, 1\} \tag{3.107}$$

$$A_i = 0 \qquad \forall i = 0 \tag{3.108}$$

$$B_j = 0 \qquad \forall j = 0 \tag{3.109}$$

$$\sum_{i \in I} A_i = 1 \tag{3.110}$$

$$\sum_{j \in J} B_j = 1 \tag{3.111}$$

The following four equations limit the weights in the same way they would be restricted for one dimension or the three point method, but will lead to forcing all but four weights in a rectangular pattern to be zero. Since the weights are dependent on both independent variables, the binary constraints must be active for every index of the piecewise points in the other independent variable dimension.

$$\alpha_{i,j} \leq A_i + A_{i+1} \qquad \forall i \neq N_x \tag{3.112}$$

$$\alpha_{i,j} \leq A_i \qquad \forall i = N_x \tag{3.113}$$

$$\alpha_{i,j} \leq B_j + B_{j+1} \qquad \forall j \neq N_y \tag{3.114}$$

$$\alpha_{i,j} \leq B_j \qquad \forall j = N_y \tag{3.115}$$

One example of these constraints at work could be if $A_2 = 1$ and $B_4 = 1$. This means that only $\alpha_{1,3}$, $\alpha_{2,3}$, $\alpha_{1,4}$, and $\alpha_{2,4}$ could be nonzero.

One Binary Variable

For this method, only one binary variable ($A_{i,j}$) will be used to indicate one active region in both independent variables. This section replaces all the equations and variables in the Two Binary Variable section immediately previous.

$$A_{i,j} \in \{0, 1\} \tag{3.116}$$

$$A_{i,j} = 0 \qquad \forall \{i = 0\} \cup \{j = 0\} \tag{3.117}$$

$$1 = \sum_{i \in I} \sum_{j \in J} A_{i,j} \tag{3.118}$$

The regions are essentially restricted in the same way, but the formulation must reflect the two dimensions accurately. Equation (3.119) is the general formula, but is not valid if the weight is at the upper bound of either independent variable (leading to the next three equations).

$$\alpha_{i,j} \leq A_{i,j} + A_{i+1,j} + A_{i,j+1} + A_{i+1,j+1} \qquad \forall i \neq N_x, j \neq N_y \tag{3.119}$$

$$\alpha_{i,j} \leq A_{i,j} + A_{i,j+1} \qquad \forall i = N_x, j \neq N_y \tag{3.120}$$

$$\alpha_{i,j} \leq A_{i,j} + A_{i+1,j} \qquad \forall i \neq N_x, j = N_y \tag{3.121}$$

$$\alpha_{i,j} \leq A_{i,j} \qquad \forall i = N_x, j = N_y \tag{3.122}$$

Benefits and Drawbacks of the Four Point Method

The main theoretical benefit of using this method when compared to the three point method is that it improves the accuracy of the upper portion of the rectangular region without adding much complexity because it simply includes the fourth point as opposed to approximating for it. The four point method is an alternative to the Tringular and Rectangular methods seen in D'Ambrosio *et al.* [2010]. The drawback to the four point method as it currently stands is that there is not a unique mapping of weights for an arbitrary pair of independent variable values. However, this can be fixed by adding one simple constraint that balances the ratios of upper bound to lower bound weights as seen in the following equations.

$$\frac{\alpha_{i,j}}{\alpha_{i+1,j}} = \frac{\alpha_{i,j+1}}{\alpha_{i+1,j+1}} \tag{3.123}$$

$$\frac{\alpha_{i,j}}{\alpha_{i,j+1}} = \frac{\alpha_{i+1,j}}{\alpha_{i+1,j+1}} \tag{3.124}$$

Both of these equations simplify to the following equation which is valid even for inactive regions (as the equation would reduce to $0 = 0$).

$$\alpha_{i,j}\alpha_{i+1,j+1} = \alpha_{i+1,j}\alpha_{i,j+1} \tag{3.125}$$

This constraint forces one mapping of weights to any pair of independent variable values, but at the cost of introducing a bilinear constraint. For a general region where $x \in [\tilde{x}_i, \tilde{x}_{i+1}]$, $y \in [\tilde{y}_j, \tilde{y}_{j+1}]$, we know from eqs. (3.102) to (3.104) that:

$$1 = \alpha_{i,j} + \alpha_{i+1,j} + \alpha_{i,j+1} + \alpha_{i+1,j+1} \tag{3.126}$$

$$x = (\alpha_{i,j} + \alpha_{i,j+1})\tilde{x}_i + (\alpha_{i+1,j} + \alpha_{i+1,j+1})\tilde{x}_{i+1} \tag{3.127}$$

$$y = (\alpha_{i,j} + \alpha_{i+1,j})\tilde{y}_j + (\alpha_{i,j+1} + \alpha_{i+1,j+1})\tilde{y}_{j+1} \tag{3.128}$$

Using eqs. (3.125) to (3.128), one can actually calculate the appropriate weights using x, y, and the discrete points.

$$\alpha_{i,j} = \frac{(\tilde{x}_{i+1} - x)(\tilde{y}_{j+1} - y)}{(\tilde{x}_{i+1} - \tilde{x}_i)(\tilde{y}_{j+1} - \tilde{y}_j)} \tag{3.129}$$

$$\alpha_{i+1,j} = \frac{(x - \tilde{x}_i)(\tilde{y}_{j+1} - y)}{(\tilde{x}_{i+1} - \tilde{x}_i)(\tilde{y}_{j+1} - \tilde{y}_j)} \tag{3.130}$$

$$\alpha_{i,j+1} = \frac{(\tilde{x}_{i+1} - x)(y - \tilde{y}_j)}{(\tilde{x}_{i+1} - \tilde{x}_i)(\tilde{y}_{j+1} - \tilde{y}_j)} \tag{3.131}$$

$$\alpha_{i+1,j+1} = \frac{(x - \tilde{x}_i)(y - \tilde{y}_j)}{(\tilde{x}_{i+1} - \tilde{x}_i)(\tilde{y}_{j+1} - \tilde{y}_j)} \tag{3.132}$$

However, there is still the issue of using a bilinear constraint in an MILP (which also defeats the purpose of creating a linear approximation method). As a result, this bilinear constraint (eq. (3.125)) is not included in the PLA formulation because it does not add any benefit outside enforcing one mapping of weights to a pair of independent variable values. The anticipated error caused by this nonunique mapping is small and can be overlooked since the PLA is an approximation method.

3.6 PLA Method

3.6.1 Description for Hydropower Application

The PLA method replaces the nonlinearities from the MINLP with piecewise linear segments that captures the general shape of the nonlinear functions. Since the power of each generator is dependent on both the discharge through the generator and the head of the upstream reservoir, the linear segments must approximate the power in two dimensions. Thus, instead of using two points to interpolate, one uses four adjacent points in a rectangular shape to interpolate the power.

This method is also just an approximation, and the error of that approximation is dependent on how many points are used. If the number of points in both dimensions approaches infinity, then the approximation becomes perfectly accurate. Alternatively, using a small number of points will calculate the segments for fewer regions, meaning the approximation will not be as accurate.

The downside of using such a method is that it requires a binary variable for each region of each generator at each time step. However, the benefit to using this method is that it does not require an iterative process like the SLP and it can see the general shape of the nonlinear functions for the entire feasible space (to a certain degree of error or approximation).

Another thing to note regarding this method is that it cannot accurately include the initial or final volume requirement as the volume is approximated based on the level. Thus, including these constraints may cause the problem to be infeasible if the initial or final volume do not coincide with points in the PLA grid. However, since the initial and final reservoir levels are still included as constraints, satisfaction of the volume constraints is not vital.

3.6.2 Hydropower PLA Example

The illustration of the PLA in two dimensions is much more complicated for this work and is seen in fig. 3.4. The function in this case, $f(x, y)$, is explicit and the regions describing the two independent variables, x and y, are examined. In this work x and y would represent the generator flow and reservoir head, respectively, while the function, $f(x, y)$, would represent the generator power output. In this example, the active region is outlined with a dashed line and simulates the rectangle in which $x \in [x_L, x_U]$ and $y \in [y_L, y_U]$, where L indicates the lower bound and U the upper bound of the region for each independent variable. These values are not to be confused with the weights indicated at each corner of the active rectangular region ($Y_{L,L}, Y_{U,L}, Y_{L,U}$, and $Y_{U,U}$).

To demonstrate the semicontinuous nature of the flow variable a portion has been greyed out to indicate that this section is not part of the feasible region. This is done to simulate the values between zero flow and minimum flow, which is considered infeasible in the optimization problem. However, attention is brought to the dotted line at the left to show that this "region" (which is feasible) indicates a generator being off and thus not having any flow (being a zero value). This "region" is needed to allow the head to vary when the generator is off and not be restricted to a specific point used in the PLA approximation.

Continuing with the example, the independent variables and nonlinear function are approximated by the variable weights of the active region with the following equations. It is important to note that these example equations are only valid for the current active region, which will cause all other weights to be zero.

$$f(x, y) = f(x_L, y_L)Y_{L,L} + f(x_U, y_L)Y_{U,L} + f(x_L, y_U)Y_{L,U} + f(x_U, y_U)Y_{U,U} \tag{3.133}$$

$$x = x_L(Y_{L,L} + Y_{L,U}) + x_U(Y_{U,L} + Y_{U,U}) \tag{3.134}$$

$$y = y_L(Y_{L,L} + Y_{U,L}) + y_U(Y_{L,U} + Y_{U,U}) \tag{3.135}$$

Then, the weights will be forced to be between zero and one, and the sum of all weights of each generator must be equal to one.

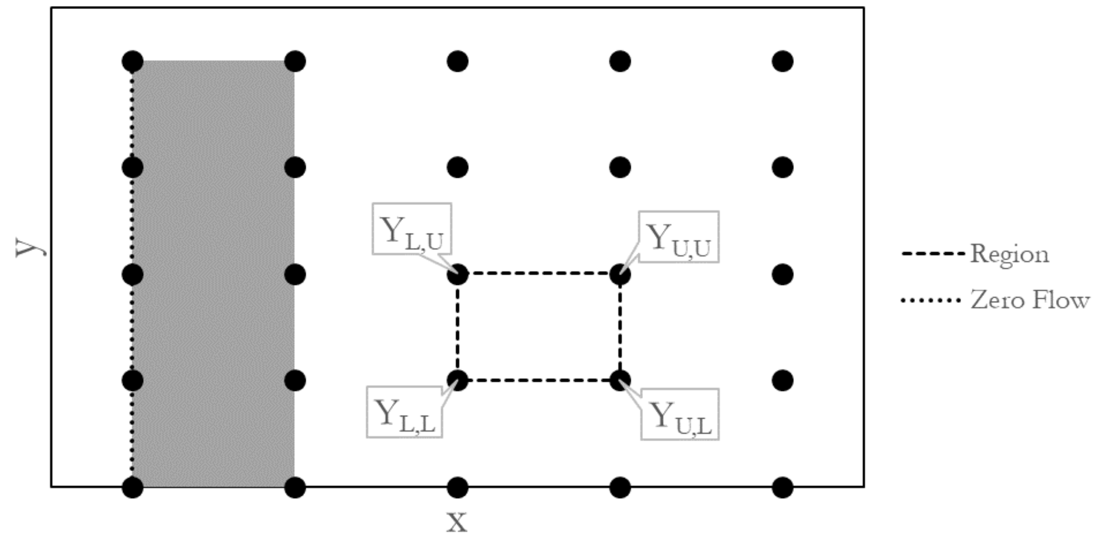

Figure 3.4: An illustration of the PLA (Piecewise Linear Approximation) method in two dimensions.

3.6.3 PLA New/Modified Model Equations

The first four adapted model equations change the way the volume, power, flow, and heads, respectively, are calculated (eqs. (3.136) to (3.139)). Each of them are now the summation of the weights at piecewise points multiplied by the value at that point, thus creating a linear approximation between two points (or four points for the power).

The piecewise points for volume, power, flow, and head are, respectively, $\tilde{V}_{i,m}$, $\tilde{P}_{i,j,n,m}$, $\tilde{F}_{i,j,n}$, and $\tilde{H}_{i,m}$, where n and m index the piecewise points in the flow and head dimensions, respectively. These are calculated based on the parameters given in the original MINLP later in section 3.6.4.

One may notice that the volume and head for each reservoir are not dependent on the generator number j, but depend on the weights, which have independent values for each generator. This is done because the generators must be allowed to have different discharges (requiring the index for each generator j), but all the generators within one reservoir at a certain time step must use the same head to calculate the power produced. In other words, the head and volume equations must be valid for the weights associated with each and every generator even though the head and volume are not dependent on the generators. To reiterate this, the equations are explicitly stated to be valid for all reservoirs, generators, and time steps (where other equations imply this unless indicated otherwise).

$$V_{i,t} = \sum_{m \in M} \tilde{V}_{i,m} \sum_{n \in N} Y_{i,j,t,n,m} \qquad \forall i \in I, j \in J, t \in T \tag{3.136}$$

$$P_{i,j,t} = \sum_{n \in N} \sum_{m \in M} \tilde{P}_{i,j,n,m} Y_{i,j,t,n,m} \qquad \forall i \in I, j \in J, t \in T \tag{3.137}$$

$$F_{i,j,t} = \sum_{n \in N} \tilde{F}_{i,j,n} \sum_{m \in M} Y_{i,j,t,n,m} \qquad \forall i \in I, j \in J, t \in T \tag{3.138}$$

$$H_{i,t} = \sum_{m \in M} \tilde{H}_{i,m} \sum_{n \in N} Y_{i,j,t,n,m} \qquad \forall i \in I, j \in J, t \in T \tag{3.139}$$

As stated before, the initial and final volumes can not be explicitly constrained to the exact value as they are in eq. (3.17) in the MINLP formulation as this may cause the problem to be infeasible, but are still enforced to be equal to each other. Instead, another piecewise weight is introduced strictly for the final reservoir level which will be used to approximate the final reservoir volume.

$$V_{i,Final} = \sum_{m \in M} \tilde{V}_{i,m} Y_{i,m,Final} \qquad \forall i \in I \tag{3.140}$$

$$L_{i,Final} = \sum_{m \in M} \left[\tilde{H}_{i,m} Y_{i,m,Final} \right] + L_{i,Down} \qquad \forall i \in I \tag{3.141}$$

Equations (3.142) and (3.143) mathematically represent the limits on the binary variables $Z_{i,j,t,n,m}$ due to nonexistance or physical limitation. Equation (3.142) forces the binary variable $Z_{i,j,t,n,m}$ to be zero when $n = 1$ because this represents the region between zero and minimum flow, which is impossible (the grey region in fig. 3.4). Equation (3.143) forces $Z_{i,j,t,n,m}$ to be zero when $m = 0$ because there is no region described by this occurance (having head below the minimum value, which is the area beneath the grid in fig. 3.4).

$$Z_{i,j,t,n,m} = 0 \qquad \forall n = 1 \tag{3.142}$$

$$Z_{i,j,t,n,m} = 0 \qquad \forall m = 0 \tag{3.143}$$

The next four equations allow the weights to be nonzero when there is an adjacent active region. When either discretization point (n or m) is at the maximum, there is not a region beyond, which is why they must be constrained differently. In the example in fig. 3.4, $Z_{3,2}$ is active (removing the indices for reservoir number, generator number, and time step), meaning only the weights $Y_{2,1}, Y_{3,1}, Y_{2,2}$, and $Y_{3,2}$ can be nonzero, which correspond directly on the figure to $Y_{L,L}, Y_{U,L}, Y_{L,U}$, and $Y_{U,U}$.

$$\begin{aligned} Y_{i,j,t,n,m} \leq Z_{i,j,t,n,m} + Z_{i,j,t,n,m+1} + \\ Z_{i,j,t,n+1,m} + Z_{i,j,t,n+1,m+1} \qquad \forall n \neq N_F, m \neq N_H \end{aligned} \tag{3.144}$$

$$Y_{i,j,t,n,m} \leq Z_{i,j,t,n,m} + Z_{i,j,t,n+1,m} \qquad \forall n \neq N_F, m = N_H \tag{3.145}$$

$$Y_{i,j,t,n,m} \leq Z_{i,j,t,n,m} + Z_{i,j,t,n,m+1} \qquad \forall n = N_F, m \neq N_H \tag{3.146}$$

$$Y_{i,j,t,n,m} \leq Z_{i,j,t,n,m} \qquad \forall n = N_F, m = N_H \tag{3.147}$$

Lastly, there should only be one active region for each generator of each reservoir at each time step, and the sum of weights should equal one to ensure a correct approximation.

$$1 = \sum_{n \in N} \sum_{m \in M} Z_{i,j,t,n,m} \tag{3.148}$$

$$1 = \sum_{n \in N} \sum_{m \in M} Y_{i,j,t,n,m} \tag{3.149}$$

$$1 = \sum_{m \in M} Y_{i,m,Final} \tag{3.150}$$

$$0 \leq Y_{i,j,t,n,m} \leq 1 \tag{3.151}$$

$$0 \leq Y_{i,m,Final} \leq 1 \tag{3.152}$$

3.6.4 PLA New/Modified Parameter Equations

The equations in this section define the piecewise points at equidistant positions within the feasible region. These are created by introducing two indices for generator discharge and reservoir head, n and m, which vary from 0 to N_F and from 0 to N_H, respectively. These piecewise points include the definitions for $\tilde{F}_{i,j,n}$, $\tilde{H}_{i,m}$, $\tilde{V}_{i,m}$, and $\tilde{P}_{i,j,n,m}$, which respectively calculate the flow, head, volume, and power at each of the discretization points.

$$\tilde{F}_{i,j,n} = 0 \qquad \forall n = 0$$

$$\tilde{F}_{i,j,n} = F_{i,j,Min} + \left[F_{i,j,Max} - F_{i,j,Min}\right] \frac{n-1}{N_F - 1} \qquad \forall n \neq 0 \quad (3.153)$$

$$\tilde{H}_{i,m} = L_{i,Min} - L_{i,Down} + (L_{i,Max} - L_{i,Min}) \frac{m}{N_H} \quad (3.154)$$

$$\tilde{V}_{i,m} = RS_{i,C0} + RS_{i,C1} \left[\tilde{H}_{i,m} + L_{i,Down} - RS_{i,C2}\right]^{RS_{i,C3}} \quad (3.155)$$

$$\tilde{P}_{i,j,n,m} = 0 \qquad \forall n = 0$$

$$\begin{aligned}\tilde{P}_{i,j,n,m} = &\left(GC_{i,j,a_1} + GC_{i,j,a_2}\tilde{H}_{i,m} + GC_{i,j,a_3}\left(\tilde{H}_{i,m}\right)^2\right) + \\ &\left(GC_{i,j,b_1} + GC_{i,j,b_2}\tilde{H}_{i,m} + GC_{i,j,b_3}\left(\tilde{H}_{i,m}\right)^2\right)\tilde{F}_{i,j,n} + \\ &\left(GC_{i,j,c_1} + GC_{i,j,c_2}\tilde{H}_{i,m} + GC_{i,j,c_3}\left(\tilde{H}_{i,m}\right)^2\right)\left(\tilde{F}_{i,j,n}\right)^2 + \\ &\left(GC_{i,j,d_1} + GC_{i,j,d_2}\tilde{H}_{i,m} + GC_{i,j,d_3}\left(\tilde{H}_{i,m}\right)^2\right)\left(\tilde{F}_{i,j,n}\right)^3 \qquad \forall n \neq 0 \quad (3.156)\end{aligned}$$

3.7 User Chosen Parameters

There are two parameters common to the SLP and Hybrid AG methods that are chosen by the user and these are the initial trust region size and the trust region shrinking factor. These methods terminate when the trust region is below a certain size, the allotted time is surpassed, or if the number of iterations reaches some predetermined value. Increasing the value of either the initial trust region or the trust region shrinking factor will increase the number of iterations that are possible before termination, which will likely increase the computational time required to terminate. However, allowing the solutions to slowly approach the optimum over more iterations will likely yield a better solution. The trade-off between computational time and solution quality is important and subjective depending on how much time the user is willing to spend obtaining a better quality solution. This is why the first test conducted is a comparison of computational time and solution quality using different values for both of these parameters.

Since the SLP and Hybrid AG methods are each an iterative process, many optimization subproblems will have to be solved for an individual problem. As the first few iterations are not very accurate, it would waste computational time if they were solved to a dual gap of zero. Thus, the optimality gap required to move to the next iteration is dependent on the iteration. The Hybrid AG method for the daily case has the requirement for iteration termination start at 1%, then decreases to 0.1% after two iterations (or starting at the third iteration), then to 0.01% after four iterations, and finally to 0% after nine iterations. The Hybrid AG method for the base case has the requirement of 0% for all iterations due to the small problem size. Since the SLP method is less accurate than the Hybrid for one individual iteration, the requirement for iteration termination starts at 0.1%, then decreases to 0.01% after two iterations, then to 0.001% after four iterations, and finally to 0% after nine iterations (and this is for both the daily and base cases). These values were chosen arbitrarily to provide an increasing accuracy as the trust region shrinks. The Hybrid FG method is slightly different because it typically solves within a few iterations, which is why the requirement for every iteration is 0%.

Like the other linearization methods, the PLA method allows the user to define values for two other parameters. These two parameters are the number of points in the head dimension and the discharge dimension. The Hybrid method (both the Hybrid FG and AG methods) also has the choice for the number of points in the discharge dimension. Using a greater number of points will allow a more accurate solution to be found, but will increase the computational complexity. Once again, the user must determine what trade-off they are willing to give.

Another thing to note is that because these methods are approximations, the generator discharges from the final solutions are utilized in the original MINLP equations and the volumes, levels, heads, and generator powers are correctly calculated so that the objective value is accurate for reporting the final solution. As mentioned before, the objective value (Obj. Val.) in this work is the profit obtained over the entire time horizon considered. The corrections due to this error in approximation for the SLP and Hybrid AG methods are negligible and are not reported, and thus only a single objective value is shown. However, the corrections are given for the Hybrid FG and PLA methods to give a fair comparison between the approximate objective value (App. Obj. Val.) obtained from the optimization and the true objective value (True Obj. Val.) obtained when the solution is implemented on the true nonlinear equations. This error is present because the Hybrid FG and PLA methods have one rough approximation and may optimize to have a significantly different value when the solution is implemented on the original MINLP (depending on the degree of the approximation).

3.8 Base Case Comparison

In order to ensure that the linearization methods are performing accurately and efficiently, a comparison is shown between the linearization methods and the original MINLP for small base case problems. The main goal of these base case tests will be to determine whether each linearization method can find the globally optimal solution, and to discard the method if it is unable to find the global optimum or if the method uses more computational time than the original MINLP formulation. Another aspect to these tests is to demonstrate that the linearization methods are mathematically depicting the problem correctly and that the solutions found by these methods are feasible within the original MINLP formulation.

These base case problems only have one reservoir, two generators, and six time steps, however the inflow changes to create three problems that are meant to show different points. The inflows for the high, medium, and low inflow base cases are 10.012, 5.012, and 1.012 thousand cubic feet per hour respectively. To put that into perspective, the minimum flow to generate power and the maximum flow allowable for the two generators considered are each 1.2 and 6.502 thousand cubic feet per hour, respectively. This means that the high inflow base case should have both generators on at all time steps and the low inflow base case will only allow the generators to be on at key points, and may not even turn on the second generator. The medium inflow base case will determine the optimal time steps to produce power and when to turn generators off or if it is optimal to keep all the generators on for all time steps at lower discharges.

For each base case and method, results will be shown comparing how the method fares given some possible values for each user chosen parameter, as described previously. The key aspects of each result are the computational time required and the objective value obtained, as the best solution is desired, but not worth waiting an exorbitant amount of time. The best method will obtain the global optimum with the greatest computational effeciency.

For the SLP and Hybrid AG methods, the initial trust region (In. T. R.) and trust region shrinking factor (T. R. Factor) are the main user chosen parameters to consider. Two values were chosen for the initial trust region to be 10 and 20 thousand cubic feet per hour as these values are large enough to allow the methods to maneuver the feasible region and small enough to not waste iterations shrinking the trust region with no change from the previous iteration (occurs when the trust region is larger than the feasible space). Four values were chosen for the trust region shrinking factor to be 0.95, 0.9, 0.75, and 0.5. These are suitable values because larger values than these will waste time with unnecessary iterations and any values smaller will not allow suitable progression towards the solution.

Since the number of points used in the Hybrid and PLA methods can be chosen like the initial trust region and trust region factor, two different values were tested (six points and eleven points) for the Hybrid AG method and multiple combinations were used for the Hybrid FG and PLA methods. There is no justification for the specific number of points used. The only thing to consider is that the more points used allows a greater accuracy of approximation to be utilized and a fewer number of points allows greater computational efficiency. The Hybrid AG method converges on the solution like the SLP method so the number of points plays an important part more on earlier iterations and plays almost no part on the final iterations. This is because as the method converges on the optimum, the piecewise points are placed so close together that they will have similar values, whereas more aspects of the nonlinearity can be captured in earlier iterations because the points are further apart. This also means that the number of points is not as vital a parameter for the Hybrid AG method as the initial trust region and trust region factor, which is why only two values are tested.

The optimization software used in this work is GAMS and its associated solvers described briefly in appendix B. For the nonlinear solvers, a dual bound is shown if the optimization was unable to find global optimality to solver tolerance. This dual bound represents an upper bound on the optimal solution, but is not guaranteed to be a feasible solution (only that the best feasible solution is less than this value). The relative optimality gap is the absolute difference between the current objective value

(Obj. Val.), which is also the best feasible solution found (the primal bound), and the dual bound divided by the dual bound. When the relative optimality gap is reduced to zero (computationally considered to be within 10^{-6}% for MINLP optimizations), then global optimality has been achieved.

3.8.1 High Flow

For the high inflow base case, the MINLP results can be seen in Table 3.1, the SLP results in Table 3.2, the Hybrid FG results in Table 3.3, the Hybrid AG results in Tables 3.4 and 3.5, and the PLA results in Table 3.6. For reference, 1,000 seconds is 16 minutes and 40 seconds, 10,000 seconds is equal to 2 hours 46 minutes and 40 seconds, and 100,000 seconds is equal to 27 hours 46 minutes and 40 seconds.

Table 3.1: High Inflow MINLP Base Case Results

Solver	Obj. Val. ($)	Dual Bound ($)	Opt. Gap (%)	Time (s)
ANTIGONE	52,439.90	53,611.56	2.19	10,001.870*
ANTIGONE	52,439.90	53,313.15	1.64	100,000.17**
SCIP	52,439.904	52,789.184	0.66	10,874.840*
SCIP	52,439.908	52,439.915	1.33×10^{-5}	100,001.50**
BARON	52,439.904	65,756.384	20.25	10,036.77*
BARON	52,439.904	64,812.848	19.09	100,122.66**
COUENNE	52,437.206	52,615.26	0.34	100,066.507**

*=Terminated based on a 10,000 second time limit

**=Terminated based on a 100,000 second time limit

It can be seen in table 3.1 that all of the MINLP global solvers used in this work except BARON (ie. ANTIGONE, SCIP, and COUENNE) are able to find the global optimum within a fairly small optimality gap. However, BARON is able to find the same solution as the other solvers and the solution with the best optimality gap was found by SCIP. COUENNE was able to find a high quality solution, but this is a slightly worse solution when compared to the solutions found by the other solvers.

Some of these simulations have proven the location of a global optimum to this problem within a satisfactory tolerance, with the best run having an absolute optimality gap within one cent ($0.01) (or within a relative optimality gap of $1.33 \times 10^{-5}\%$). This is close enough to say that the global optimum has been found within a small margin of error and that this is sufficient for comparison purposes. Thus, it will be assumed that the optimal objective value is $52,439.91 and any linearization methods that can find this solution (within a small margin of error) will be deemed acceptable. The next step is to determine which method can find this solution in the lowest amount of time for all or most of the scenarios considered.

Table 3.2: High Inflow SLP Base Case Results

Method	In. T. R.	T. R. Factor	Time (s)	Iter.	Obj. Val. ($)
SLP	20	0.95	89.490	194	52,439.903
SLP	20	0.9	32.457	94	52,439.902
SLP	20	0.75	8.944	35	52,439.903
SLP	20	0.5	3.577	15	52,424.534
SLP	10	0.95	80.806	180	52,439.903
SLP	10	0.9	30.795	88	52,439.903
SLP	10	0.75	7.825	33	52,439.903
SLP	10	0.5	3.371	14	52,305.220

The SLP has no problem finding a similar objective value to the optimum proven by the MINLP global solvers as long as it is given sufficient iterations (Iter.) to do so. Specifically, a trust region factor of 0.5 is not large enough for the two initial trust regions tested. It seems that the intial trust region is not a significant factor, but as expected, the larger initial trust region takes longer to terminate.

Table 3.3: High Inflow Hybrid Fixed Grid Base Case Results

Method	N_F	Time (s)	Iter.	App. Obj. Val. ($)	True Obj. Val. ($)
Hybrid FG	6	0.507	2	52,289.41	52,298.70
Hybrid FG	11	1.155	3	52,403.17	52,406.50
Hybrid FG	26	1.211	3	52,437.60	52,438.53
Hybrid FG	51	3.582	4	52,438.93	52,439.15
Hybrid FG	101	14.992	3	52,439.55	52,439.62
Hybrid FG	251	855.615	4	52,439.77	52,439.78
Hybrid FG	501	3002.338*	3	52,439.88	52,439.88

*=Terminated based on 1,000 second time limit for each iteration

The Hybrid FG method (results seen in table 3.3) is able to converge on a stable solution within a few iterations regardless of the number of piecewise points used (N_F). However, even with 500 linear segments the final solution is still a few cents off the globally optimal solution. This is simply a limitation of the approximation method.

The Hybrid AG method, like the SLP method, seems to find the global optimum within a small margin of error with similar computational times as the SLP method for this base case. However, even with the small trust region factor of 0.5 the Hybrid AG method is still able to find an objective value similar to the optimum. Also, as expected, the eleven point Hybrid AG method takes longer than the six point Hybrid AG method, and this is simply because there are more binary variables for each iteration. It is also apparent that the adaptive grid method is much more effective than the fixed grid method.

Table 3.4: High Inflow Hybrid Six-Point Adaptive Grid Base Case Results

Method	In. T. R.	T. R. Factor	Time (s)	Iter.	Obj. Val. ($)
Hybrid AG	20	0.95	61.009	149	52,439.901
Hybrid AG	20	0.9	28.061	73	52,439.901
Hybrid AG	20	0.75	7.581	27	52,439.900
Hybrid AG	20	0.5	3.162	11	52,439.898
Hybrid AG	10	0.95	56.411	135	52,439.900
Hybrid AG	10	0.9	26.094	66	52,439.898
Hybrid AG	10	0.75	6.551	25	52,439.902
Hybrid AG	10	0.5	2.616	10	52,439.898

Table 3.5: High Inflow Hybrid Eleven-Point Adaptive Grid Base Case Results

Method	In. T. R.	T. R. Factor	Time (s)	Iter.	Obj. Val. ($)
Hybrid AG	20	0.95	72.218	149	52,439.903
Hybrid AG	20	0.9	31.594	73	52,439.902
Hybrid AG	20	0.75	8.600	27	52,439.903
Hybrid AG	20	0.5	3.292	11	52,439.902
Hybrid AG	10	0.95	67.994	135	52,439.902
Hybrid AG	10	0.9	27.234	66	52,439.902
Hybrid AG	10	0.75	7.449	25	52,439.903
Hybrid AG	10	0.5	2.897	10	52,439.902

As one can see from table 3.6, the PLA method is not as reliable for this base case as the SLP and Hybrid methods, and this is most likely due to the approximation not being detailed enough (ie. not enough points). The PLA method comes close, but does not manage to satisfy the same level of accuracy as the SLP and Hybrid

Table 3.6: High Inflow PLA Base Case Results

Method	N_F	N_H	App. Obj. Val. ($)	True Obj. Val. ($)	Time (s)
PLA	101	100	52,439.624 (dual=52,464.766 Opt. Gap=0.0479%)	52,439.779	100,003.729*
PLA	101	100	52,438.351 (dual=52,464.766 Opt. Gap=0.0503%)	52,438.558	10,003.577**
PLA	101	50	52,439.512	52,439.486	4,700.661
PLA	101	25	52,440.767	52,439.338	1,251.450
PLA	51	50	52,438.872	52,439.388	339.115
PLA	51	25	52,439.133	52,436.646	571.974
PLA	26	25	52,437.345	52,439.411	31.364
PLA	26	10	52,438.236	52,437.531	7.382
PLA	11	10	52,407.466	52,414.034	2.314

*=Terminated based on a 100,000 second time limit

**=Terminated based on a 10,000 second time limit

methods. Not only this, but the PLA method uses longer computational times. One must compare the other base case results to determine the best method to use.

3.8.2 Medium Flow

A subset of the tests performed on the high inflow base case are completed for the medium and low inflow base cases as the results follow the same pattern as before. The global optimum will need to be found for this problem as well as the low case to show that the best method will be able to adapt to different scenarios and not just the best for one individual case like an anomaly.

Different tests were performed for the medium inflow base case that varies the termination requirement (Term. Req.) to return a solution. The two sets of requirements are: (i) an optimality gap of zero or a specified maximum computational time (MT) (whichever occurs first); and (ii) a specified achieved optimality gap (OG) with no maximum computational time. These specific tests are chosen based on the results from the high inflow base case. These are included to show how quickly the best solution may be found and how long it may take to prove optimality. These results are shown in table 3.7. To be clear, the last column is the termination requirement specified by the user (along with the solver in the first column) and the interior columns are obtained by the optimization.

Table 3.7: Medium Inflow MINLP Base Case Results

Solver	Obj. Val. ($)	Dual ($)	Opt. Gap (%)	Time (s)	Term. Req.
SCIP	29,113.101	29,113.102	3.43×10^{-6}	100,066.61	MT=100,000s
SCIP	29,113.101	29,113.102	3.43×10^{-6}	10,010.62	MT=10,000s
SCIP	29,113.101	29,113.391	9.96×10^{-4}	1,753.00	OG=0.001%
SCIP	29,113.101	29,115.983	9.90×10^{-3}	1,761.80	OG=0.01%
BARON	29,113.101	36,195.859	19.57	10,054.55	MT=10,000s

SCIP once agains perfoms the best amongst all MINLP global solvers and one run by BARON shows the same solution for consistency. It is odd that the two runs that specify the optimality gap have similar computational times and that the stricter requirement (OG=0.001%) also takes less time. Logically, the stricter optimality gap requirement should take more time if the solver performs the same solving methodolgy each time and that the solver must achieve an optimality gap of 0.01% before 0.001% (unless they happen simultaneously). However, this logical contradiction can be attributed to small inconsistencies in computer performance.

As with the high inflow base case, the optimal solution was found within a very small tolerance and has a value of $29,113.10 for the medium inflow base case. As only a subsection of the tests performed on the high inflow base case are carried out for the medium inflow base case, the SLP and Hybrid AG results are combined into table 3.8.

Table 3.8: Medium Inflow SLP and Hybrid Adaptive Grid Base Case Results

Method	In. T. R.	T. R. Factor	Time (s)	Iter.	Obj. Val. ($)
SLP	20	0.95	81.799	194	28,640.437
SLP	20	0.9	32.116	94	29,113.100
SLP	10	0.75	8.327	33	29,113.101
Hybrid (6 pt.) AG	20	0.95	72.523	149	29,111.473
Hybrid (6 pt.) AG	10	0.75	6.483	25	29,113.099
Hybrid (11 pt.) AG	20	0.95	71.798	149	29,113.100
Hybrid (11 pt.) AG	10	0.75	7.639	25	29,111.414

There are a few runs from both the SLP and Hybrid AG methods that fail to find the global optimum. The linearization methods cannot guarentee that they will find the global optimum and this is shown here. These mishaps may be attributed to the method, but it is more likely that these results are anomalies because changing the user chosen parameters slightly fixes this problem. However, it is worth noting that although the Hybrid AG method failed to find the optimum in more than one scenario, it found a solution with the objective value within a small amount of the optimum (ie. a high quality solution).

It has been observed that with the fixed grid method it is possible for iterations to alternate between solutions. When the current iteration's solution is identical to the solution occured two iterations previously (within computational tolerances),

Table 3.9: Medium Inflow Hybrid Fixed Grid Base Case Results

Method	N_F	Time (s)	Iter.	App. Obj. Val. ($)	True Obj. Val.($)
Hybrid FG	6	0.953	3	29,006.40	29,053.22
Hybrid FG	11	0.948	2	29,046.97	29,053.22
Hybrid FG	26	1.235	3	29,110.79	29,111.90
Hybrid FG	51	2.001	4*	29,109.78	29,110.35
Hybrid FG	101	3.214	4	29,112.60	29,112.84
Hybrid FG	251	13.844	5	29,111.31	29,111.34
Hybrid FG	501	17.580	2	29,113.09	29,113.09
Hybrid FG	1001	322.676	4*	29,111.41	29,111.41

*=Terminated based on alternating solutions

indicating alternating solutions, the iterative process is terminated and the current solution is returned. This occurs in two runs in table 3.9.

Since it is more likely that generators will be off when there is lower inflow, it is worth investigating whether branching downwards would save computational time. Branching downwards will force the solver (CPLEX) to explore the branch on the binary variables towards zero first. This means the solver will explore solutions where generators are primarily off and will hopefully assist in cutting other branches that are suboptimal faster. The branching direction (B. Dir.) is only tested on the PLA method as an individual iteration is particularly quick for the SLP and Hybrid methods and thus would not change the computational time by a significant amount. For the high inflow base case the inflows are high enough to know that all generators should be on, meaning that this test is unnecessary for that particular problem. Since the inflow for the medium inflow base case is lower than the maximum capacity of one generator, it is possible to have one generator off for the entire time horizon and still utilize the incoming flow completely. However, the medium inflow base case also has sufficient flow to have both generators on for the entire time horizon. This means that there is no expectation as to which is better.

Table 3.10: Medium Inflow PLA Base Case Results

Method	N_F	N_H	App. Obj. Val. ($)	True Obj. Val. ($)	Time (s)	B. Dir.
PLA	51	50	29,111.752	29,112.519	1,849.242	Up
PLA	51	50	29,111.752	29,112.519	170.570	Down
PLA	26	25	29,110.445	29,112.003	30.556	Up
PLA	26	25	29,110.445	29,111.899	19.211	Down

It can be observed from table 3.10 that branching down is significantly better for this case, but branching down with one set of N_F and N_H values (26 and 25, respectively) achieved the same approximate objective value as branching upwards but did not obtain the same true objective value. This may be attributed to a minor approximation error that creates a nonunique global optimum in the approximation, but obtains different true objective values.

3.8.3 Low Flow

Again, a search for the global optimum is completed for the low inflow base case using MINLP solvers, seen in table 3.11.

Table 3.11: Low Inflow MINLP Base Case Results

Solver	Obj. Val. ($)	Dual Bound ($)	Opt. Gap (%)	Time (s)
ANTIGONE	5,897.254	Global Optimum	0.00	5.504
COUENNE	5,897.254	Global Optimum	0.00	82.217

Unlike the high or medium inflow base cases, the global optimum has been proven using two different solvers to be $5,897.25 (within a computational tolerance). The swiftness in which this solution was found is most likely due to the lack of feasible solutions, and may be the one scenario where the MINLP is possibly faster than any linearization method. However, the likelihood of such a scenario happening is low and this test is completed to show that the linearization methods can perform well under different circumstances.

Table 3.12: Low Inflow SLP and Hybrid Adaptive Grid Base Case Results

Method	In. T. R.	T. R. Factor	Time (s)	Iter.	Obj. Val. ($)
SLP	20	0.95	83.719	194	5,897.254
SLP	10	0.75	7.883	33	5,897.254
Hybrid (6 pt.) AG	20	0.95	68.743	149	5,897.254
Hybrid (6 pt.) AG	10	0.75	7.546	25	5,897.254
Hybrid (11 pt.) AG	20	0.95	67.361	149	5,897.254
Hybrid (11 pt.) AG	20	0.75	8.297	27	5,896.915
Hybrid (11 pt.) AG	20	0.5	3.076	11	5,896.915
Hybrid (11 pt.) AG	10	0.95	63.060	135	5,896.915
Hybrid (11 pt.) AG	10	0.9	26.257	66	5,896.915
Hybrid (11 pt.) AG	10	0.75	8.943	25	5,896.915
Hybrid (11 pt.) AG	10	0.5	2.970	10	5,896.915

In table 3.12 it can be seen that the SLP and six point Hybrid AG methods found the global optimum within a reasonable amount of time under different user chosen parameters, but the eleven point Hybrid AG method failed to find the global optimum in most tests (finding an only slightly worse solution). Due to the consistently better performance of the six point over the eleven point Hybrid method, the latter will be dropped in favour of the former.

Table 3.13: Low Inflow Hybrid Fixed Grid Base Case Results

Method	N_F	Time (s)	Iter.	App. Obj. Val. ($)	True Obj. Val. ($)
Hybrid FG	6	0.599	2	5,823.45	5,896.92
Hybrid FG	11	0.795	2	5,884.52	5,896.92
Hybrid FG	26	1.090	2	5,896.93	5,897.25
Hybrid FG	51	2.953	2	5,897.09	5,897.25
Hybrid FG	101	6.013	2	5,897.18	5,897.25
Hybrid FG	251	36.667	2	5,897.23	5,897.25
Hybrid FG	501	82.826	2	5,896.91	5,896.92

For the low inflow case, it is curious that the approximate objective values are different for the Hybrid FG method, but have the same two true objective values (seen in table 3.13). However, this is well explained by the fact that they have the same two solutions, which is dispelling all the inflow at once through one generator either at time step 3 or 4. These time steps have the same electricity price, but since the head can build slightly more in time step 4, it yields a greater power output, which leads to a higher profit. This is also the same solution the eleven point Hybrid AG method found in most tests.

Table 3.14: Low Inflow PLA Base Case Results

Method	N_F	N_H	App. Obj. Val. ($)	True Obj. Val. ($)	Time (s)	B. Dir.
PLA	51	50	5,897.027	5,897.254	809.064	Up
PLA	51	50	5,897.027	5,897.254	303.119	Down
PLA	26	25	5,896.639	5,897.254	104.518	Up
PLA	26	25	5,896.639	5,897.254	13.495	Down

Each linearization method has been able to find the global optimum or a similar quality solution, but the PLA method takes more computational time and is more likely to find a slightly sub-optimal solution. The Hybrid FG method is reasonably quick to find its final solution, but is also inconsistent. Thus, the best methods are the SLP and the six point Hybrid AG methods both with an initial trust region of 10 thousand cubic feet per hour and a trust region factor of 0.75. This does not mean that these settings will always be the best, but for similar cases it will allow the optimizer to obtain a high quality solution while being reasonably quick. The base case is quite easy to solve with the SLP and Hybrid AG methods as it is not very complex. The daily case must be the true test for fine tuning these parameters. The cascading reservoirs add complexity that may not be well observed by the linearization methods, and it may not be well captured by the iterative processes (the SLP and Hybrid methods).

3.9 Daily Case Comparison

The daily case contains three reservoirs with five, four, and three generators, respectively, and 24 time steps, as mentioned in the introduction. One aspect that is present in the daily case that was not present in the base cases is the introduction of a nonzero minimum reservoir discharge, which is only present in the second reservoir. Linearization methods may not deal well with the minimum reservoir discharge, which requires the trade-off between spilling a small amount or turning on a generator at a time step with low electricity price.

The MINLP results are not shown for this case because the problem size is intractable and cannot solve to an acceptable optimality gap within a reasonable amount of time. The best simulation was executed by COUENNE achieving an objective value of \$961,465 with an optimality gap of 39.9% after a computational time of 100,000 seconds. This is easily proven by the linearization methods not to be the global optimum as they find a better feasible solution.

The daily case results for the SLP and Hybrid methods are shown in tables 3.15 to 3.19. As mentioned before, the daily case uses a decreasing optimality gap requirement. To show the significance of the benefit, the constant zero optimality gap requirement results for the SLP and Hybrid methods are shown in Tables 3.16 and 3.18 as a comparison. However, the Hybrid FG method has a constant zero gap requirement for all iterations for all cases.

The SLP method results seen in tables 3.15 and 3.16 show how the SLP solutions are inconsistent for the daily case. Also, the decreasing optimality gap requirement takes less time and achieves similar solution qualities to the zero optimality gap requirement.

Table 3.15: SLP Daily Case Results with Decreasing Gap

Method	In. T. R.	T. R. Factor	Time (s)	Iter.	Obj. Val. ($)
SLP	20	0.95	64.132	194	981,041.882
SLP	20	0.9	29.136	94	982,932.092
SLP	10	0.95	59.157	180	983,745.806
SLP	10	0.9	28.493	88	982,098.755
SLP	10	0.75	9.572	33	978,205.271

To show that the eleven point Hybrid AG method was dropped for valid reasons, the results are shown for the daily case in tables 3.17 and 3.18. As was concluded in the previous section, the eleven point Hybrid method is worse than the six point Hybrid method.

Unexpectedly, the eleven point Hybrid AG method generally returns a worse objective value than the six point Hybrid AG method while also taking more computational time. This is most likely due to the method approaching a different local optimum.

Table 3.16: SLP Daily Case Results with Zero Gap

Method	In. T. R.	T. R. Factor	Time (s)	Iter.	Obj. Val. ($)
SLP	20	0.95	112.571	194	983,156.355
SLP	20	0.9	79.096	94	981,122.837
SLP	10	0.95	209.131	180	982,287.834
SLP	10	0.9	35.466	88	983,364.572
SLP	10	0.75	10.554	33	977,963.953

Table 3.17: Hybrid Adaptive Grid Daily Case Results with Decreasing Gap

Method	In. T. R.	T. R. Factor	Time (s)	Iter.	Obj. Val. ($)
Hybrid (6 pt.) AG	20	0.95	132.197	149	996,608.774
Hybrid (6 pt.) AG	10	0.9	47.074	66	996,608.775
Hybrid (6 pt.) AG	10	0.75	16.459	25	996,482.945
Hybrid (11 pt.) AG	20	0.95	150.352	149	996,511.537
Hybrid (11 pt.) AG	10	0.9	54.948	66	996,511.534
Hybrid (11 pt.) AG	10	0.75	18.284	25	996,529.649

As there is no guarentee of this linearization method approaching the global optimum, one must select the combination of parameters that fares the best in these tests and assume that they will be the best for similar problems. As with the SLP method, the zero optimality gap takes longer for the Hybrid AG method while also achieving similar quality solutions.

After examining the SLP results in comparison to the Hybrid results, one can determine that the SLP method generally takes less time than the Hybrid AG method, but the extra amount of time is worth the benefit of a higher objective value when the computational times are low. However, this is not true when compared to the Hybrid

Table 3.18: Hybrid Adaptive Grid Daily Case Results with Zero Gap

Method	In. T. R.	T. R. Factor	Time (s)	Iter.	Obj. Val. ($)
Hybrid (6 pt.) AG	20	0.95	173.161	149	996,609.368
Hybrid (6 pt.) AG	10	0.9	64.614	66	996,609.372
Hybrid (6 pt.) AG	10	0.75	34.712	25	996,609.499
Hybrid (11 pt.) AG	20	0.95	178.312	149	996,511.535
Hybrid (11 pt.) AG	10	0.9	71.616	66	996,511.535
Hybrid (11 pt.) AG	10	0.75	32.298	25	996,511.538

Table 3.19: Hybrid Fixed Grid Daily Case Results

Method	N_F	Time (s)	Iter.	App. Obj. Val. ($)	True Obj. Val. ($)
Hybrid FG	6	8,464.936	25*	993,046.05	993,242.50
Hybrid FG	11	1,096.303	6	995,961.84	995,989.32
Hybrid FG	26	1,915.154	7**	996,540.75	996,549.30
Hybrid FG	51	4,035.263	10**	996,628.47	996,630.50
Hybrid FG	101	6,674.448	15	996,653.15	996,653.56
Hybrid FG	251	10,028.630*	10	996,659.07	996,659.18

*=Solution method terminated due to 25 iteration limit or 10,000 second time limit
**=Terminated based on alternating solutions

FG method results (seen in table 3.19) as the computational times are significantly larger. The solutions provided by the Hybrid FG method are slightly higher quality than the Hybrid AG method when a large number of piecewise points are used in the Hybrid FG method. However, the inconsistent terminations due to alternating solutions and computational limitations (either iteration or time limits) lead to the conclusion that the Hybrid FG method is not a good replacement for the original

MINLP.

It has been discovered that the shrinking factor of 0.75 is not large enough for the Hybrid AG method to achieve a similar quality solution for the daily case when the decreasing optimality gap method is used. Alternatively, a trust region factor of 0.75 is more efficient and achieves a similar quality solution for the Hybrid AG method when a zero optimality gap is used instead.

In conclusion, the six point Hybrid method with an inital trust region of 10 thousand cubic feet per hour and a trust region factor of 0.9 with the decreasing optimality gap is the best method amongst all methods considered.

Chapter 4

Nervousness and Uncertainty

4.1 Formulation Adaptations

The detailed version of the formulation in Chapter 3 is meant to maximize profit while meeting all constraints. However, the formulation has no concern for the stability of the solution and how it might adapt to small or large changes. In reality one must consider the amount of monitoring required to start up or shut down a generator and whether changes in parameters, particularly small ones, might cause the solution to change significantly. These considerations lead to two main adaptations to the formulation based on nervousness and uncertainty.

4.1.1 Nervousness

When used in this context, nervousness refers to the changes in a generator's discharge either from time step to adjacent time steps, especially the changes in a generator's status, or from one scenario to another. In other words, when a generator is turning on and off frequently, when it changes from large flows to low flows to closely follow the price profile, and/or when the solution changes drastically if a small change is made in the problem parameters (usually the result of a different price profile). Thus, nervousness occurs due to the optimization finding the best solution possible, but this can result in difficult implementations, particularly if the solutions changes often with the revelation of new information.

It is desired to mitigate nervousness to achieve a stable solution and there are two easy and common ways to try and complete this mission. Both methods involve adding penalties to the optimization. The first method penalizes the change in individual generator discharge from time step to time step and the second method penalizes turning on a generator. Using the first method adds an artificial goal into the optimization which may result in losing a significant amount of optimality by influencing the generators to flatten their discharge profiles. An issue with this method is that the user must decide on the severity of the penalty, which leads to subjective decisions, which, in turn, can cause a greater loss in profit than necessary. Alternatively, the second method, known as a generator start-up cost, represents a real cost of the energy required to get a generator started (which can be estimated as a monetary value). This method will encourage generators to stay on for a prolonged period of time instead of turning on and off when the price profile changes, which will stabilize the solution. Due to the compilation of reasons listed previously, the second method will be used in this work.

4.1.2 Uncertainty

One cannot experience everyday life without also experiencing uncertainty. A hydroelectric plant experiences uncertainty in many forms, whether it be unexpected rainfall, varying upstream inflows, shutdown periods, additional power demand, machine malfunctions, price flucuations, or otherwise. In order to improve the performance of an optimization in a real setting, one can identify sources of uncertainty and use past data to predict future values or scenarios. Unfortunately, one cannot predict all possible realizations of future events, which leads to the creation of a set of possible future events to use in the optimization. Including several scenarios of possible future events can allow one to find the best inputs to obtain the best outcome amongst all scenarios.

For this work, the inclusion of ten price scenarios simulates some of the possible future events. Since one cannot know all the infinite number of possible events, another scenario, that is not one of the ten considered, is used to simulate the "true" future events. These scenarios are created by taking random samples from the normal distribution with the nominal price profile being the mean and having the standard deviation to be a particular percentage of the nominal price profile (each time step being considered individually). Varying this percentage allows the creation of multiple sets of scenarios. This means that the greater the standard deviation, the higher amount of uncertainty is seen, and thus, the solution will be less stable as a result. For this work, three sets of price profile scenarios are created with standard deviations of 1%, 5%, and 10% of the nominal price profile. Since each time step is considered individually, time steps with higher prices will also have a higher absolute value of standard deviation than other time steps as a result.

To accurately consider all ten price profile scenarios in reality, decisions must be made during the current time step to improve the outcome of all or as many as possible scenarios within those considered. This is achieved with a stochastic implementation, separating decision variables into first stage and second stage decisions (or into multiple stages in the general case). First stage decisions must be made before the revelation of any uncertain information, and second stage decisions may be made after the revelation of uncertain information, meaning one may have a set of second stage decisions for each scenario considered. The revelation of uncertain information is realizing which scenario is occuring, which, to reiterate, is not known when the first stage decisions are made. In this work, the first stage decisions comprise all the generator and spill discharges within the first three time steps of the problem, with the remaining time steps making up the second stage decisions.

In reality, the true price profile would reveal itself time step by time step as each hour (or other time duration somtimes changing every fifteen minutes depending on the energy market) passes allowing one to make decisions about the best option for the current time step. However, the first part of this chapter (section 4.2) does not include the revelation of uncertain information in the form of the electricity price. It simply assumes the electricity price of the entire time horizon will follow one of the ten scenarios included and best adjusts the first stage decisions to optimize the expected value of the profit without revealing the "true" price profile in any time step. Thus, the key is to optimize the first three time steps leaving freedom to change the second stage decsions. This also means that the first stage decisions have different prices for each scenario, even though the same discharge and power is planned and executed. The last part of this chapter (section 4.3) will assume that the true price profile reveals three hours in advance and that those three hours will be part of the first stage of the stochastic implementation (meaning that all scenarios will change to have the true price profile for the first stage).

Deciding to make the first stage decisions to be the first three time steps creates more stability by forcing the first three time steps to have a distinct plan which must be followed. The common alterantive is to make the first stage decisions only the first time step, which creates more variability in the following time steps as the scenarios become different. The advantages of making the first stage three time steps are that the optimization will solve less frequently and that operators will have a stable plan for a longer duration. The three time step stochastic solution method described here will be abbreviated as Sto. 3 TS.

4.1.3 Mathematical Formulation

Since the start-up cost and uncertain electricity price profile are new to the mathematical formulation, a few adaptations are necessary to accurately include these changes. The start-up cost can be introduced rather easily into the formulation by adding the variable $COST$ (which is the summation of all start-up costs for the time horizon considered), including an additional binary variable ($SU_{i,j,t}$) signifying when a generator starts up, defining the start-up cost for each generator with the parameter $SUC_{i,j}$, and including eqs. (4.1) to (4.4). The profit is simply redefined as the revenue minus the cost and the cost is the sum of all generators' start-up costs multiplied by how many times that generator starts up. Equation (4.4) forces the binary variable $SU_{i,j,t}$ to be 1 when a generator starts up (meaning that it is on in time step t and was off in time step $t-1$) while eq. (4.3) forces the binary variable $SU_{i,j,t}$ to be 1 if the generator is on in time step 0. Otherwise the start-up cost binary variable will be free implying that it will be zero as the optimization is trying to minimize the amount of cost.

$$PROF = REV - COST \tag{4.1}$$

$$COST = \sum_{i \in I} \sum_{j \in J} SUC_{i,j} \sum_{t \in T} SU_{i,j,t} \tag{4.2}$$

$$SU_{i,j,t} = S_{i,j,t} \qquad \forall t = 0 \tag{4.3}$$

$$SU_{i,j,t} \geq S_{i,j,t} - S_{i,j,t-1} \qquad \forall t \neq 0 \tag{4.4}$$

An assumption made is that all generators are off in the time step immediately before the start of the time horizon considered. Alternatively, one may also assume that all generators are already on (or only a subset are on) but some preliminary tests have shown generators starting on in the first time step to avoid the start-up cost then remaining on for prolonged durations. Typically in practice a rolling horizon will be utilized which will take the previous time step solution into consideration which will avoid this issue because the optimization will determine the best subset of generators to be on (which may also be none or all of them). However, this work will assume each generator needs to be started in order for it to be utilized as if it were a new hydroelectric plant.

Since including the uncertainty requires multiple scenarios be present in the optimization, all variables will have to include another index, k, signifying the scenario number. One example is the generator discharges changing from $F_{i,j,t}$ to $F_{i,j,t,k}$. This addendum will also affect the linearization coefficients and linearization points as these are dependent on each individual generator and reservoir which may have different solutions for each scenario. The optimization will then try to maximize the expected profit ($EXPROF$), which is the average profit amongst all scenarios. For the general case, any number of scenarios may be used (indicated by N_K), but in this work $N_K = 10$.

$$EXPROF = \sum_{k \in K} PROF_k / N_K \tag{4.5}$$

$$k \in K = \{1, 2, ...N_K\}$$

In reality one may have knowledge that indicates that some scenarios are more likely than others to occur, which can be included with a weight on each scenario. In this work, each scenario will be given equal likelihood of occuring.

4.2 One Phase Case Study

4.2.1 Discription

As discussed previously, by varying the standard deviation, one can create three sets of random electricity prices from a normal distribution. In addition to this, three alternate solution methods are used to provide a comparison between the Sto. 3 TS method and other realistic and optimistic methods. First, each scenario is solved individually to provide a perfect information case (being the best possible solution) which will be called the individual deterministic solution method (Ind. Det.). The Ind. Det. method cannot be implemented in reality because it relies on knowing which scenario will occur and does not necessarily make a decision common to all scenarios in the current time step. This allows this method to find a better solution than possible in reality, which should make it better than all other solution methods. However, since global optimality can not be proved for the full daily case in this work, it is not a guaranteed perfect information solution, it simply allows the best solution possible given the solution methods available.

Second, all scenarios are solved simulataneously to provide one single solution that is the best amongst all scenarios which will be called the single deterministic solution method (Sin. Det.). Third, a single deterministic optimization on the average price profile of all scenarios considered is completed (Avg. P.) then this solution is implemented on each scenario. This is a common way of dealing with uncertainty in a simple manner, as it only solves one artificial scenario that averages the prices of all scenarios into one price profile and does not require solving across all scenarios simultaneously. These two methods give a sense of the optimum of the worst case possible when considering uncertainty since it considers the uncertainty without making any corrections after the revelation of uncertain information. In other words, these methods find one solution that yields the best expected objective value and accepts the results of the solution if any scenario occurs, whether they be good or bad.

The stochastic method is expected to be the best solution method that can be implemented in reality because it makes an optimal decision for the first stage and then improves the solution after incorporating uncertain information that has become known. To summarize, in the results it is expected that the Ind. Det. method provides the best solution and the Sto. 3 TS method should never be worse than the Sin. Det. or Avg. P. methods, but this may not be the case as the Hybrid solution method does not guarantee global optimality.

A comparison of solutions with and without start-up costs included for each case will provide the rationale for including start-up costs to stabilize generator statuses by examining how often generators turn on and off. For example, if generators never turn on then it is likely that the start-up costs are too high and if generators are turning on and off multiple times then it may be likely that the start up costs are too low. One must also consider the effect that including the start-up costs has on the revenue. A small loss in revenue is expected when the start-up costs are included, but too large of a loss may indicate that the generator statuses have more importance in the optimization than the revenue. A fine balance is needed to optimize revenue while stabilizing the generators' statuses, which is achieved by estimating the monetary value of energy needed to start each generator as mentioned before.

4.2.2 The 1% Case

The first case considered here has the standard deviation at 1% of the nominal price profile because it varies the price profile only slightly. Solutions should be very similar and will provide a good basis to determine the validity of the assumptions made, particularly if the generator statuses become more stable after adding the start-up costs and whether or not the stochastic implementation performs well.

Without Start-Up Costs

The revenues for the 1% case without start-up costs can be seen in table 4.1. The revenue is given for each scenario (Scen.) in addition to the expected revenue (Ex. Rev.) for each solution method. As expected, the Sto. 3 TS method obtains a better expected solution than the Sin. Det. and the Avg. P. methods but is not better than the Ind. Det. solution method.

Table 4.1: The 1% case revenues (in dollars) without start-up costs for each solution method.

Scen.	Ind. Det.	Sin. Det.	Avg. P.	Sto. 3 TS
1	993,580.08	992,597.89	993,181.03	993,510.77
2	996,388.91	995,610.02	995,702.77	996,370.78
3	991,852.69	991,342.68	991,500.76	991,753.85
4	993,844.59	993,309.52	993,655.61	993,819.27
5	992,799.60	992,329.61	992,157.08	992,718.34
6	990,647.02	989,816.41	990,141.01	990,678.72
7	989,108.02	988,552.21	988,818.14	989,027.62
8	995,701.93	995,248.48	995,279.67	995,610.11
9	996,842.13	996,424.84	996,765.77	996,778.85
10	993,318.84	992,817.70	992,794.333	993,189.99
Ex. Rev.	993,408.38	992,804.93	992,999.62	993,345.83

The generator statuses obtained in scenario 1 for each solution method can be seen in figs. 4.1 to 4.4 and the power profiles can be seen in figs. 4.5 to 4.8. It is clear that the generator statuses are unstable and although the solution methods have similarlities in generator power profiles and revenue values, there are quite a few differences. It is likely that the Hybrid method converges on one of several solutions that are practically identical in revenue but noticeably different when comparing power outputs and generator statuses. It is worthwhile bringing attention to one pattern that is seen in each solution method. That pattern is how generators alternate being on and off in consecutive time steps and it is possible that this is due to reservoirs building up head to produce additional power. One specific example of this can be seen in fig. 4.6 in time steps 10 to 14 where the second and third reservoirs alternate between producing medium and low or no power.

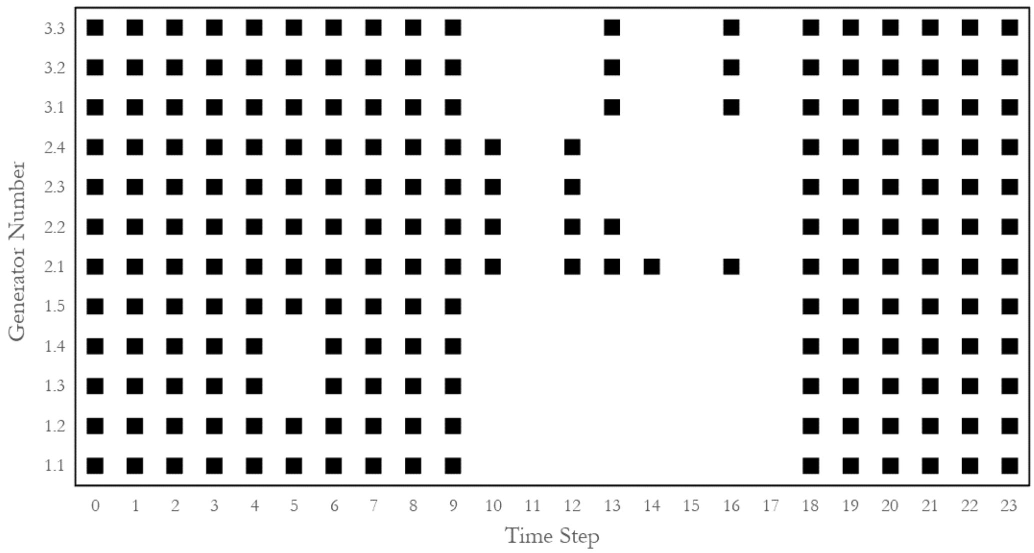

Figure 4.1: Generating unit statuses for scenario 1 from the 1% individual deterministic (Ind. Det.) case without cost.

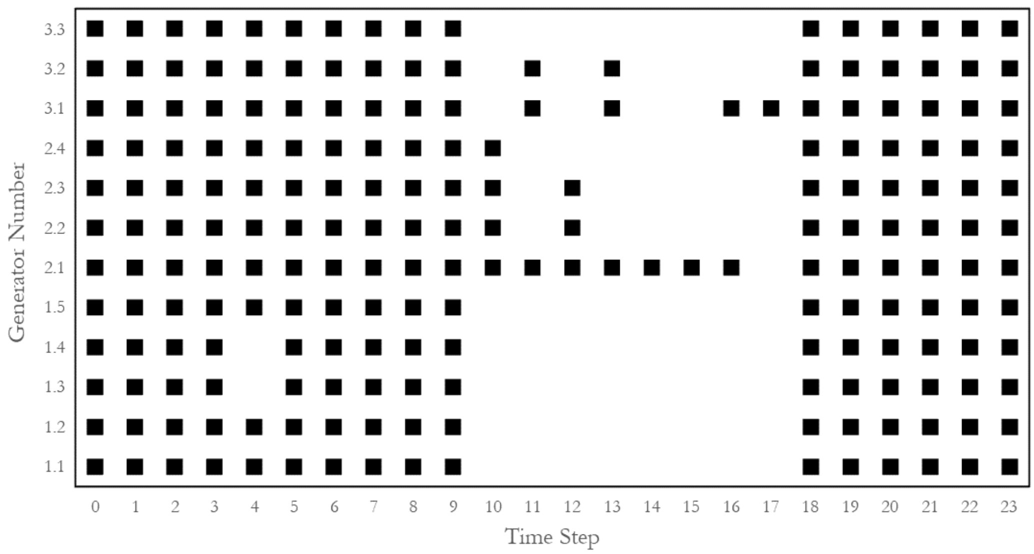

Figure 4.2: Generating unit statuses for scenario 1 from the 1% single deterministic (Sin. Det.) case without cost.

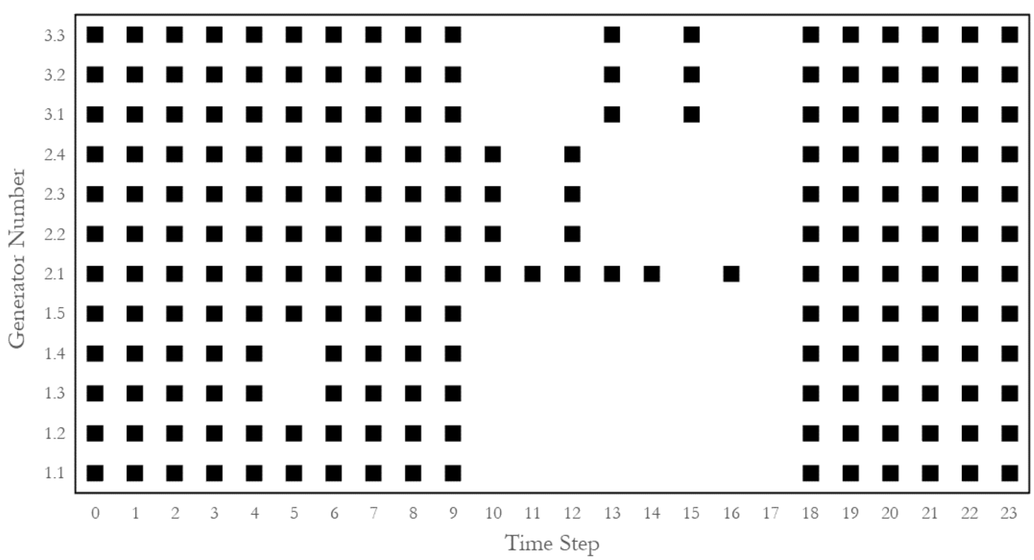

Figure 4.3: Generating unit statuses for scenario 1 from the 1% average price deterministic (Avg. P.) case without cost.

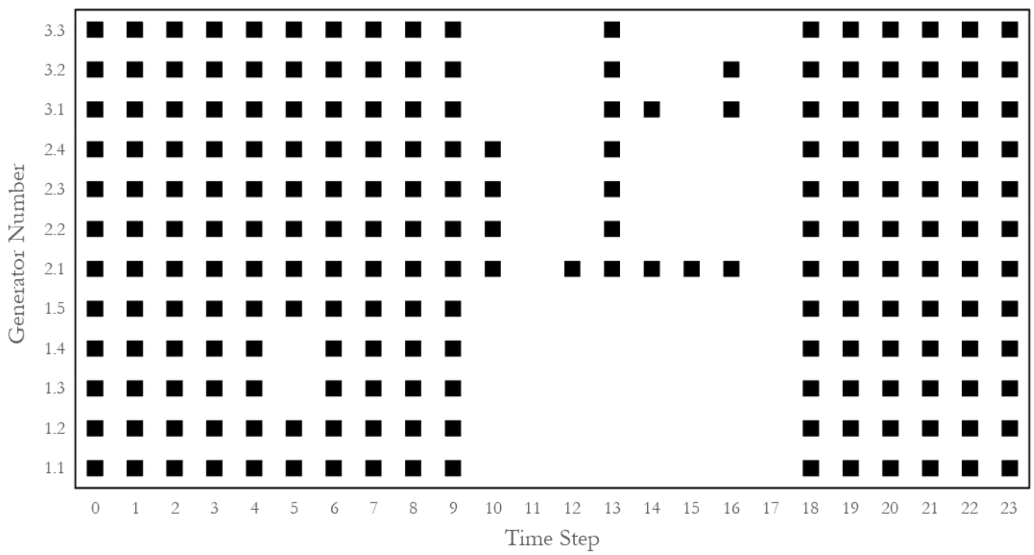

Figure 4.4: Generating unit statuses for scenario 1 from the 1% 3 time step stochastic (Sto. 3 TS) case without cost.

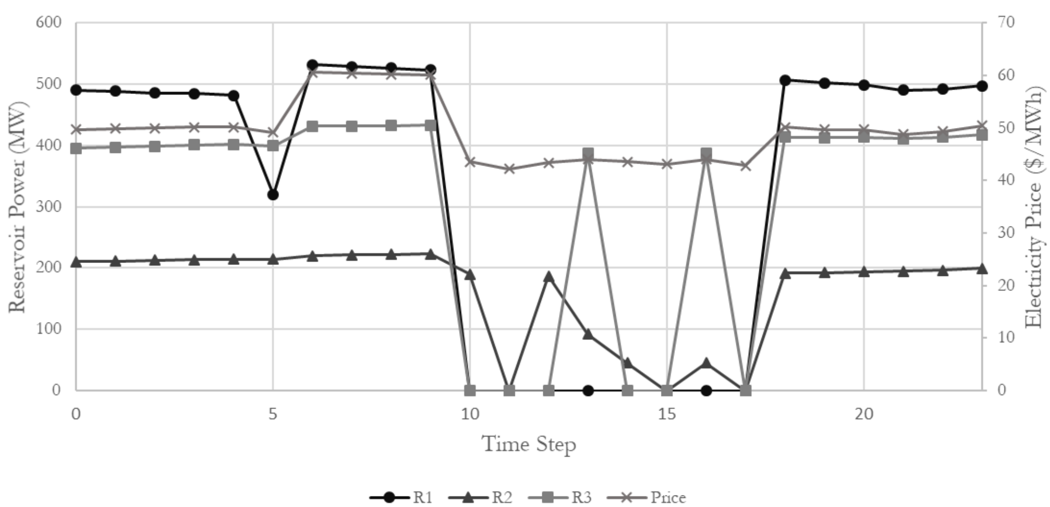

Figure 4.5: Total reservoir power outputs for scenario 1 from the 1% individual deterministic (Ind. Det.) case without cost with the electricity price profile.

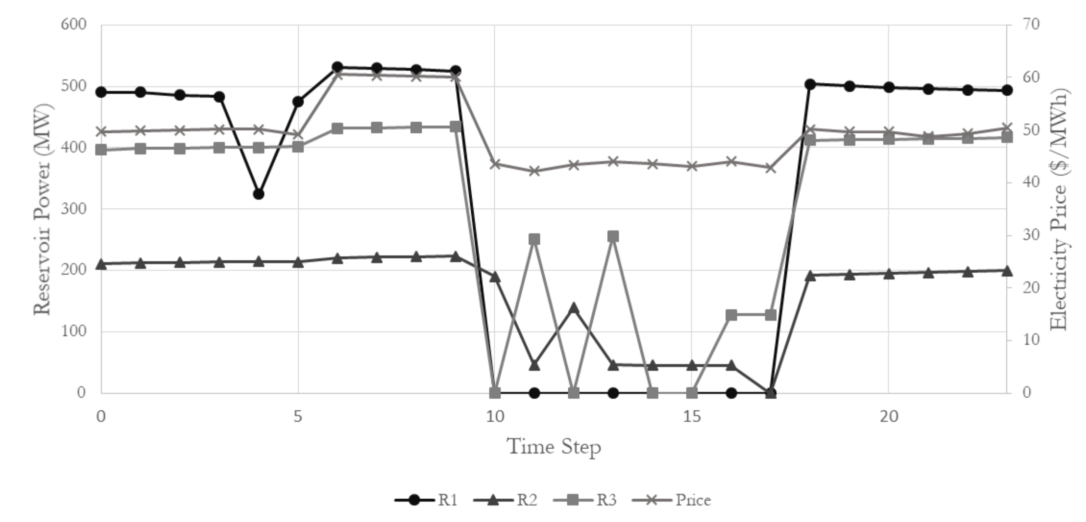

Figure 4.6: Total reservoir power outputs for scenario 1 from the 1% single deterministic (Sin. Det.) case without cost with the electricity price profile.

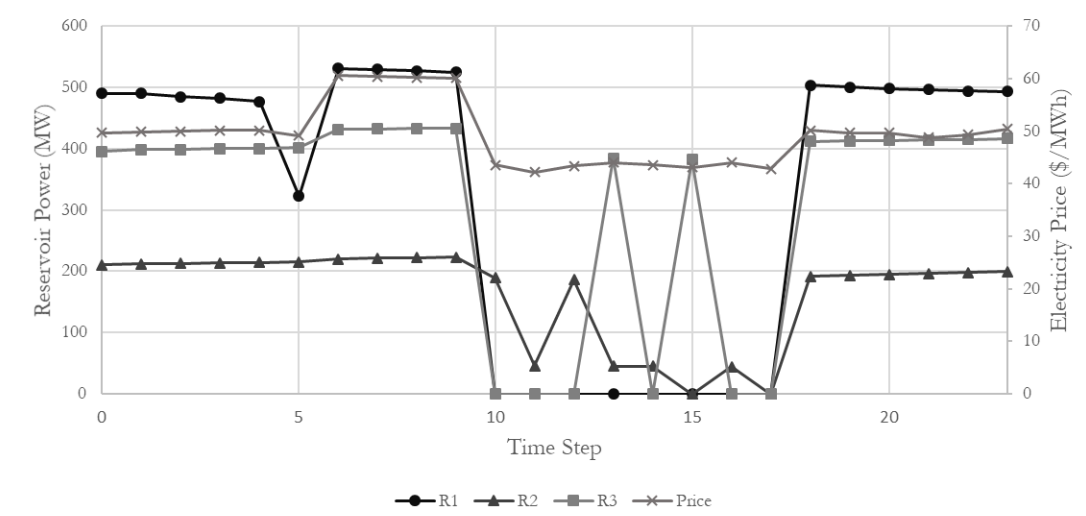

Figure 4.7: Total reservoir power outputs for scenario 1 from the 1% average price deterministic (Avg. P.) case without cost with the electricity price profile.

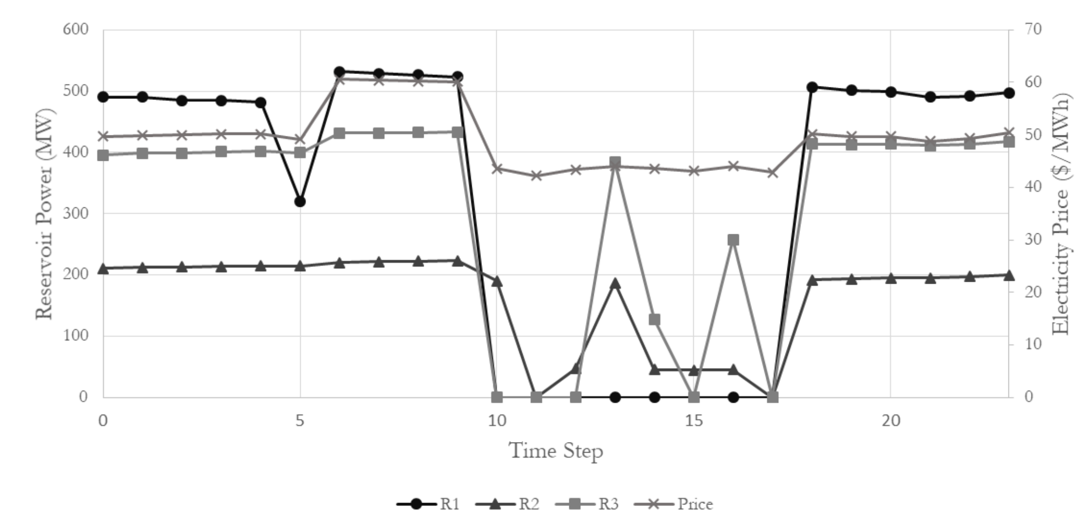

Figure 4.8: Total reservoir power outputs for scenario 1 from the 1% 3 time step stochastic (Sto. 3 TS) case without cost with the electricity price profile.

With Start-Up Costs

The inclusion of start-up costs stabilizes the solution and creates more consistency amongst the solution methods. There are a few instances in which solution methods have different generator status solutions and total start-up costs which can result in revenues that are significantly different. Costs must be the same for all ten scenarios in each of the Sin. Det. and Avg. P. methods as they must have the same solution, but the Ind. Det. and Sto. 3 TS methods may have different costs amongst their scenarios. It is likely due to the fact that the price profiles vary so little in the 1% case that each scenario has the same cost for the Ind. Det. method, but this is not required as they can have unique solutions for each scenario. As can be seen in table 4.2, the costs are different in scenarios 6 and 10 when compared to other scenarios for the Sto. 3 TS method, but the profits are similar to other methods. These scenarios are a perfect example of how turning on fewer generators (and thereby incurring less start-up costs) can lead to a loss in potential revenue and can also result in less profit overall. In other words, the hypothesis is that turning generators on and keeping them on may lead to a worse solution. This is no doubt another effect of the way the Hybrid method approaches the solution. It may assess that a particular set of generator statuses is better in an earlier iteration, which may converge on a local optimum that is worse overall than a different set of generator statuses. To reiterate, when the start-up costs are included, the profit is optimized which is the revenue minus the costs. In the results tables that include start-up costs, the revenue is displayed alongside the cost. Two examples in table 4.2 are that the profit of the Ind. Det. method in scenario 10 is \$951,508.62 and the profit of the Sto. 3 TS method in scenario 10 is \$951,009.89.

In figs. 4.9 to 4.12 we can see that the generator statuses are much more stable and one can observe that some generators stay on during low electricity prices and some others turn off. This is a good indication that the start-up costs are a good estimation

Table 4.2: The 1% case revenues (in dollars) with start-up costs (in thousands of dollars) included in parentheses for each solution method.

Scen.	Ind. Det.	Sin. Det.	Avg. P.	Sto. 3 TS
1	984,754.90 (34)	984,736.95 (34)	984,737.14 (34)	984,853.57 (34)
2	987,976.96 (34)	987,951.63 (34)	987,951.96 (34)	988,066.87 (34)
3	983,124.70 (34)	983,074.89 (34)	983,074.76 (34)	983,196.20 (34)
4	985,006.77 (34)	984,982.70 (34)	984,982.66 (34)	985,078.80 (34)
5	985,010.66 (34)	984,865.02 (34)	984,864.35 (34)	985,008.68 (34)
6	981,823.33 (34)	981,674.94 (34)	981,675.43 (34)	974,860.16 (28)
7	980,113.18 (34)	979,973.12 (34)	979,972.80 (34)	980,112.18 (34)
8	987,419.46 (34)	987,408.34 (34)	987,408.24 (34)	987,502.13 (34)
9	987,892.85 (34)	987,880.02 (34)	987,879.94 (34)	987,960.15 (34)
10	985,508.62 (34)	985,367.57 (34)	985,367.78 (34)	979,009.89 (28)
Ex. Rev.	984,863.14 (34)	984,791.52 (34)	984,791.50 (34)	983,564.86 (32.8)

and that they serve the intended purpose well. We can also observe that the fifth generator of the first reservoir stays on and the first four generators (which are the same type) turn off. This may imply that the fifth generator has a higher cost than necessary or it may simply mean that it is a larger generator with a larger start-up cost. Another thing of note is that the second reservoir has a minimum flow and we can see in the case without start-up costs there are time steps in which all generators are off. This means that the Hybrid solution method determined that it was better to spill the necessary amount rather than have one generator on to achieve this minimum flow. In the case with start-up costs, there are at least two generators on in each time step even though only one is necessary to achieve this minimum flow. Again, this may indicate that the start-up costs for the generators in the second reservoir may be too high, or it may mean that the operation of these generators is worthwhile enough during those time steps of low electricity price to avoid additional start-up costs.

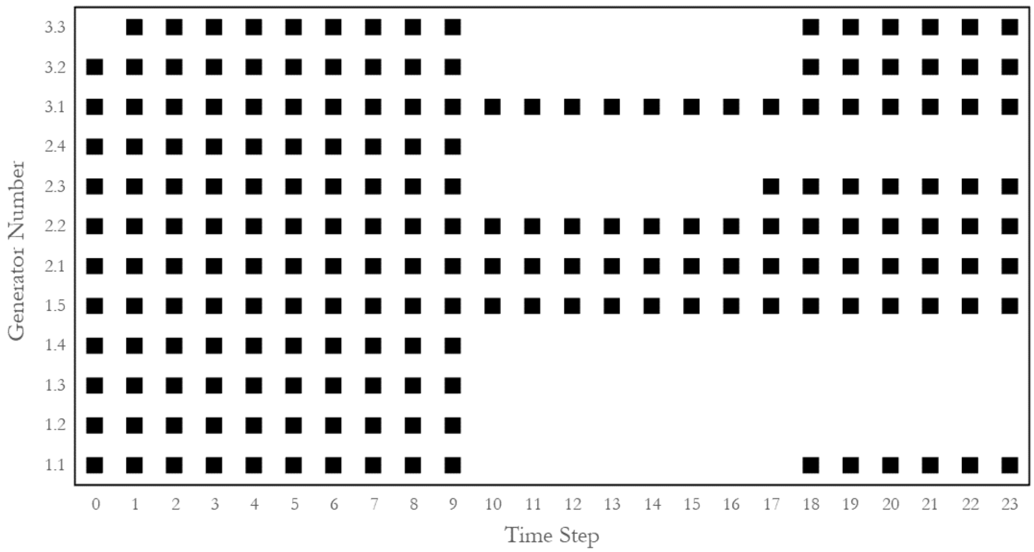

Figure 4.9: Generating unit statuses for scenario 1 from the 1% individual deterministic (Ind. Det.) case with cost.

The power profiles can be seen in figs. 4.13 to 4.16 and although there is no penalty on flow between time steps it can be observed that the power profiles follow the price profile, but are much flatter than the case without start-up costs. This means that the generator costs also assist in stabilizing generator discharges without the first artificial penalty method discussed previously. The key argument is whether or not the loss in revenue is worth obtaining these stable flat power profiles and generator statuses. For the 1% case, the loss in revenue is approximately \$9,000 on average when start-up costs are included, which is about 1% of the revenue obtained in the case without start-up costs. This loss in revenue is reasonable, but we must ensure this loss does not increase when higher uncertainty is seen.

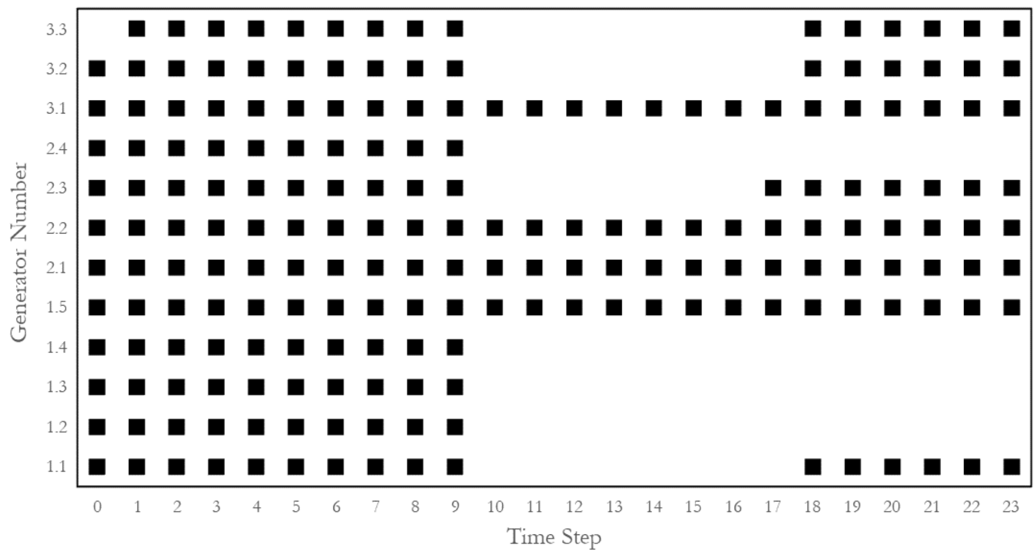

Figure 4.10: Generating unit statuses for scenario 1 from the 1% single deterministic (Sin. Det.) case with cost.

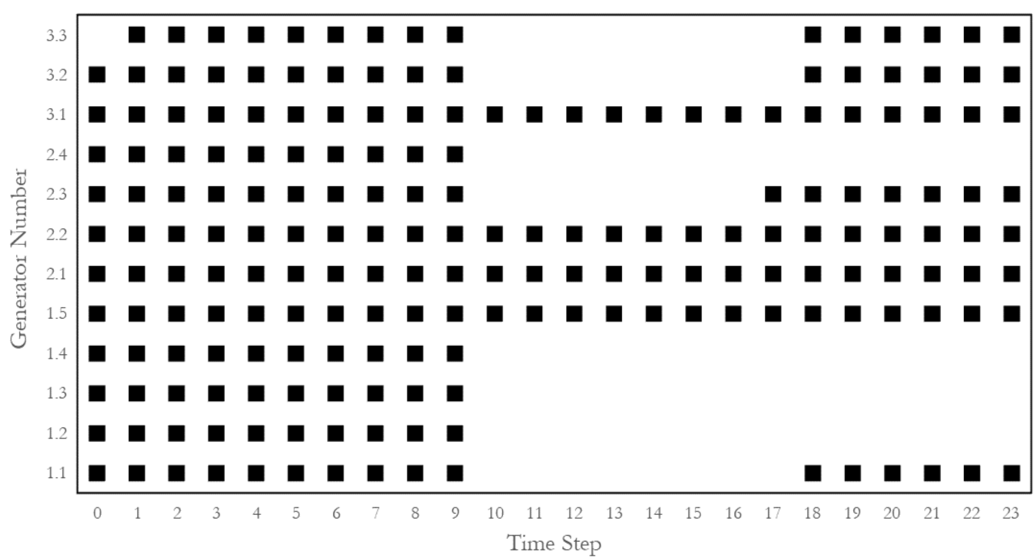

Figure 4.11: Generating unit statuses for scenario 1 from the 1% average price deterministic (Avg. P.) case with cost.

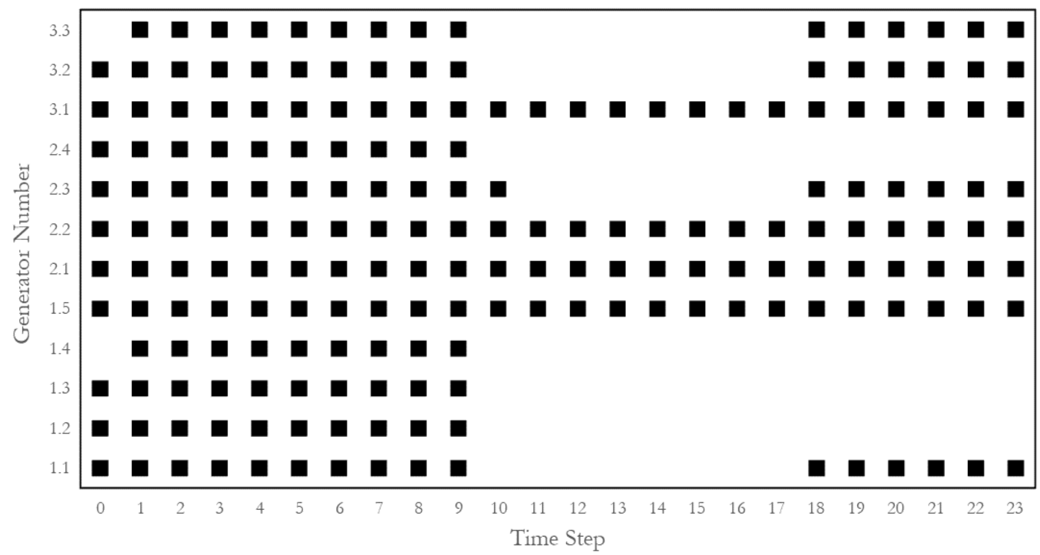

Figure 4.12: Generating unit statuses for scenario 1 from the 1% 3 time step stochastic (Sto. 3 TS) case with cost.

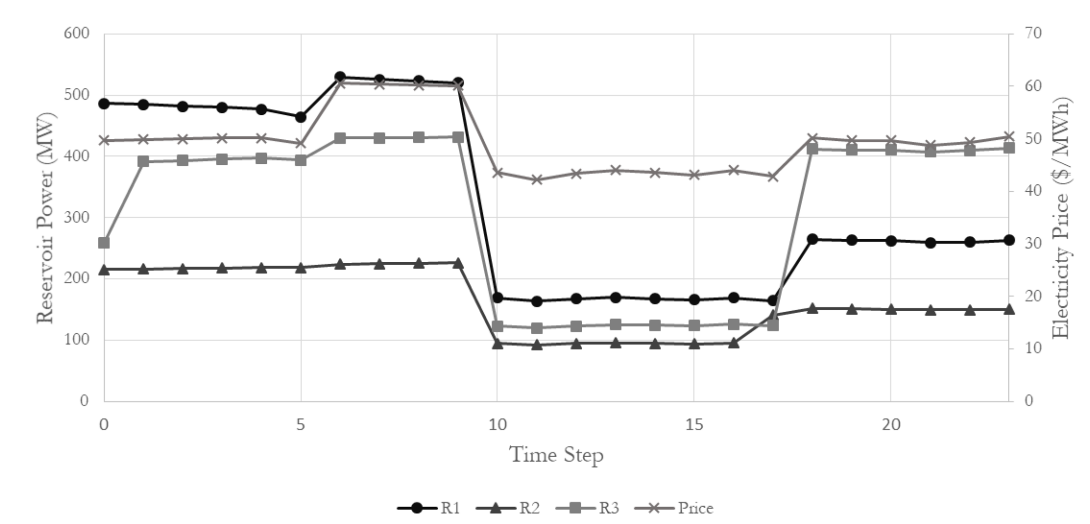

Figure 4.13: Total reservoir power outputs for scenario 1 from the 1% individual deterministic (Ind. Det.) case with cost with the electricity price profile.

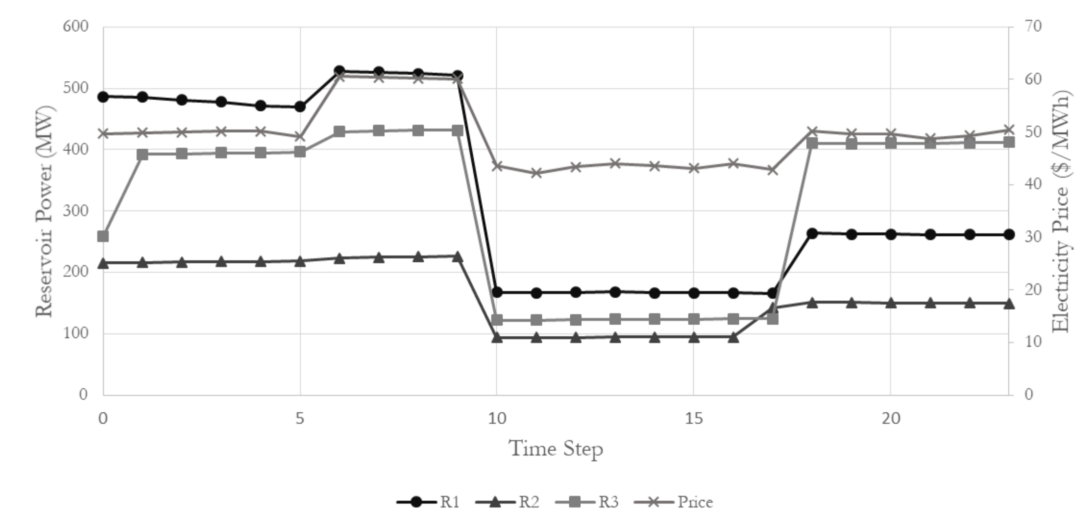

Figure 4.14: Total reservoir power outputs for scenario 1 from the 1% single deterministic (Sin. Det.) case with cost with the electricity price profile.

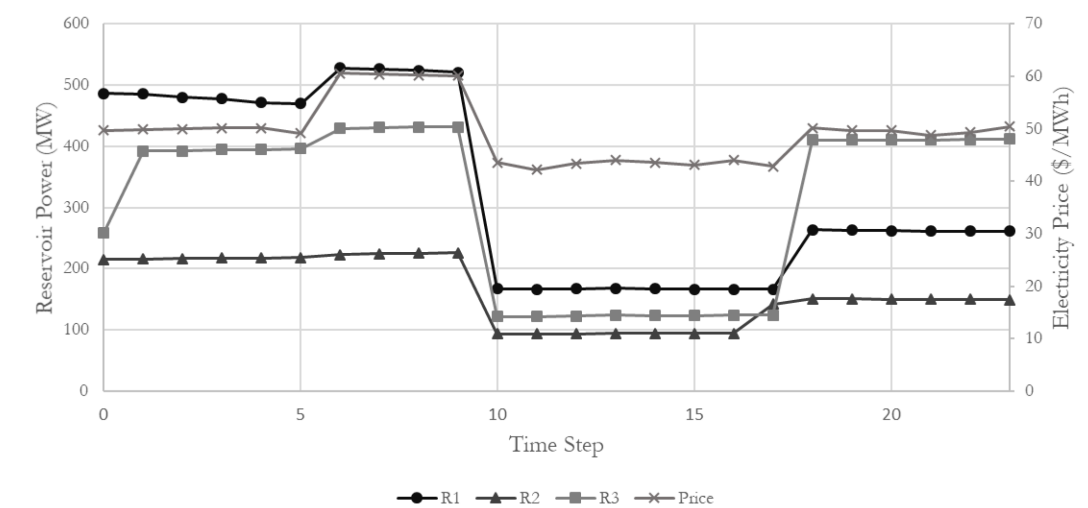

Figure 4.15: Total reservoir power outputs for scenario 1 from the 1% average deterministic (Avg. P.) case with cost with the electricity price profile.

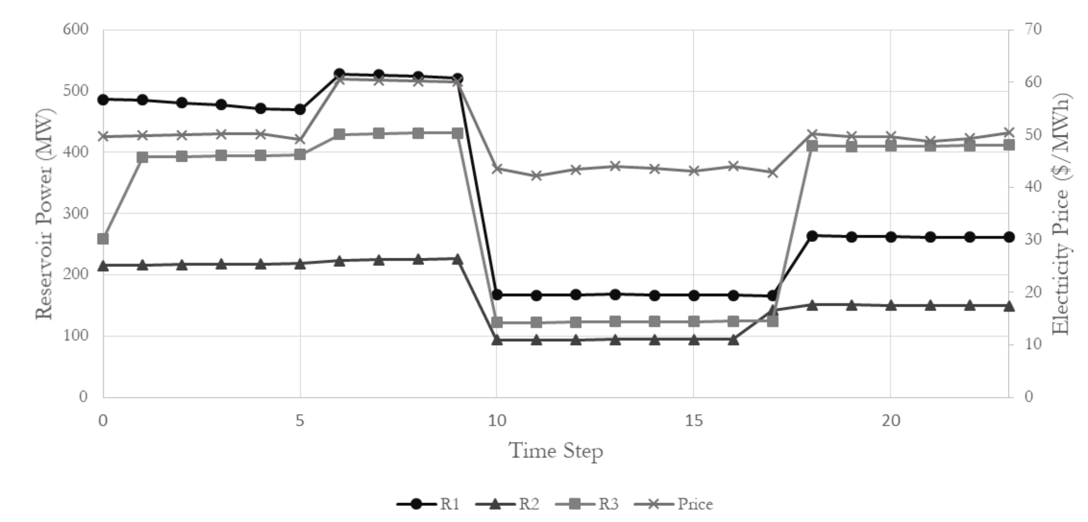

Figure 4.16: Total reservoir power outputs for scenario 1 from the 1% 3 time step stochastic (Sto. 3 TS) case with cost with the electricity price profile.

4.2.3 The 5% Case

Without Start-Up Costs

In the 5% case we start to see greater variation in revenues obtained for each scenario in table 4.3, but we can still see the expected outcome of the Sto. 3 TS method performing better than the two other realistic methods. It is also worth mentioning that the Sto. 3 TS method is very close to the Ind. Det. method, meaning that the Sto. 3 TS solution is close to being as optimal as possible even when the uncertain events are known in advance. Figures 4.17 to 4.24 show that when the start-up costs are absent, the optimization tries to follow the price profile closely, meaning that generators will turn on for time steps with even a slight increase in price and turn off after the price decreases again. This can be seen in time steps 13 and 16 when all or most generators turn on for the Ind. Det. and Sto. 3 TS methods, and then the opposite is seen in time steps 2 and 5 when generators turn off for one time step. These jumps in power production and generator statuses are undesirable and should become more stable when the start-up costs are included. As expected, the Sin. Det. and Avg. P. methods do not make the same jumps and most generators are off in the peak price time step of 13 and some turn on after the price goes down in time step 14, but this is likely due to other scenarios having higher prices in time step 14. In other words, since the Sin. Det. and Avg. P. methods must optimize for all scenarios at once, the generator power profiles do not always follow the price profile in each scenario, which can be seen here.

Table 4.3: The 5% case revenues (in dollars) without start-up costs for each solution method.

Scen.	Ind. Det.	Sin. Det.	Avg. P.	Sto. 3 TS
1	1,009,168.58	998,385.10	999,746.69	1,008,459.32
2	994,047.03	988,290.71	989,526.02	993,805.08
3	1,017,059.80	1,013,484.58	1,014,458.79	1,016,402.67
4	995,792.94	987,777.32	989,339.60	995,420.60
5	998,316.94	993,241.81	992,351.24	997,747.64
6	1,009,643.38	1,004,744.84	1,005,936.91	1,009,613.51
7	972,431.16	965,813.56	965,147.49	969,683.66
8	996,698.70	990,400.58	990,471.86	996,187.56
9	999,112.57	989,188.33	988,939.21	997,761.86
10	994,773.57	985,983.13	986,744.85	994,005.73
Ex. Rev.	998,704.47	991,731.00	992,266.27	997,908.76

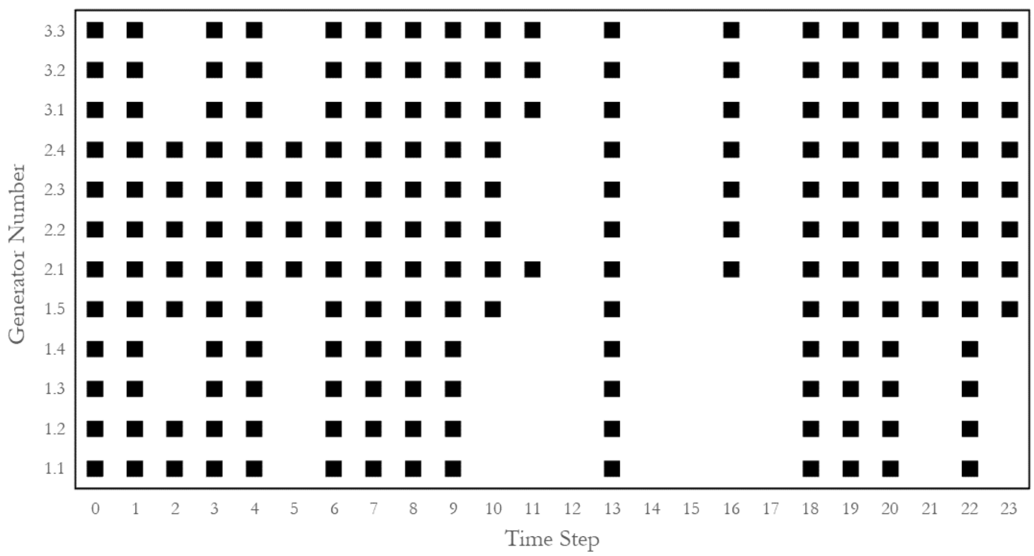

Figure 4.17: Generating unit statuses for scenario 1 from the 5% individual deterministic (Ind. Det.) case without cost.

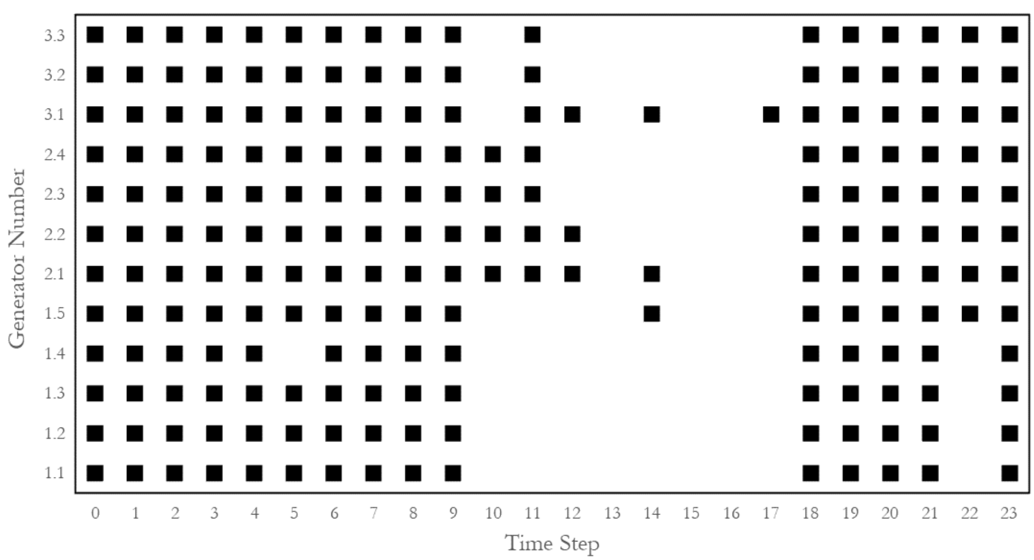

Figure 4.18: Generating unit statuses for scenario 1 from the 5% single deterministic (Sin. Det.) case without cost.

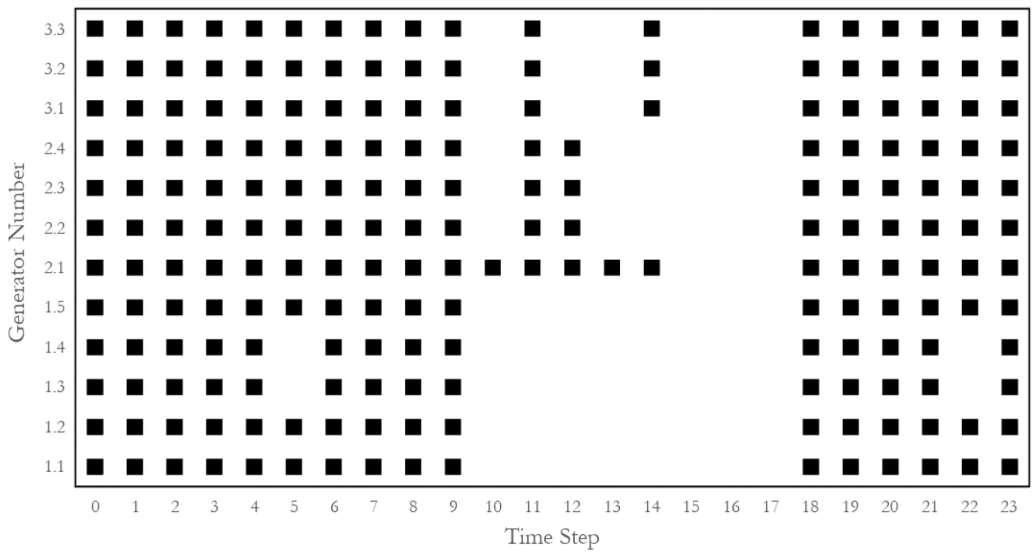

Figure 4.19: Generating unit statuses for scenario 1 from the 5% average price deterministic (Avg. P.) case without cost.

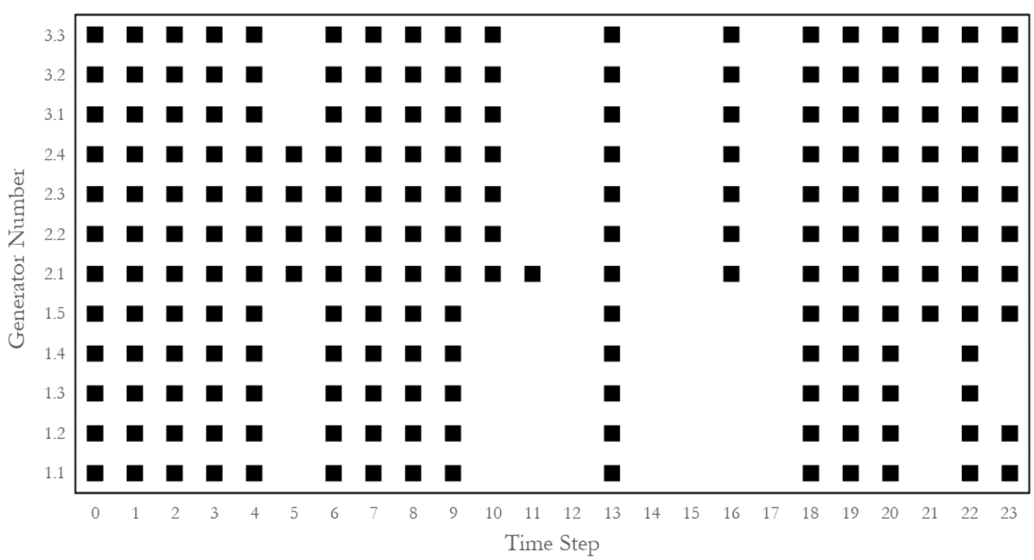

Figure 4.20: Generating unit statuses for scenario 1 from the 5% 3 time step stochastic (Sto. 3 TS) case without cost.

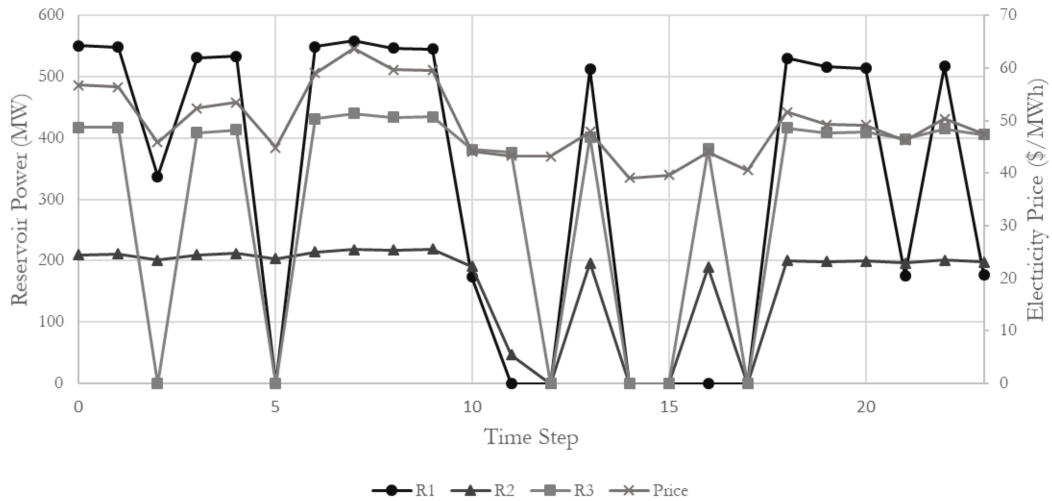

Figure 4.21: Total reservoir power outputs for scenario 1 from the 5% individual deterministic (Ind. Det.) case without cost with the electricity price profile.

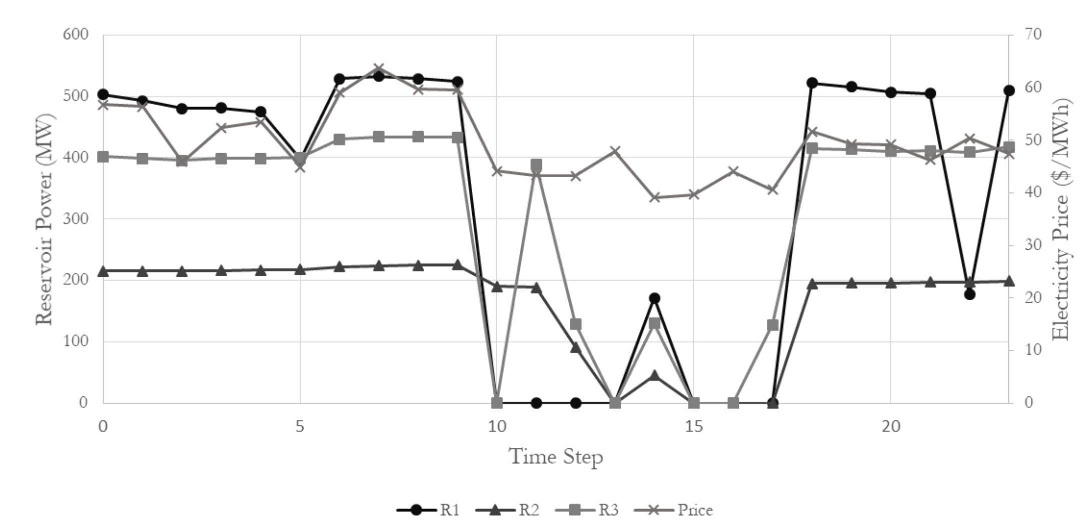

Figure 4.22: Total reservoir power outputs for scenario 1 from the 5% single deterministic (Sin. Det.) case without cost with the electricity price profile.

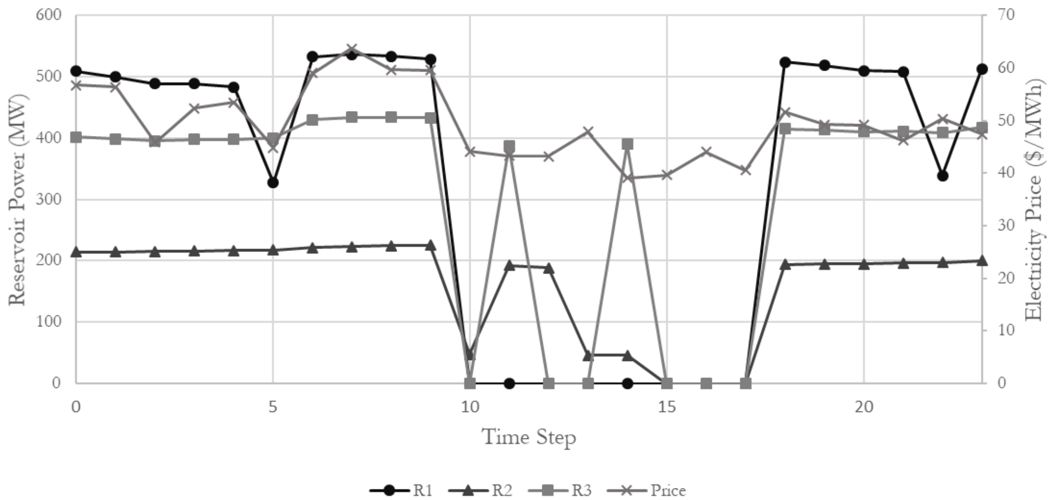

Figure 4.23: Total reservoir power outputs for scenario 1 from the 5% average deterministic (Avg. P.) case without cost with the electricity price profile.

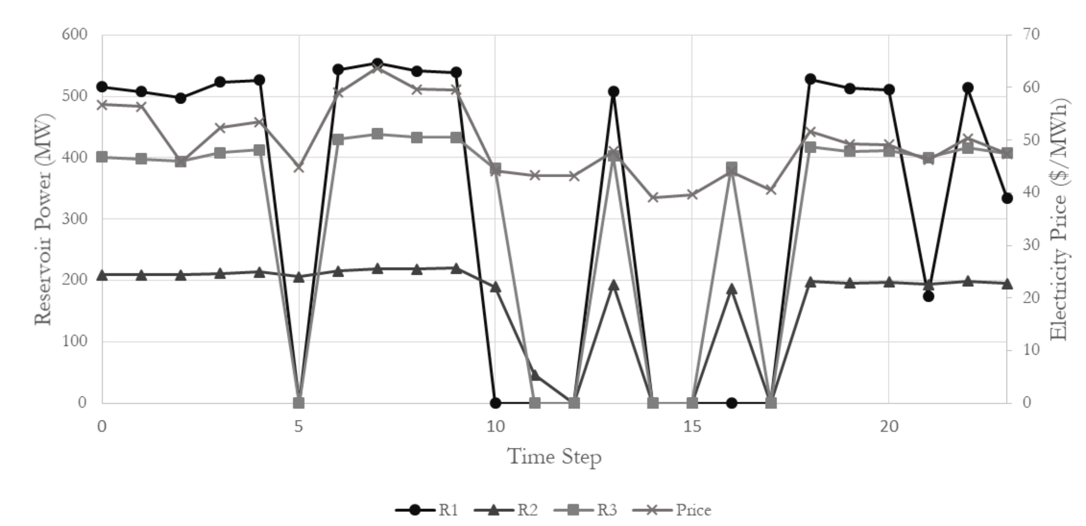

Figure 4.24: Total reservoir power outputs for scenario 1 from the 5% 3 time step stochastic (Sto. 3 TS) case without cost with the electricity price profile.

With Start-Up Costs

Table 4.4 shows the first instance of how the start-up costs can be misleading. In scenarios 7 and 8 we see that the Sto. 3 TS method achieves a higher revenue than the Ind. Det. method, but after incorporating the start-up costs one realizes that the profit is lower. This inference states that the Ind. Det. method has a better optimum according to the optimization solver, but a worse revenue which is the basis for comparison in this work. There are two scenarios (4 and 5) where the Sto. 3 TS method performs slightly worse than both the Sin. Det. and Avg. P. methods, but this can be overlooked since the expected revenues still yield the hypothesized result.

Table 4.4: The 5% case revenues (in dollars) with start-up costs (in thousands of dollars) included in parentheses for each solution method.

Scen.	Ind. Det.	Sin. Det.	Avg. P.	Sto. 3 TS
1	984,105.91 (25)	981,940.90 (25)	981,011.15 (25)	983,569.29 (25)
2	980,444.66 (34)	968,132.57 (25)	968,296.22 (25)	974,165.22 (28)
3	1,004,945.27 (34)	994,943.88 (25)	994,628.93 (25)	1,004,897.95 (34)
4	976,719.47 (25)	974,941.96 (25)	975,193.51 (25)	973,269.08 (25)
5	984,814.64 (25)	982,508.29 (25)	982,989.21 (25)	981,071.45 (25)
6	995,412.92 (34)	981,370.10 (25)	981,739.41 (25)	993,295.51 (34)
7	952,802.85 (25)	951,843.56 (25)	951,618.40 (25)	958,271.03 (32)
8	976,978.39 (25)	975,271.88 (25)	975,518.99 (25)	982,515.10 (32)
9	982,502.90 (25)	979,952.10 (25)	980,123.22 (25)	980,679.51 (25)
10	973,498.73 (28)	962,528.18 (25)	962,988.87 (25)	977,432.14 (35)
Ex. Rev.	981,222.58 (28)	975,343.34 (25)	975,410.79 (25)	980,916.63 (29.5)

As expected, we can see stable generator statuses in figs. 4.25 to 4.28 when we reintroduce the start-up costs. However, this is slightly misleading when one observes the power profiles shown in figs. 4.29 to 4.32, particularly the drops in power production for the Ind. Det. and Sto. 3 TS methods at time steps 5 and 14. This shows that even when there are no generator status changes, the generator discharges can still be reduced drastically to conserve water in their respective reservoirs while keeping the generators on. This avoids the start-up costs that would occur if the generators were to completely turn off, but instead operates at a low throughput, which is a side effect of the start-up cost method. Perhaps if the start-up cost was not present in real operation, one might consider removing the start-up costs and manually turn off the generators in these low price time steps to improve the solution.

Alternatively, this is one benefit of the other two methods (the Sin. Det. and Avg. P. methods), as they consider all scenarios simultaneously they are not influenced by a drop in price in one scenario. However, this is due to the price profiles being samples from a normal distribution which, when averaged, approach the nominal price profile. If the prices were forecasted with realistic future events, it may result that there is a price drop in all or most scenarios which would bring us back to the problem discussed in the previous paragraph.

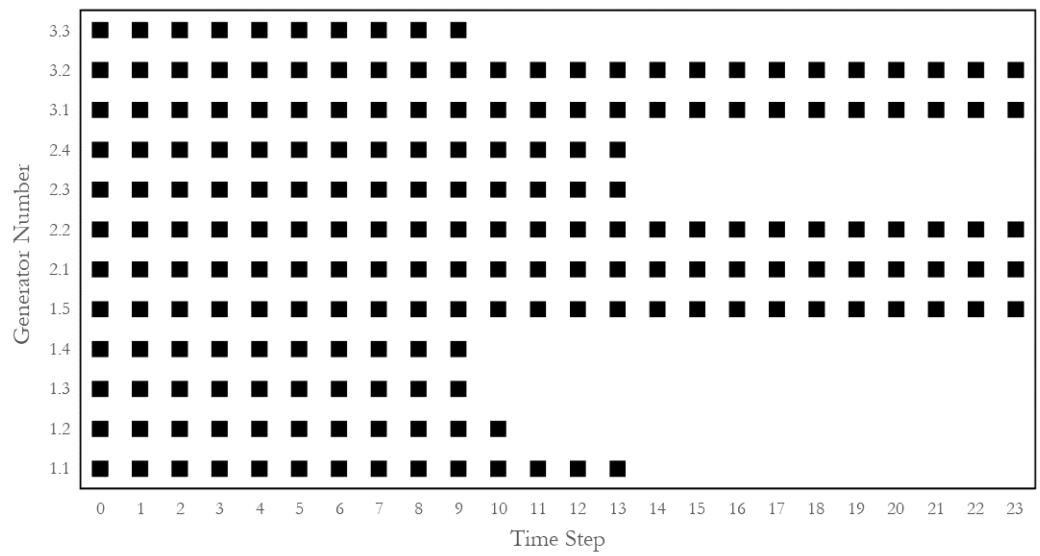

Figure 4.25: Generating unit statuses for scenario 1 from the 5% individual deterministic (Ind. Det.) case with cost.

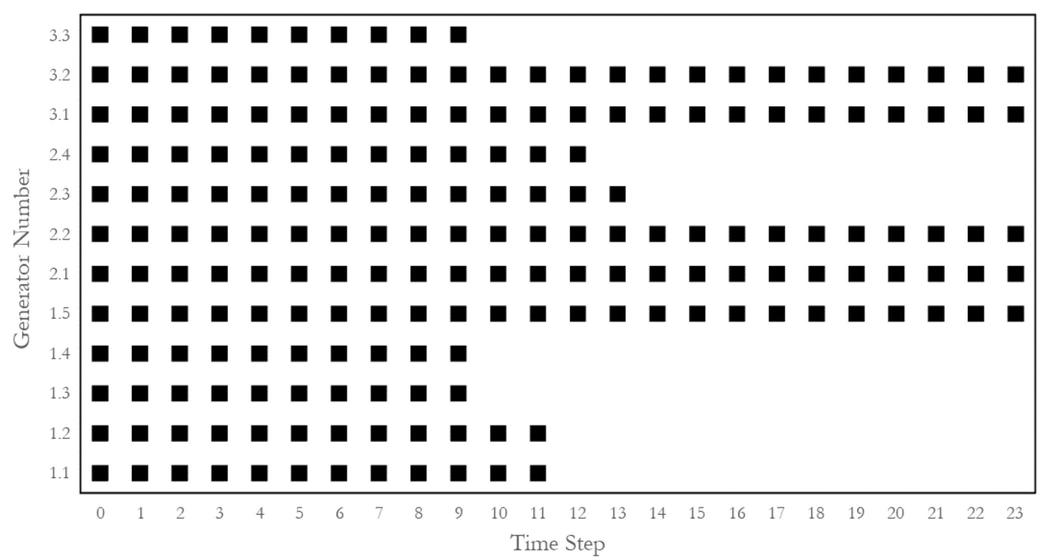

Figure 4.26: Generating unit statuses for scenario 1 from the 5% single deterministic (Sin. Det.) case with cost.

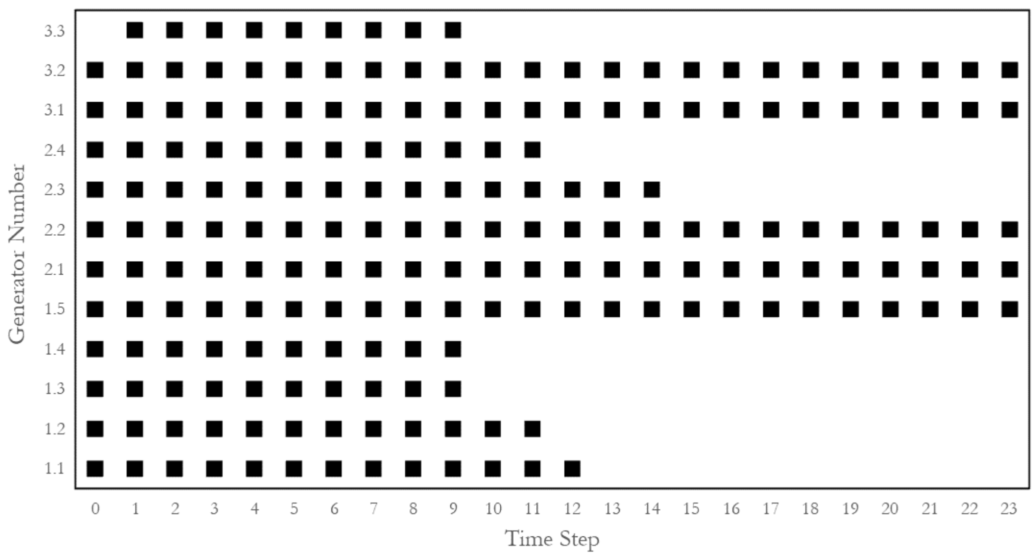

Figure 4.27: Generating unit statuses for scenario 1 from the 5% average price deterministic (Avg. P.) case with cost.

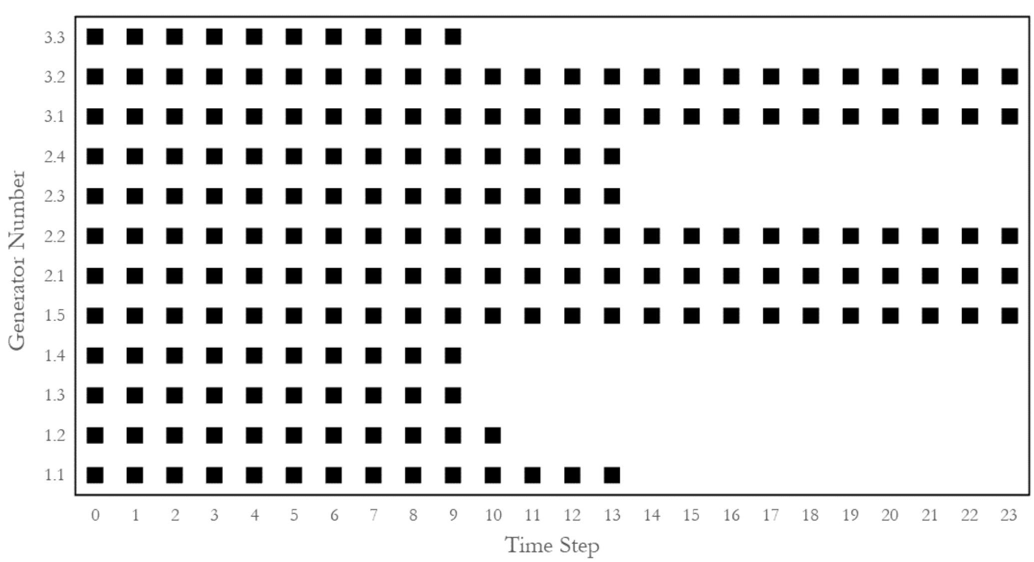

Figure 4.28: Generating unit statuses for scenario 1 from the 5% 3 time step stochastic (Sto. 3 TS) case with cost.

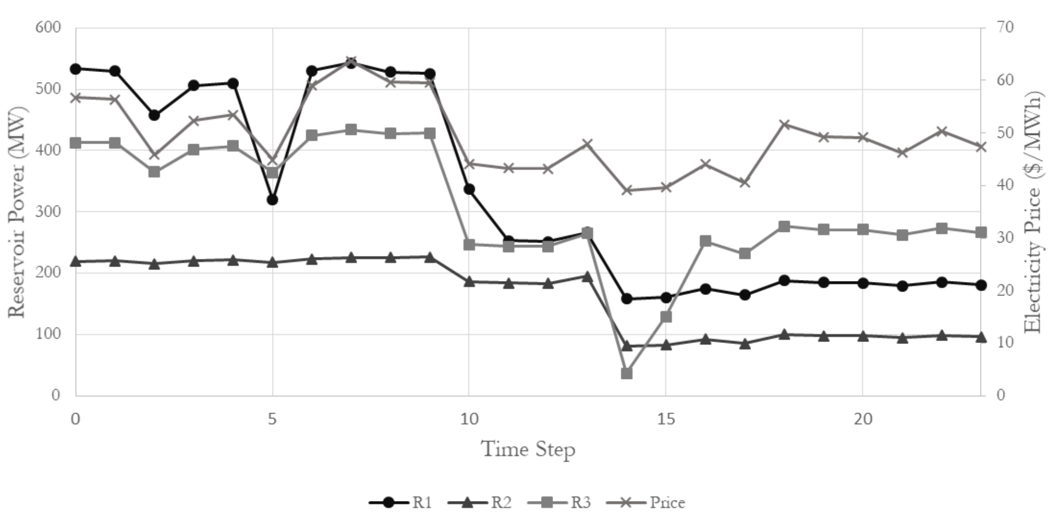

Figure 4.29: Total reservoir power outputs for scenario 1 from the 5% individual deterministic (Ind. Det.) case with cost with the electricity price profile.

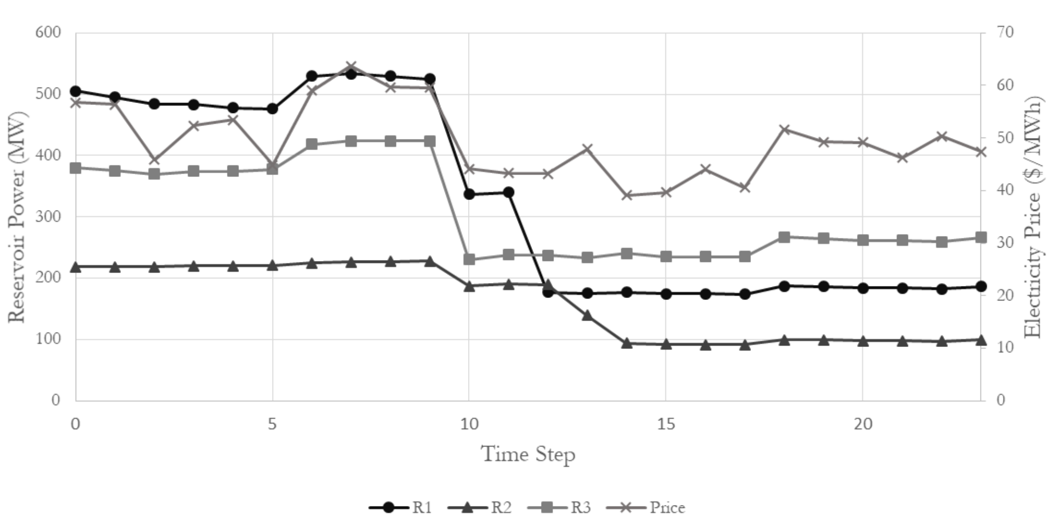

Figure 4.30: Total reservoir power outputs for scenario 1 from the 5% single deterministic (Sin. Det.) case with cost with the electricity price profile.

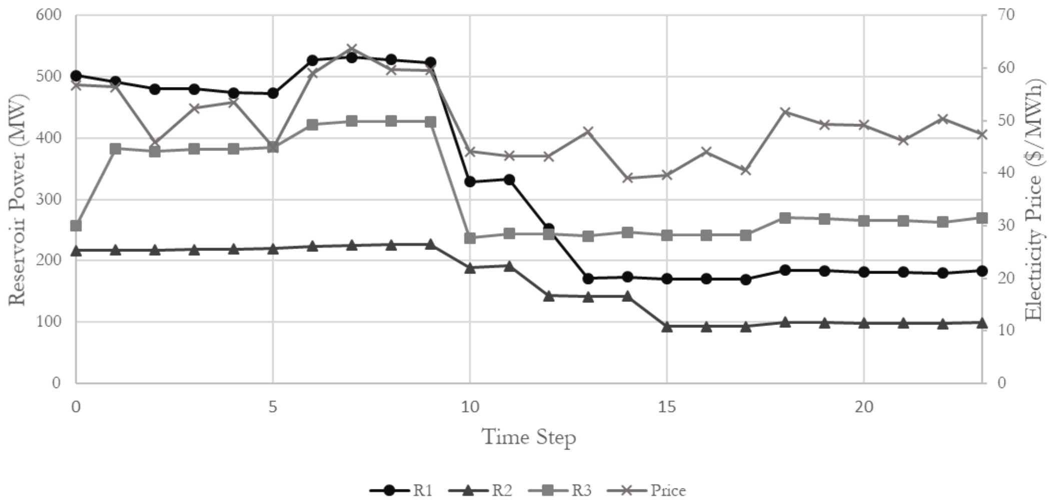

Figure 4.31: Total reservoir power outputs for scenario 1 from the 5% average price deterministic (Avg. P.) case with cost with the electricity price profile.

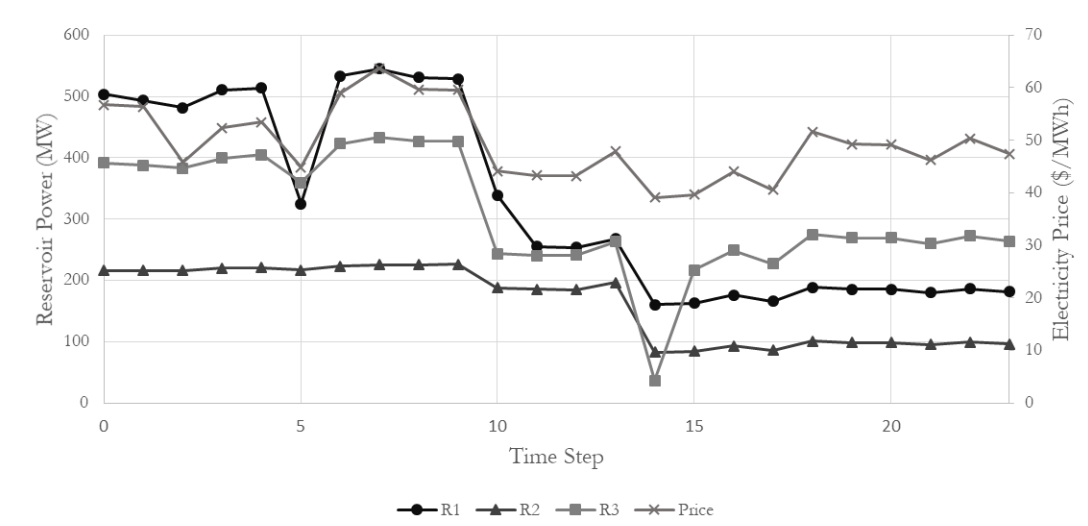

Figure 4.32: Total reservoir power outputs for scenario 1 from the 5% 3 time step stochastic (Sto. 3 TS) case with cost with the electricity price profile.

4.2.4 The 10% Case

Without Start-Up Costs

As the scenarios vary more greatly from the nominal price profile the optimal revenues also vary in value. In the 10% case we can clearly identify the segregation in revenues between the solution methods in table 4.5. The Sto. 3 TS method performs significantly better than the Sin. Det. and Avg. P. methods as expected, but still remains fairly close behind to the Ind. Det. method.

Table 4.5: The 10% case revenues (in dollars) without start-up costs for each solution method.

Scen.	Ind. Det.	Sin. Det.	Avg. P.	Sto. 3 TS
1	989,685.51	972,356.30	971,453.39	978,854.23
2	992,926.15	982,028.69	981,919.16	990,948.24
3	986,187.12	957,010.72	957,346.50	983,829.53
4	1,022,263.83	1,015,627.63	1,015,972.39	1,019,464.80
5	1,008,572.53	989,445.00	989,082.24	1,006,602.71
6	989,018.04	971,103.01	969,941.79	983,387.77
7	1,025,666.99	1,008,103.12	1,009,125.80	1,023,458.36
8	1,055,769.56	1,035,168.03	1,035,266.11	1,052,947.71
9	1,037,417.11	1,028,549.45	1,028,594.64	1,035,136.49
10	1,021,427.25	999,182.58	999,862.75	1,016,889.01
Ex. Rev.	1,012,893.41	995,857.45	995,856.48	1,009,151.88

We still see unstable generator statuses in figs. 4.33 to 4.36 and significant spikes in power production in figs. 4.37 to 4.40, but the nervousness seen may also be mitigated if the price profiles gradually increased and decreased instead of randomly changing from time step to time step. Another consideration that could be worthwhile would be to include ramping limitations that force the changes in a generator's discharge to be under some absolute value that is chosen by the user or decided by some realistic constraint. However, this will likely lead to a significant loss in revenue as it is often quite beneficial to have a large rise or fall in generator discharges as the price profile enters or leaves the peak pricing time step(s).

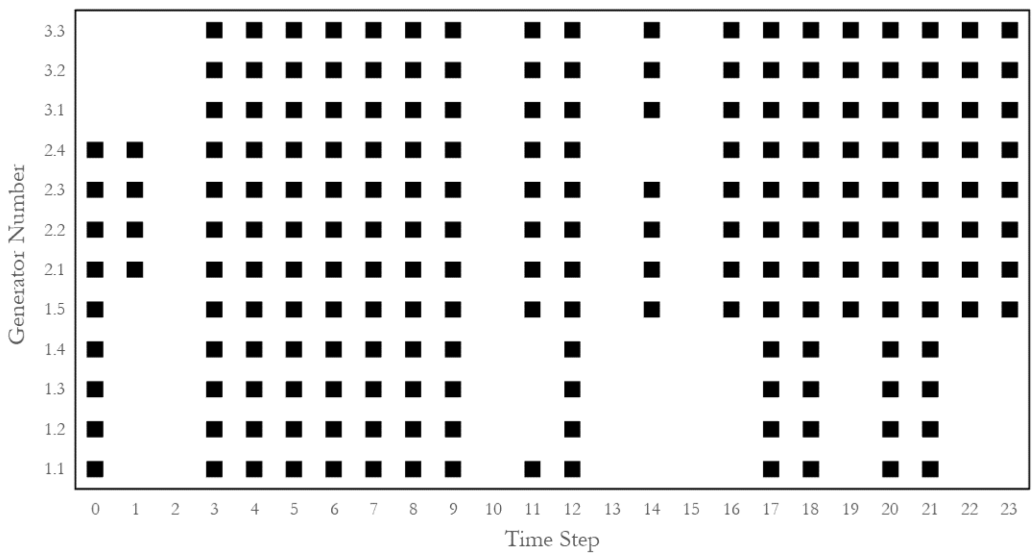

Figure 4.33: Generating unit statuses for scenario 1 from the 10% individual deterministic (Ind. Det.) case without cost.

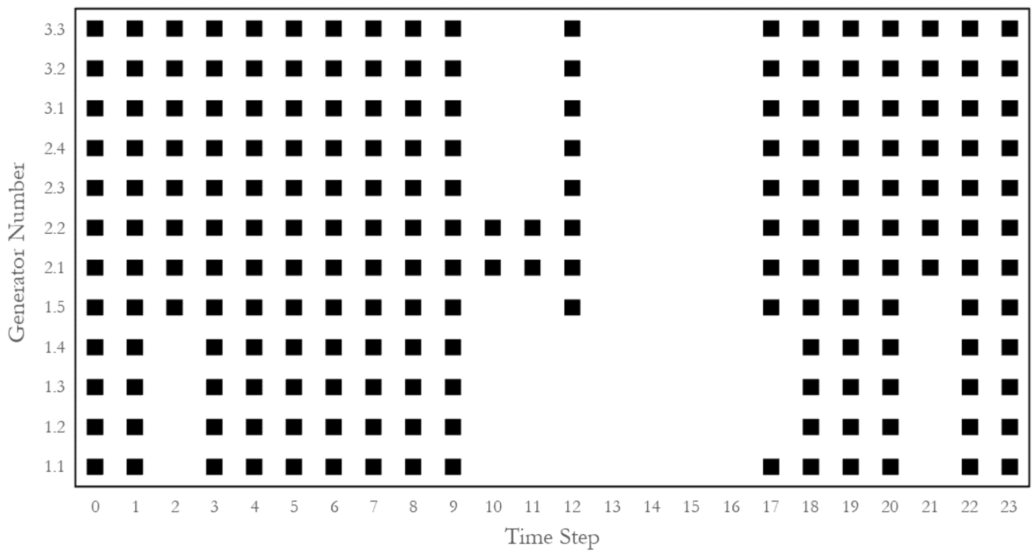

Figure 4.34: Generating unit statuses for scenario 1 from the 10% single deterministic (Sin. Det.) case without cost.

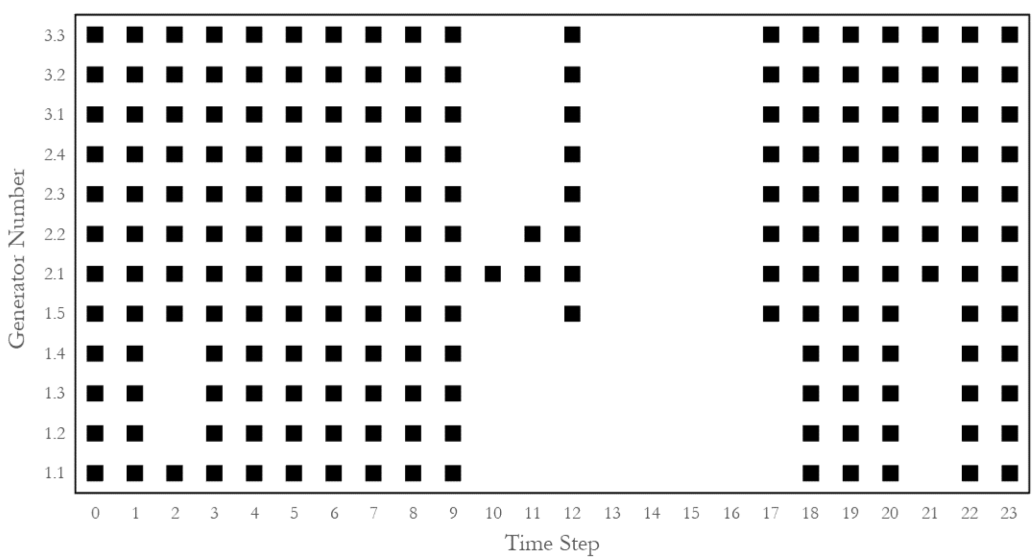

Figure 4.35: Generating unit statuses for scenario 1 from the 10% average price deterministic (Avg. P.) case without cost.

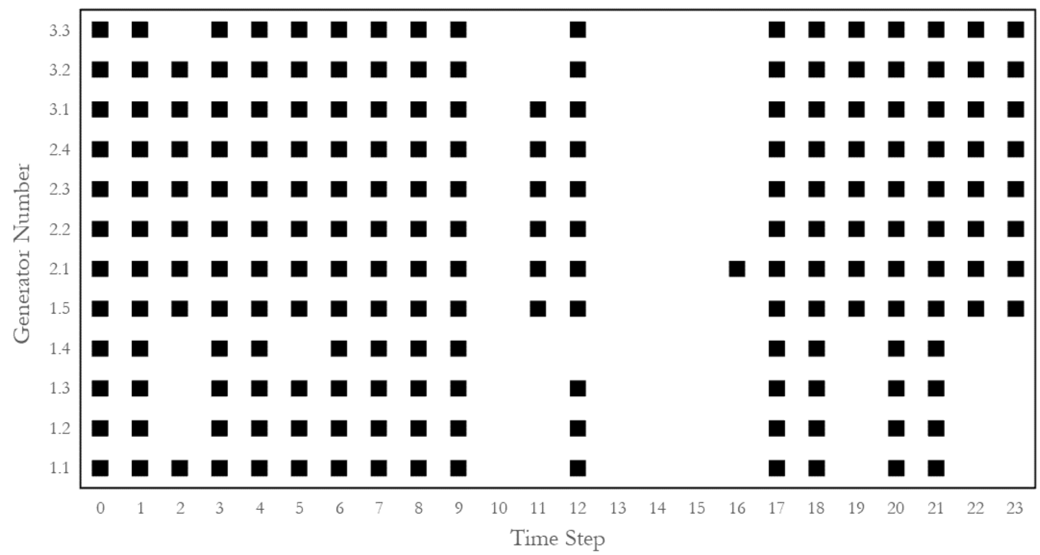

Figure 4.36: Generating unit statuses for scenario 1 from the 10% 3 time step stochastic (Sto. 3 TS) case without cost.

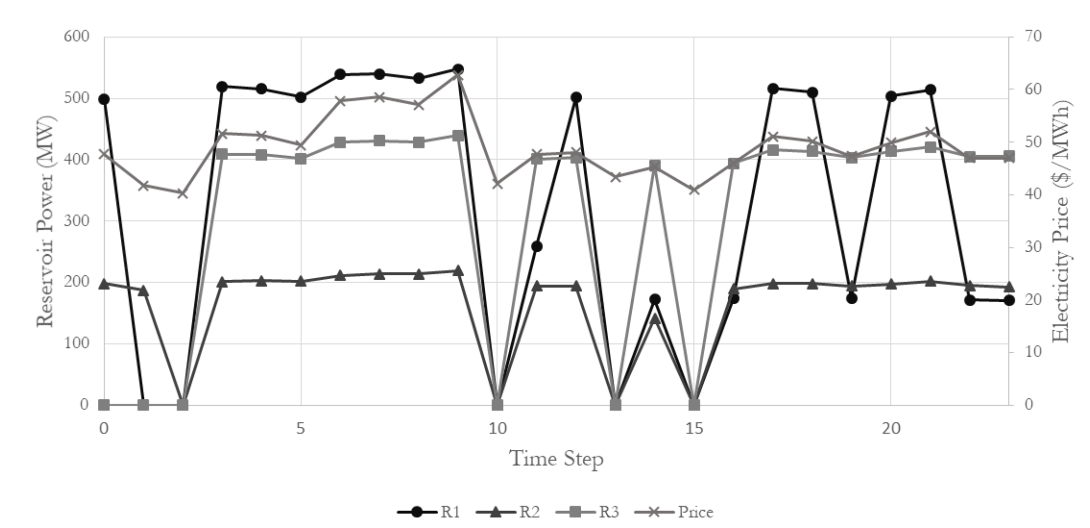

Figure 4.37: Total reservoir power outputs for scenario 1 from the 10% individual deterministic (Ind. Det.) case without cost with the electricity price profile.

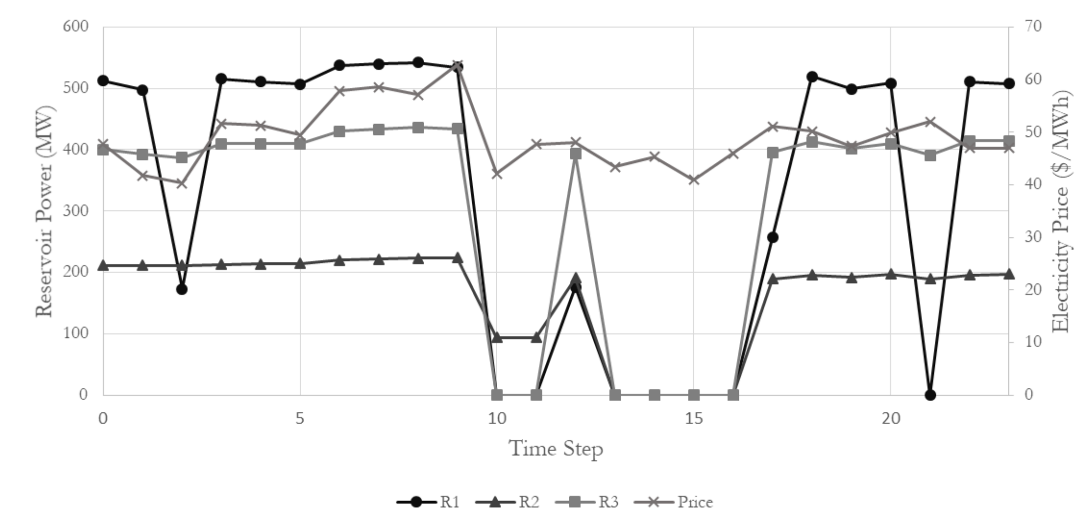

Figure 4.38: Total reservoir power outputs for scenario 1 from the 10% single deterministic (Sin. Det.) case without cost with the electricity price profile.

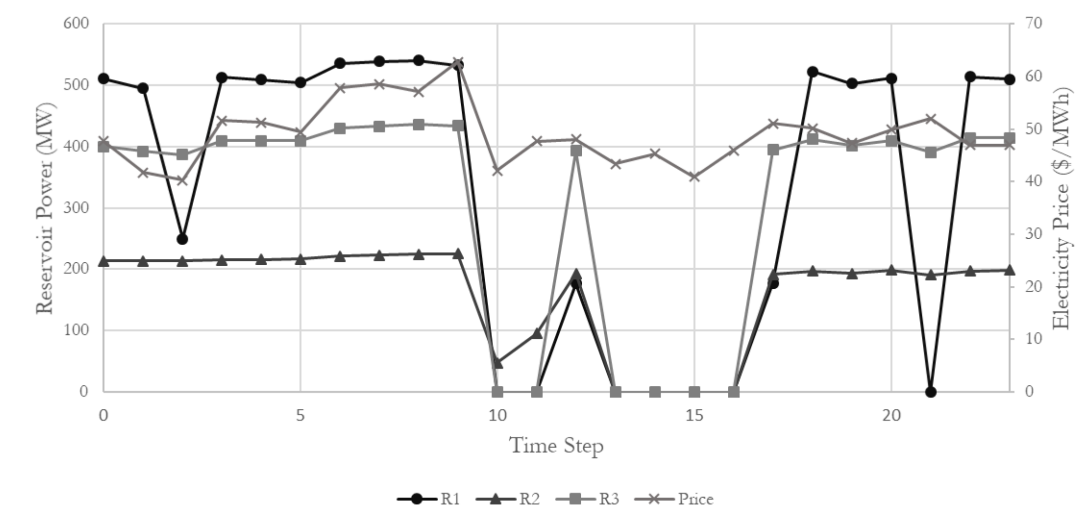

Figure 4.39: Total reservoir power outputs for scenario 1 from the 10% average price deterministic (Avg. P.) case without cost with the electricity price profile.

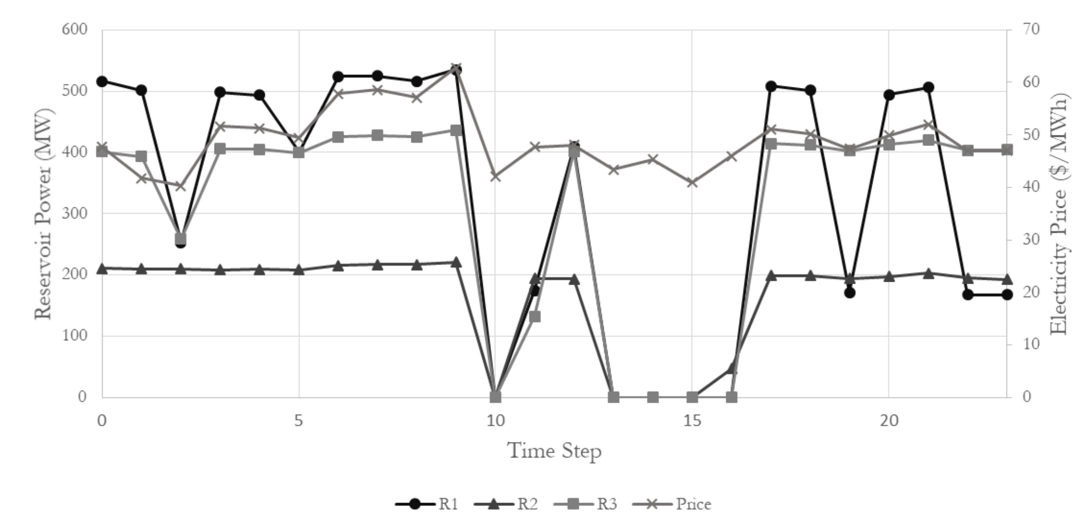

Figure 4.40: Total reservoir power outputs for scenario 1 from the 10% 3 time step stochastic (Sto. 3 TS) case without cost with the electricity price profile.

With Start-Up Costs

Once again it can be seen that revenues in some solution methods are higher than others but the profits are the opposite. One may also see in table 4.6 the counterintuitive result of the Sto. 3 TS method achieving better revenues than the Ind. Det. method in scenarios 2, 3, 4, and 7 and better profits in scenarios 8 and 9. This is a good indication that the Hybrid method may need a better initialization point. The only reason the Sto. 3 TS method should perform better than the Ind. Det. method is that the Ind. Det. method converges on a local optimum instead of the global optimum. It is also highly likely that the generator start-up costs strongly affect the convergence in earlier iterations which leads to a suboptimal solution since the optimization problem is so highly non-linear with binary variables. On the other hand, since the Sto. 3 TS method has a stable start in the first three time steps it assists in finding a better solution by managing its own convergence to find the best first stage decisions (leaving the second stage decisions as free for each scenario). This means that the major focus is on the first three time steps as they must be common to all scenarios, which implies that the first iterations do not get locked into a suboptimal set of generator statuses.

The generator statuses can be seen in figs. 4.41 to 4.44 and when the Ind. Det. method is examined one can see that most generators are off in the first three time steps which contradicts the solution of the other three methods. This has already been discussed as likely being caused by low prices in just scenario 1 which would not be enough to cause the other methods to turn off the generators in these time steps as the solution is common to all scenarios. In other words it is only beneficial to turn off the generators in this individual scenario while most or all other scenarios it would be detrimental.

In figs. 4.45 to 4.48 we see the solutions are stabilized by introducing the start-up

Table 4.6: The 10% case revenues (in dollars) with start-up costs (in thousands of dollars) included in parentheses for each solution method.

Scen.	Ind. Det.	Sin. Det.	Avg. P.	Sto. 3 TS
1	975,866.41 (28)	957,735.03 (25)	960,198.76 (25)	960,451.02 (28)
2	962,269.41 (32)	944,298.20 (25)	944,519.24 (25)	966,549.38 (38)
3	960,945.18 (31)	938,202.04 (25)	939,417.00 (25)	961,891.66 (25)
4	1,004,399.04 (28)	994,376.32 (25)	995,824.89 (25)	1,004,860.19 (25)
5	986,830.76 (25)	982,024.68 (25)	981,217.54 (25)	984,089.70 (25)
6	972,617.66 (25)	964,479.69 (25)	966,057.90 (25)	967,460.70 (25)
7	995,744.54 (25)	991,452.00 (25)	990,064.45 (25)	997,234.84 (25)
8	1,034,953.67 (40)	1,008,941.56 (25)	1,008,801.76 (25)	1,034,628.80 (25)
9	1,025,666.46 (38)	1,005,856.25 (25)	1,006,477.81 (25)	1,021,617.06 (25)
10	996,851.99 (25)	991,677.41 (25)	991,756.46 (25)	993,436.11 (25)
Ex. Rev.	991,614.51 (29.7)	977,904.32 (25)	978,433.58 (25)	984,321.95 (26.3)

costs as before, but as the prices become more erratic the power profiles of the Sto. 3 TS and Ind. Det. methods also include large rises and falls to follow the crests and troughs of the price profile respectively.

Overall, the start-up costs achieved the intended purpose of stabilizing the generator statuses and also assisted greatly in the stabilization of the power production profiles. This was also achieved while not sacrificing too much revenue, otherwise it would be counter-productive. From the results it is likely that the generator start-up costs are higher than desired as many generators stay on during the entire time horizon. However, apart from reestimating the costs or improving the generators this may not be accurate to lower as it represents a real cost. And although global optimality cannot be proven, it was still shown that the stochastic method performed well in

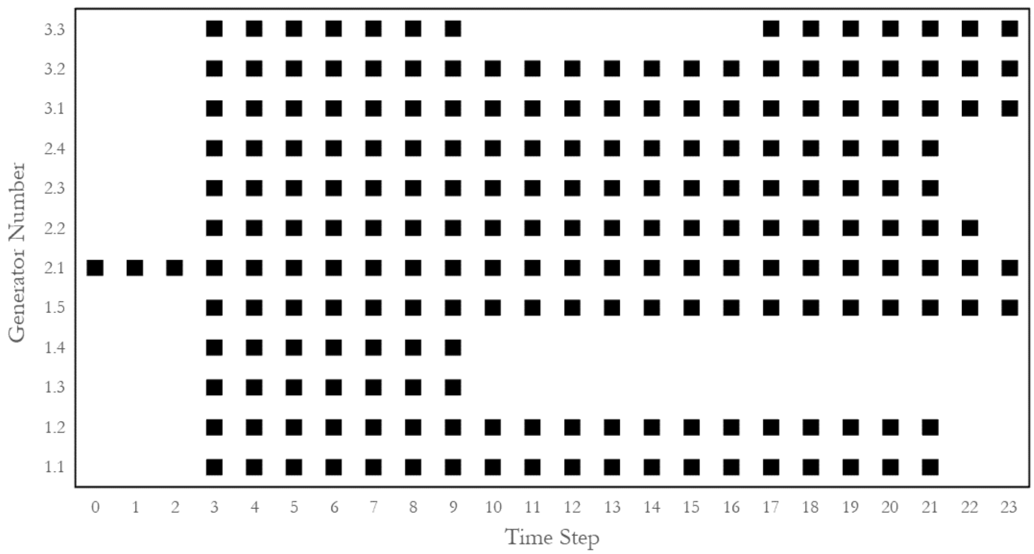

Figure 4.41: Generating unit statuses for scenario 1 from the 10% individual deterministic (Ind. Det.) case with cost.

most cases as expected, and only slightly worse in all other cases. The real test will be how well it performs as the passing of time is simulated in the next section.

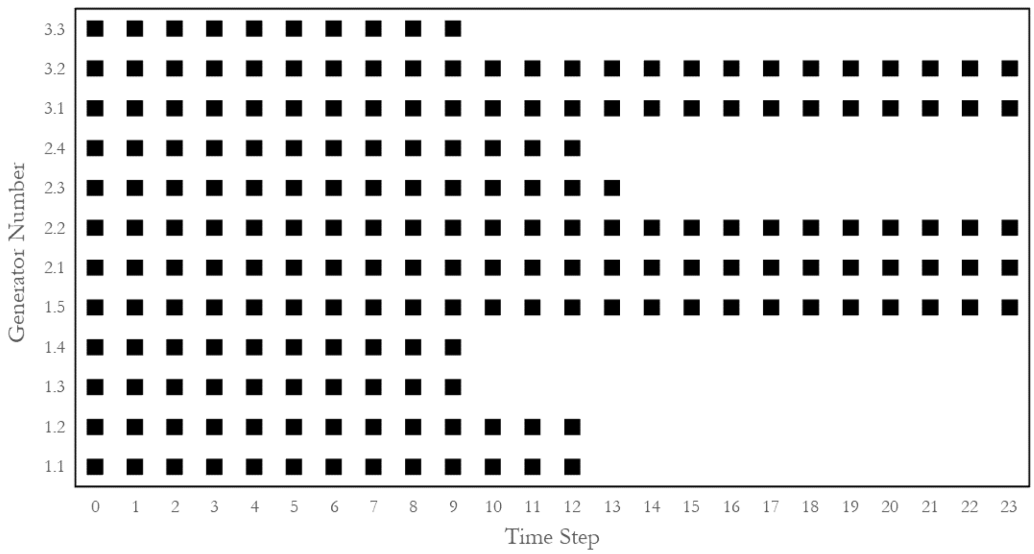

Figure 4.42: Generating unit statuses for scenario 1 from the 10% single deterministic (Sin. Det.) case with cost.

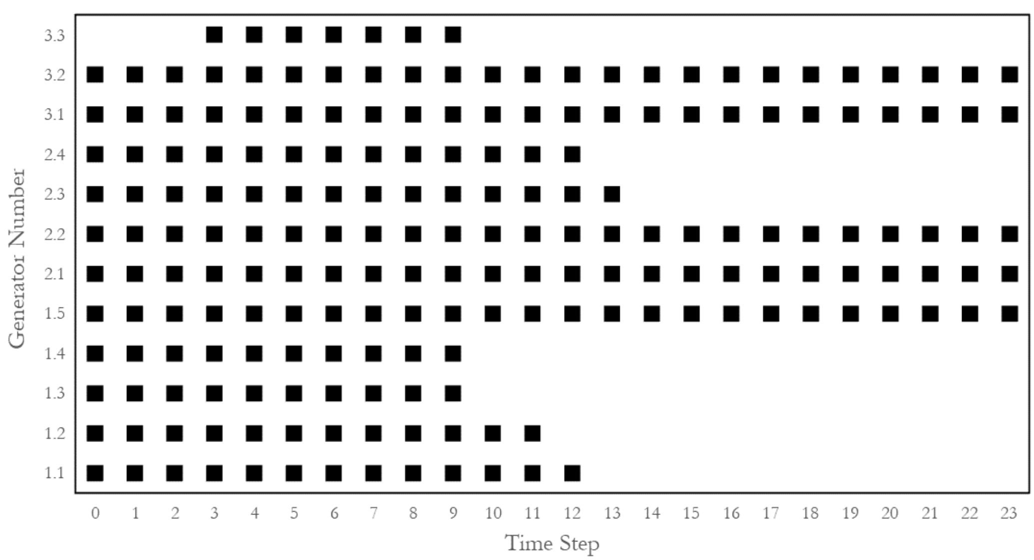

Figure 4.43: Generating unit statuses for scenario 1 from the 10% average price deterministic (Sin. Det.) case with cost.

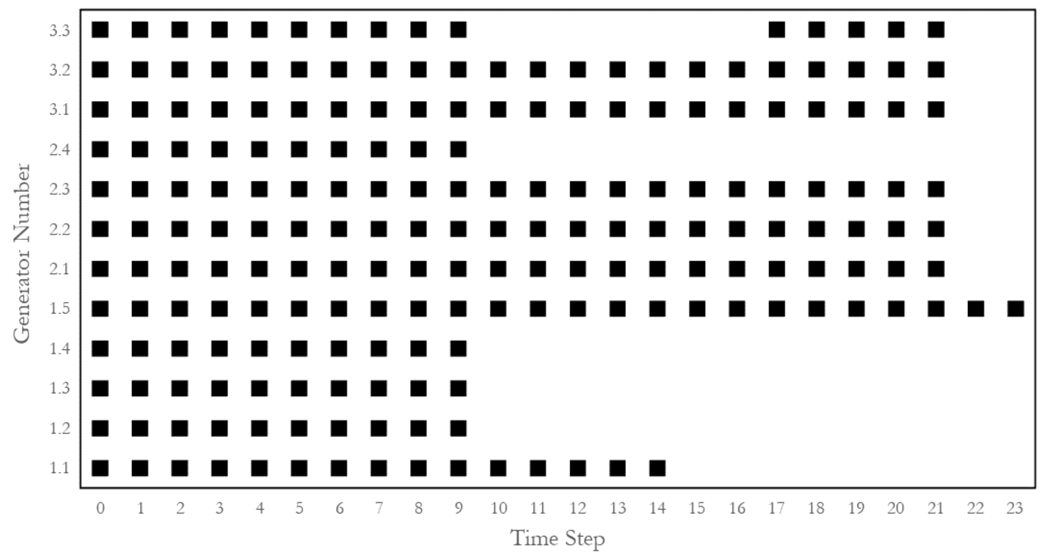

Figure 4.44: Generating unit statuses for scenario 1 from the 10% 3 time step stochastic (Sto. 3 TS) case with cost.

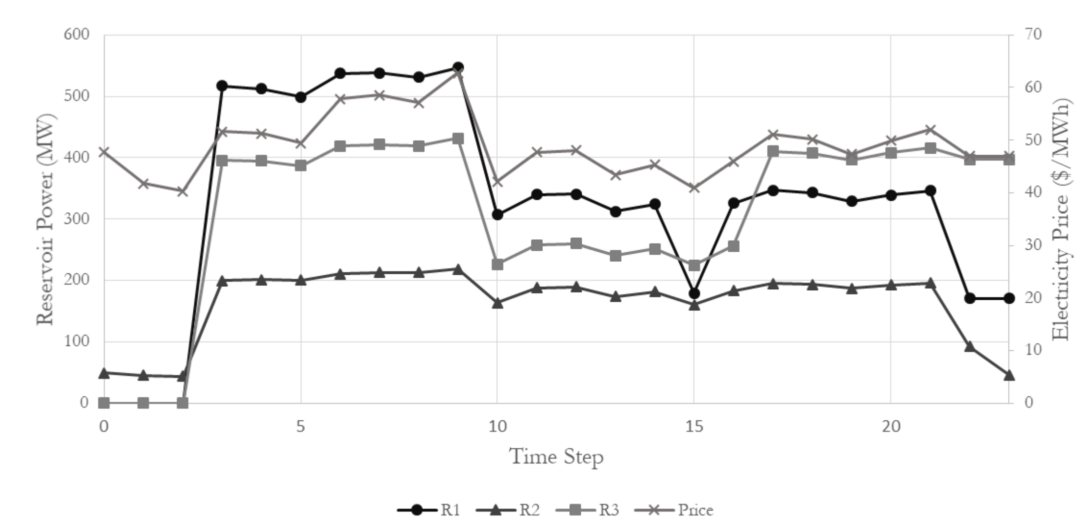

Figure 4.45: Total reservoir power outputs for scenario 1 from the 10% individual deterministic (Ind. Det.) case with cost with the electricity price profile.

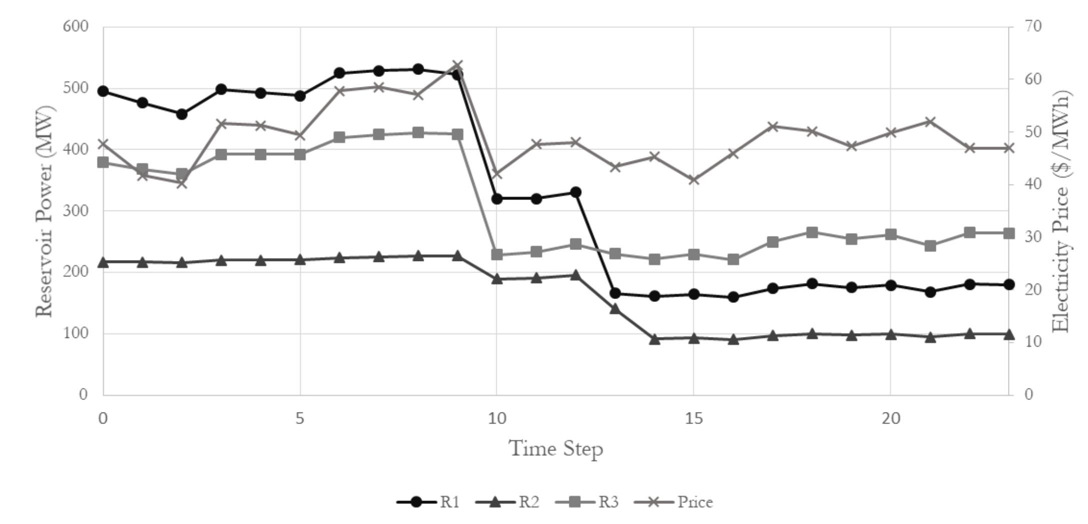

Figure 4.46: Total reservoir power outputs for scenario 1 from the 10% single deterministic (Sin. Det.) case with cost with the electricity price profile.

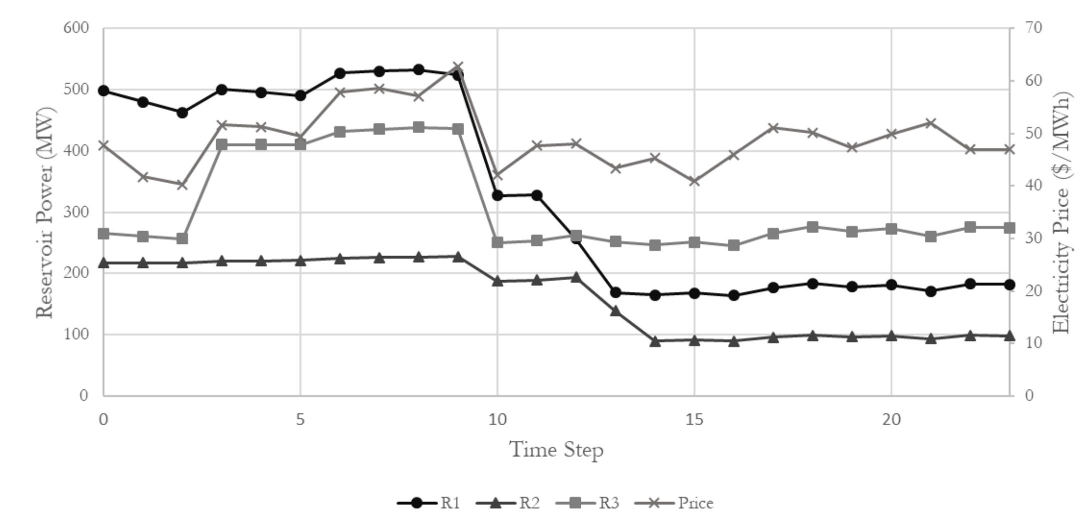

Figure 4.47: Total reservoir power outputs for scenario 1 from the 10% average price deterministic (Avg. P.) case with cost with the electricity price profile.

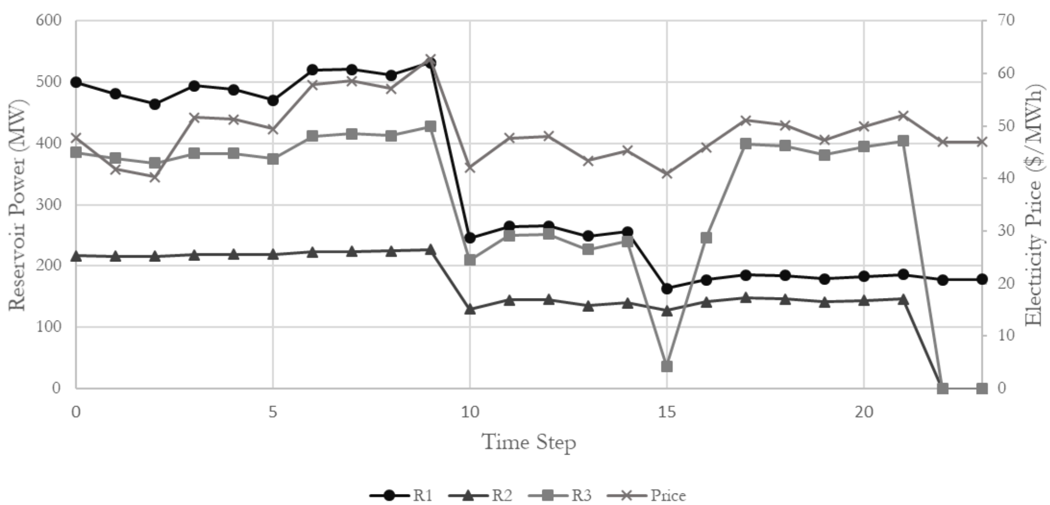

Figure 4.48: Total reservoir power outputs for scenario 1 from the 10% 3 time step stochastic (Sto. 3 TS) case with cost with the electricity price profile.

4.3 Pseudo-Rolling Horizon

4.3.1 Description

In literature a rolling horizon is a type of optimization problem that simulates the passing of time and reoptimizes with new information to improve the solution while maintaining the same time horizon length, thus extending the time horizon into the future. However, in this work the ending time step is kept fixed as the simulation of passing of time is simulated, therefore shrinking the time horizon length. This will be referred to as a pseudo-rolling horizon.

One of the biggest reasons the time horizon is not extended in this work is due to the final level constraint. In practice, reservoir levels must be kept within specific elevation regions as a constraint of the system, but there are also target elevation regions for each reservoir to be within so that the system can be managed on a long-term basis. As mentioned before, in this work the final level is constrained to be equal to the initial level, so that all the generators don't run at maximum throughput for the entire time horizon. Instead of extending this final level constraint to future tme steps outside the initial time horizon considered (as it would in a true rolling horizon), it is kept at time step 24 (ie. the end of the last time step in the horizon).

An alternative could be to extend the horizon in a true rolling horizon fashion and keep the level requirement at time step 24 and add an additional constraint after the last time step considered in the updated time horizon. However, this could be decomposed into two optimization problems as they are completely separated by the level constraint at time step 24 because the first 24 time steps utilize the upstream inflows exactly and any time steps after would have its own inflows to utilize. Thus, there would be no interesting results in implementing this alternative.

The pseudo-rolling horizon used here will have three time steps in the first stage and each stage after, meaning the 24 hour duration will be separated into eight stages. As stated previously, the "true" price profile will be simulated to be a different random sample from a normal distribution with the nominal price for each time step being the mean and the standard deviation varying to be 1%, 5%, and 10% to obtain three price profiles. As the simulation rolls forward, the three time steps in the current stage will have the "true" price profile revealed. The optimization will then determine a solution for all scenarios with the solutions being the same in the current stage (and all stages prior).

This section will use the same solution methods from the last section with some modifications. First, the Ind. Det. method will optimize purely for the true price profile, once again simulating the perfect information case. Secondly, the same solutions from the previous section for the Sin. Det. and Avg. P. methods will be implemented on the "true" price profile to calculate what revenue would be obtained in reality. Lastly, the Sin. Det. and Sto. 3 TS methods will implemented in the pseudo-rolling horizon method described previously. This will provide a comparison of methods that should be robust for any price profile similar to the ones considered and those that improve the solution as time passes.

4.3.2 Results

The pseudo-rolling horizon comparison results are shown in tables 4.7 to 4.9 and are mostly intuitive to what one might expect. The generator statuses and power profiles for the pseudo-rolling horizon methods and the Ind. Det. method on the "true" price profile can be found in appendix C. Although the Ind. Det. method is better than every other method and the Sin. Det. and Avg. P. methods are worse, the Sin. Det. Roll method yields a better result than the Sto. 3 TS Roll method in most cases considered in this work. This last result is counterintuitive because the stochastic method has the freedom to create a solution for each scenario which should allow a better, or at the very least equal, optimum to be found. However, it is likely for that very same reason that the Sin. Det. Roll performs better because it creates a stable solution and makes slight corrections as the true price profile is revealed stage by stage. The Sto. 3 TS expects one of ten scenarios to happen which is why it must make more corrections when a completely different price profile is revealed one piece at a time. It must also collapse ten scenarios worth of solutions into one for the current stage using different linearizations for each scenario. Thus, the robust nature of the Sin. Det. Roll method allows it to perform slightly better than the Sto. 3 TS method in most of the tests considered in this work.

Table 4.7: The 1% true price profile case revenues (in dollars) without and with start-up costs (in thousands of dollars) for each solution method.

Method	Without	With
Ind. Det.	991,765.19	982,755.64 (34)
Sin. Det.	990,830.17	982,635.88 (34)
Avg. P.	991,292.75	982,635.74 (34)
Sin. Det. Roll	991,648.18	982,380.93 (34)
Sto. 3 TS Roll	991,510.24	983,257.63 (35)

This is not to say that the Sto. 3 TS Roll method performs terribly, just that it isn't better than the Sin. Det. Roll method in most cases. If one examines the revenues for each standard deviation case the Sto. 3 TS method is within approximately 1% of the Ind. Det. method every time. This difference can add up over time, but ultimately will be deemed an acceptable high quality solution method. Overall the Sin. Det. Roll method is better because of its ability to obtain a high quality solution regardless of what scenario occurs (even one that isn't included in the optimization), but the Sto. 3 TS is better for a one time use. However, this is only true because the Sto.

Table 4.8: The 5% true price profile case revenues (in dollars) without and with start-up costs (in thousands of dollars) for each solution method.

Method	Without	With
Ind. Det.	1,008,737.50	985,640.47 (31)
Sin. Det.	993,678.69	972,076.66 (25)
Avg. P.	993,728.79	972,286.72 (25)
Sin. Det. Roll	1,004,417.06	978,980.44 (28)
Sto. 3 TS Roll	1,003,005.79	987,164.77 (34)

Table 4.9: The 10% true price profile case revenues (in dollars) without and with start-up costs (in thousands of dollars) for each solution method.

Method	Without	With
Ind. Det.	1,035,193.02	1,014,694.36 (35)
Sin. Det.	1,017,437.90	996,534.03 (25)
Avg. P.	1,018,770.15	996,602.09 (25)
Sin. Det. Roll	1,033,984.75	1,009,580.67 (32)
Sto. 3 TS Roll	1,030,622.80	1,003,020.41 (29)

3 TS method finds multiple solutions with a common first stage. This could only be implemented in reality if one knew one of the ten scenarios considered would occur and it was known immediately after the third time step. The fact that a completely different scenario is revealed as the true price profile is the reason why the Sto. 3 TS Roll method falls in comparison with the robust Sin. Det. Roll method.

One may find that the Sto. 3 TS method performs better on average than the Sin. Det. method if many more tests are performed. The results seen in this work may be considered an anomaly or may be proven to be statistically true. In either case, more tests are needed to obtain a distinct conclusion on which method is better.

Chapter 5

Conclusions and Future Considerations

5.1 Conclusions

After determining that the original MINLP problem is too large to solve realistically, several linearization methods were tested as a replacement. The PLA was dropped as a viable replacement after the base cases due to poorer approximations and long computational times. The SLP performed well in the base cases, but after implementing on the daily case it was observed that the method has issues with nonconvex problems and could not find a solution of similar quality to the Hybrid method (either the fixed grid or adaptive grid methods). The Hybrid fixed grid method found a slightly higher quality solution than the adaptive grid method when a significant number of piecewise points are used in the Hybrid fixed grid method. However, due to the inconsistent performance of the Hybrid fixed grid method sometimes terminating due to repeating solutions and the fact that the method takes a significantly larger amount of computational time, the method was also dropped as a viable replacement in favour of the Hybrid adaptive grid method.

To summarize, the Hybrid adaptive grid method is the best linearization method examined in this work and is an efficient and worthwhile replacement to the hydroelectric nonconvex MINLP. It also gives options pertaining to the tradeoff of desired solution quality and computational time while still being effective at both aspects by allowing the user to change the number of piecewise points, the initial trust region, and the trust region shrinking factor.

To take uncertainty into account, three realistic methods were tested to determine which would perform the best. These methods are the single deterministic method (Sin. Det.), the average price method (Avg. P.), and the stochastic three time step method (Sto. 3 TS). These methods were compared against the perfect information case which is called the individual deterministic method (Ind. Det.). Then, a "true" price profile was used to simulate a rolling horizon solution methodology for the Sin. Det. and Sto. 3 TS methods.

As expected, the stochastic method fares better in the single stage tests than either of the other two realistic methods. Unfortunately, this is due to the fact that the stochastic method is likely to have different solutions for each scenario in the remaining time steps. This is an unfair comparison because this is dependent on the stochastic method knowing which scenario will occur as the "true" price profile in the second stage. This advantage disappears in the pseudo-rolling horizon tests because only one solution may be utilized. One observes for most cases considered in this work that the stochastic method performs slightly worse in a pseudo-rolling horizon situation when compared to the Sin. Det. pseudo-rolling horizon method. However, this is not a distinct conclusion because it is only valid for the cases considered. These tests would have to be performed on a large number of different random profiles to achieve a clear conlcusion. It can also be seen that there is a clear improvement when using the psuedo-rolling horizon methods over the deterministic solutions implemented on the “true” price profile.

5.2 Future Considerations

There are a few additions to the original problem not completed in this work that may prove to be worthwhile. The first extra inclusion that should be added is uncertain inflows as this will add unexpected complexity and will introduce a potential infeasibility problem. Another inclusion that should be considered is ramping limitations for generators, meaning that they can only gradually change the flow through them from time step to adjacent time step. Finally, of course, implementing this solution methodology on a true rolling horizon deserves investigation, particularly in comparison with the pseudo-rolling horizon results.

There are three tests that may be completed in the future to potentially improve the solution methodology proposed in this thesis. The first is examining initial generator statuses based on which generators are likely to be on and/or turn on due to their efficiencies and electricity price. This could be completed by considering the current electricity price and whether it is a peak price or a trough price as well as comparing the average inflow over the time horizon considered to the maximum throughput for each reservoir. Generators are more likely to be on when electricity prices are higher and when the average inflow is higher, which is helpful to know because this could assist in estimating initial generator statuses (which will remove the start-up costs for the generators which are estimated to be on).

The second test is calculating the maximum value of water resources for a particular reservoir with a known generator configuration at a specific head. In other words, finding a function that approximates the maximum potential power produced for any total reservoir flow that considers all possible generator configurations together as one. By doing so, the original MINLP can be separated into two subproblems that optimizes for the total reservoir flow for each time step and then optimizes the individual generators given the total reservoir flow and reservoir head for each time step in an iterative process. Ideally, this would reduce computational complexity and the accuracy would improve as the iterations converge on the solution.

The last test is implementing the Hybrid method with large number of piecewise points that reduces as the iterations progress. This would allow a greater degree of accuracy in earlier iterations where a greater amount of feasible space is examined, and greater computational efficiency in later iterations as the Hybrid method converges on an exact solution.

Additionally, it is always worthwhile trying to find the optimum in less time. Considering a decomposition method for this problem may be worth exploring particularly for removing large sections of suboptimal feasible space. Perhaps if this solution methodology is used in a rolling horizon implementation, trying to use the previous solution to substantially reduce the search space could be significantly helpful. For example, using a smaller trust region for time steps that are closer to the current time step could not only reduce the computational time needed to find the optimum but it could also assist in creating additional stability for the ongoing solution.

List of References

Achterberg, T. (2009). SCIP: solving constraint integer programs. *Mathematical Programming Computation*, **1**(1), 1–41.

Belotti, P., Lee, J., Liberti, L., Margot, F., and Wächter, A. (2009). Branching and bounds tightening techniques for non-convex MINLP. *Optimization Methods and Software*, **24**(4-5), 597–634.

Belsnes, M. M., Wolfgang, O., Follestad, T., and Aasgård, E. K. (2016). Applying Successive Linear Programming for Stochastic Short-term Hydropower Optimization. *Electric Power Systems Research*, **130**, 167–180.

Brooke, A., Kendrick, D., Meeraus, A., Raman, R., and Rasenthal, R. (1998). A user's guide, GAMS software. *GAMS Development corporation*, .

D'Ambrosio, C., Lodi, A., and Martello, S. (2010). Piecewise linear approximation of functions of two variables in MILP models. *Operations Research*, **38**, 39–46.

de Castro Amarante e Ribeiro, A. F. (2014). *Mathematical problems of hydroelectric power stations management.* PhD Thesis, Department of Mathematics, University of Porto, Portugal.

de Ladurantaye, D., Gendreau, M., and Potvin, J.-Y. (2009). Optimizing Profits from Hydroelectricity Production. *Computers & Operations Research*, **36**, 499–529.

Drouin, N., Gautier, A., Lamond, B. F., and Lang, P. (1996). Piecewise Affine Approximations for the Control of a One-Reservoir Hydroelectric System. *European Journal of Operational Research*, **89**, 53–69.

Fletcher, R. and de la Maza, E. S. (1989). Nonlinear Programming and Nonsmooth Optimization By Successive Linear Programming. *Mathematical Programming*, **43**, 235–256.

Fleten, S.-E. and Kristoffersen, T. K. (2008). Short-term Hydropower Production Planning By Stochastic Programming. *Computers & Operations Research*, **35**, 2656–2671.

Fu, J. H. G. and Scott, R. C. (2013). Piecewise Linear Approximation of Smooth Functions of Two Variables. *Advances in Mathematics*, **248**, 229–241.

Guedes, M. C. M., Ribeiro, A. F., Smirnov, G. V., and Vilela, S. (2012). On the Optimal Control of a Cascade of Hydro-electric Power Stations. *Electric Power Systems Research*, **88**, 121–129.

Hreinsson, E. B. (1988). Optimal Short Term Operation of a Purely Hydroelectric-System. *IEEE Transactions on Power Systems*, **3**(3), 1072–1077.

IBM. (2015). IBM ILOG CPLEX optimization studio CPLEX user's manual, Version 12 Release 6.

Korobeinikov, A., Kovacec, A., McGuinness, M., Pascoal, M., Pereira, A., and Vilela, S. (2010). Optimizing the Profit from a Complex Cascade of Hydroelectric Stations with Recirculating Water. *Mathematics in Industry Case Studies Journal*, **2**, 111–133.

LUENBERGER, D. G. AND YE, Y. (1984). *Linear and Nonlinear Programming.* Springer International Publishing.

MISENER, R. AND FLOUDAS, C. A. (2014). ANTIGONE: algorithms for continuous/integer global optimization of nonlinear equations. *Journal of Global Optimization*, **59**(2-3), 503–526.

OSBURN, G. (2014). Hydrogenerator Start/Stop Costs. .

PALACIOS-GOMEZ, F., LASDON, L., AND ENGQUIST, M. (1982). Nonlinear Optimization By Successive Linear Programming. *Management Science*, **28**(10), 1106–1120.

PEREIRA, M. V. F. (1989). Optimal Stochastic Sperations Scheduling of Large Hydroelectric Systems. *International Journal of Electrical Power & Energy Systems*, **11**(3), 161–169.

PEREIRA, M. V. F. AND PINTO, L. M. V. G. (1985). Stochastic Optimization of a Multireservoir Hydroelectric System: A Decomposition Approach. *Water Resources Research*, **21**(6), 779–792.

RAJŠL, I., ZIDAR, M., AND KRAJCAR, S. (2011). Model of short term hydro power plant scheduling in competitive environment. *2011 8th International Conference on the European Energy Market, EEM 11*, , 434 – 441.

RYOO, H. S. AND SAHINIDIS, N. V. (1995). Global Optimization of Nonconvex NLPs and MINLPs with Applications in Process Design. *Computers and Chemical Engineering*, **19**(5), 551–566.

SAHINIDIS, N. V. (1996). BARON: A general purpose global optimization software package. *Journal of global optimization*, **8**(2), 201–205.

Séguin, S., Fleten, S.-E., Côtéb, P., Pichler, A., and Audet, C. (2017). Stochastic Short-term Hydropower Planning With Inflow Scenario Trees. *European Journal of Operational Research*, **259**, 1156–1168.

Tomlin, J. A. (1988). Special Ordered Set and an Application to Gas Supply Operations Planning. *Mathematical Programming*, **42**, 69–84.

Zhang, J., Kim, N.-H., and Lasdon, L. (1985). An Improved Successive Linear Programming Algorithm. *Management Science*, **31**(10), 1312–1331.

Appendix A

Formulation Nomenclature

A.1 MINLP Formulation

A.1.1 MINLP Sets

t	$\in T = \{0, 1, ...T_{End}\}$	Time steps
i	$\in I = \{1, 2, 3\}$	Reservoirs
j	$\in J = \{1, 2, 3, 4, 5\}$	Generators
gs	$\in GS = \{a_1, a_2, a_3, b_1, b_2, b_3,$	
	$c_1, c_2, c_3, d_1, d_2, d_3\}$	Set for power equation coefficients
rs	$\in RS = \{C0, C1, C2, C3\}$	Set for storage equation coefficients

A.1.2 MINLP Parameters

$L_{i,Min}$	Minimum reservoir levels
$L_{i,Max}$	Maximum reservoir levels
$L_{i,Init}$	Initial and final reservoir levels
$V_{i,Min}$	Minimum reservoir volumes
$V_{i,Max}$	Maximum reservoir volumes
$V_{i,Init}$	Initial and final reservoir volumes
EP_t	Electricity selling prices
$L_{i,Down}$	Tailwater elevations for each reservoir
$L_{i,Sill}$	Sill elevations for each reservoir
$F_{i,t,In}$	Inflows to each reservoir
$FS_{i,Max}$	Maximum spill flows for each reservoir
$GC_{i,j,gs}$	Generator power coefficients
$RC_{i,rs}$	Reservoir storage coefficients
$F_{i,j,Max}$	Maximum flows for each generator
$F_{i,j,Min}$	Minimum flows for each generator
$FT_{i,Min}$	Minimum flows for each reservoir
$P_{i,j,Max}$	Maximum possible power produced for each generator
Δt	The length of each time step

A.1.3 MINLP Continuous Variables

REV	Total revenue for the entire time horizon
$FT_{i,t}$	Total flow leaving reservoir i at time step t through generators
$F_{i,j,t}$	Flow through generator j in reservoir i at time step t
$P_{i,j,t}$	Power produced with generator j in reservoir i at time step t
$FS_{i,t}$	Spill flow for reservoir i at time step t
$V_{i,t}$	Volume of reservoir i at time step t
$L_{i,t}$	Level of reservoir i at time step t
$H_{i,t}$	Head of reservoir i at time step t
$V_{i,Final}$	The final volume for reservoir i
$L_{i,Final}$	The final level for reservoir i

A.1.4 MINLP Binary Variables

$S_{i,j,t}$	Generator status for generator j in reservoir i at time step t
$SS_{i,t}$	Spill status for reservoir i at time step t

A.2 SLP Modifications

A.2.1 SLP New/Modified Parameters

$L_{i,t,S}$	Linearization points for level
$F_{i,j,t,S}$	Linearization points for individual generator flow
$H_{i,t,S}$	Linearization points for head
$V_{i,t,S}$	Linearization points for volume
$S_{i,j,t,S}$	Linearization points for generator status
$P_{i,j,t,S}$	Linearization points for power for each individual generator
$CL_{i,t}$	Coefficients for level in the linearization
$CF_{i,j,t}$	Coefficients for inidividual generator flow in the linearization
$CH_{i,j,t}$	Coefficients for head in the linearization
TR	The trust region size for the current iteration
TR_{Init}	The initial trust region size
TR_{Factor}	The shrinking factor for the trust region size

A.2.2 SLP New/Modified Continuous Variables

$PH_{i,j,t}$	The value used to replace head in the power equation
$EF_{i,j,t}$	The absolute differences between the linearization flow points and their respective flows used in the solution
ET	The total of all absolute differences between all flows and their respective linearization points

A.3 Hybrid Modifications

A.3.1 Hybrid New/Modified Sets

n $\in N = \{0, 1, ...N_F\}$ Piecewise points

A.3.2 Hybrid New/Modified Parameters

$\tilde{P}_{i,j,t,n}$ Piecewise power points

$\tilde{F}_{i,j,t,n}$ Piecewise flow points

The coefficients $CF_{i,j,t}$ and parameters $P_{i,j,t,S}$ used in the SLP formulation are not needed for the Hybrid method as their locations in eq. (3.22) are replaced with other terms in the Hybrid power equation (eq. (3.54)).

A.3.3 New/Modified Continuous Variables

$Y_{i,j,t,n}$ Piecewise weights

A.3.4 Hybrid New/Modified Binary Variables

$Z_{i,j,t,n}$ Piecewise regions (requires all but two adjacent weights to be zero)

A.4 PLA Modifications

All the parameters, variables, and equations that appear in the SLP and Hybrid method modifications are replaced with the ones that follow (these also replace eqs. (3.2), (3.15) and (3.17) from the MINLP formulation with equations seen in section 3.6).

A.4.1 PLA New/Modified Sets

n	$\in N = \{0, 1, ...N_F\}$	Generator flow piecewise points
m	$\in M = \{0, 1, ...N_H\}$	Reservoir head piecewise points

A.4.2 PLA New/Modified Parameters

$\tilde{P}_{i,j,n,m}$	Piecewise power points
$\tilde{F}_{i,j,n}$	Piecewise flow points
$\tilde{H}_{i,m}$	Piecewise head points
$\tilde{V}_{i,m}$	Piecewise volume points

A.4.3 PLA New/Modified Continuous Variables

$Y_{i,j,t,n,m}$	Piecewise weights
$Y_{i,m,Final}$	Final reservoir head piecewise weights

A.4.4 PLA New/Modified Binary Variables

$Z_{i,j,t,n,m}$	Piecewise regions (requires all but one region to be inactive)

A.5 Nervousness and Uncertainty Modifications

A.5.1 Nervousness and Uncertainty New/Modified Sets

k	$\in K = \{1, 2, ...N_K\}$	Scenarios

A.5.2 Nervousness and Uncertainty New/Modified Parameters

$SUC_{i,j}$	Start-up cost for each generator

A.5.3 Nervousness and Uncertainty New/Modified Continuous Variables

$EXPROF$	Expected total profit for the entire time horizon
$PROF$	Total profit for the entire time horizon
$COST$	Total cost for the entire time horizon

A.5.4 Nervousness and Uncertainty New/Modified Binary Variables

$SU_{i,j,t}$	Start-up indicator for each generator

Every variable, linearization coefficient, and linearization point will now require the additional index k (excluding $EXPROF$) to indicate the scenario number (eg. $F_{i,j,t}$ changing to $F_{i,j,t,k}$).

Appendix B

GAMS Solvers

GAMS is an optimization software used to solve all the optimization problems in this work [Brooke *et al.*, 1998]. Both MINLP and MILP solvers are necessary for this work and since CPLEX is an efficient MILP solver, it is the only MILP solver used in this work. CPLEX uses the simplex method to solve linear, quadratic, and quadratically constrained optimization problems with or without integer variables [IBM., 2015]. As for the MINLP solvers, the four used are ANTIGONE, BARON, COUENNE, and SCIP, which are all global solvers (meaning they can find the best solution possible to computational tolerances).

ANTIGONE (Algorithms for coNTinuous/Integer Global Optimization of Nonlinear Equations) examines the MINLP problem and classifies the objective function and constraints by term types to determine a specific relaxation method before creating underestimators for the subproblems in a branch-and-bound method [Misener and Floudas, 2014].

In order to solve nonconvex MINLP optimizations, BARON (Branch-And-Reduce Optimization Navigator) uses relaxations and a branch-and-bound technique with range reduction tests and heuristics using duality to separate the problem into subproblems that can be solved much more easily [Sahinidis, 1996].

COUENNE (Convex Over and Under-Envelopes for Nonlinear Estimation) is an MINLP solver that separates the problem into subproblems and uses underestimators for optimization problems where both the objective function and constraints are factorable (or can be defined as the product of univariate functions) [Belotti *et al.*, 2009].

SCIP (Solving Constraint Integer Problems) uses a similar branch-and-bound approach to the other MINLP solvers, but focuses on meeting integer constraints as the name suggests, even offering the option to be a pure constraint programming solver (ignoring optimality completely) [Achterberg, 2009].

For more information please refer to the referenced user manuals for each software.

Appendix C

Pseudo-Rolling Horizon Results

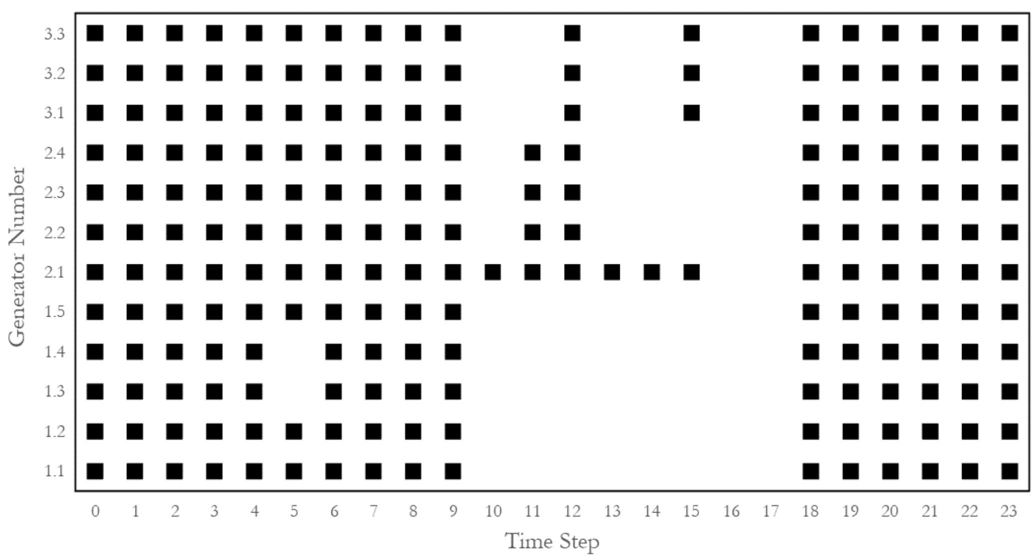

Figure C.1: Generating unit statuses for the "true" price profile from the 1% individual deterministic (Ind. Det.) case without cost.

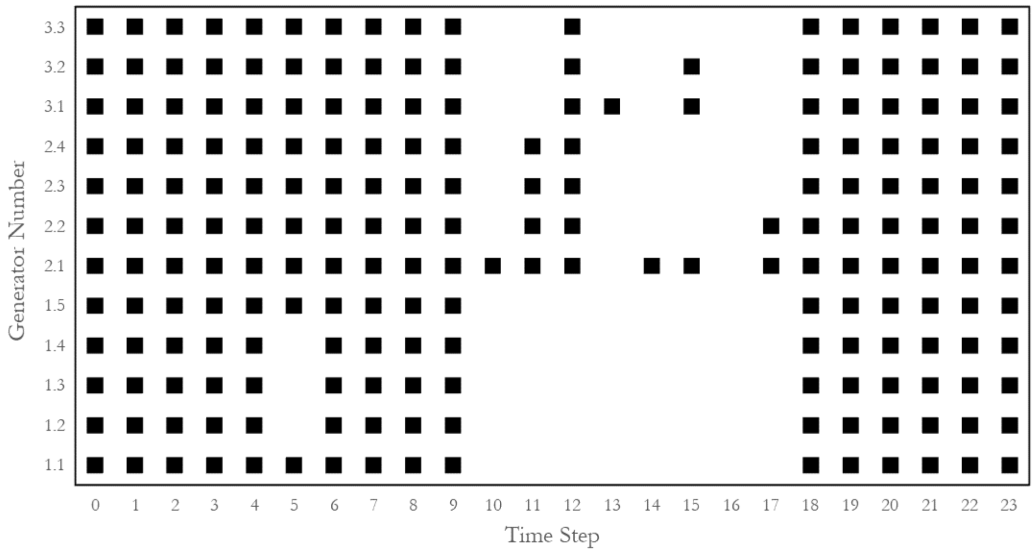

Figure C.2: Generating unit statuses for the "true" price profile from the 1% single deterministic (Sin. Det.) case without cost.

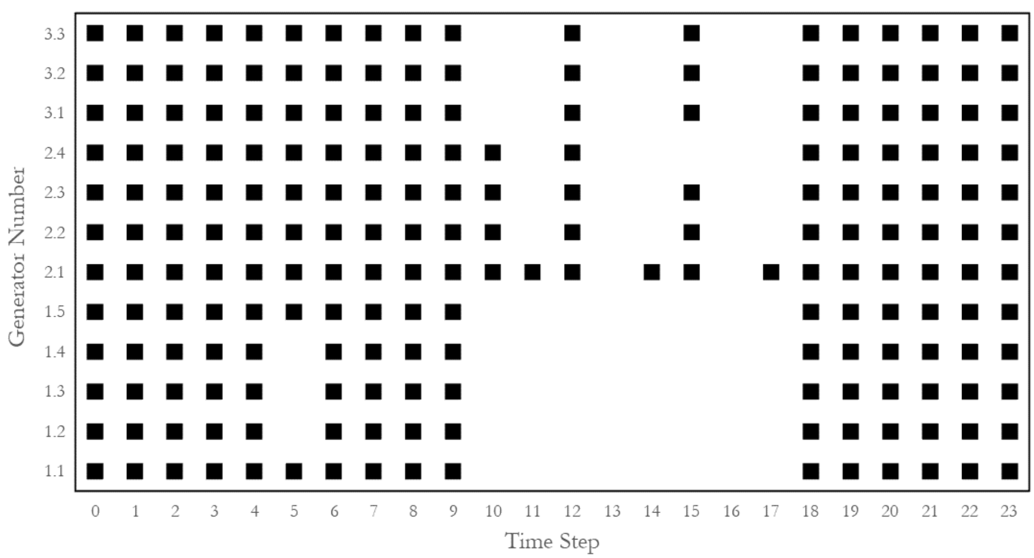

Figure C.3: Generating unit statuses for the "true" price profile from the 1% 3 time step stochastic (Sto. 3 TS) case without cost.

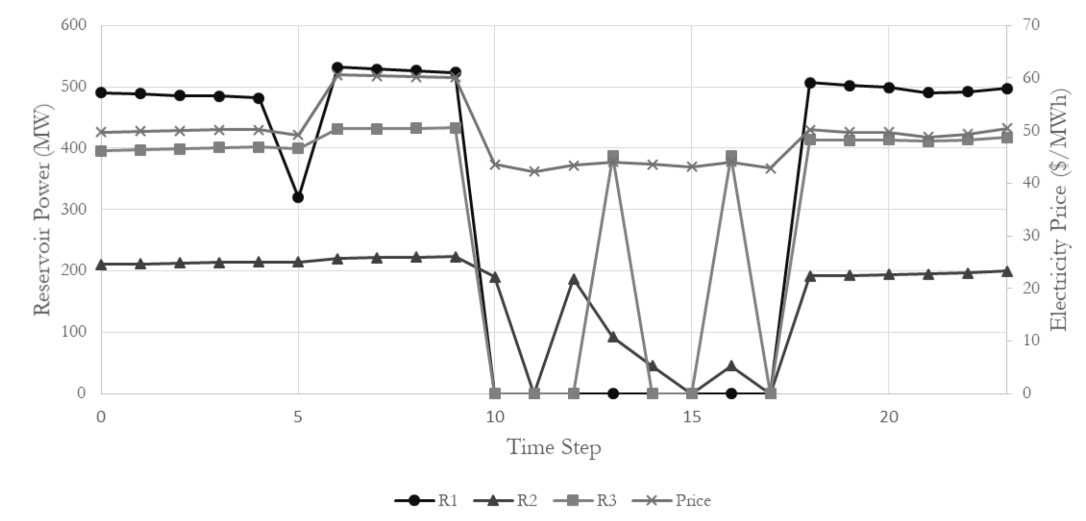

Figure C.4: Total reservoir power outputs for the “true” price profile from the 1% individual deterministic (Ind. Det.) case without cost with the electricity price profile.

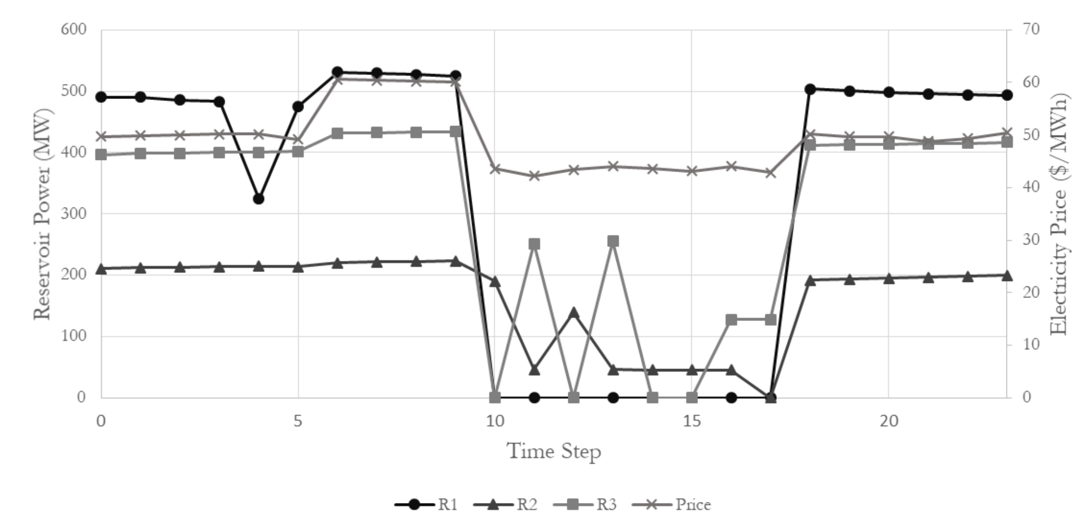

Figure C.5: Total reservoir power outputs for the “true” price profile from the 1% single deterministic (Sin. Det.) case without cost with the electricity price profile.

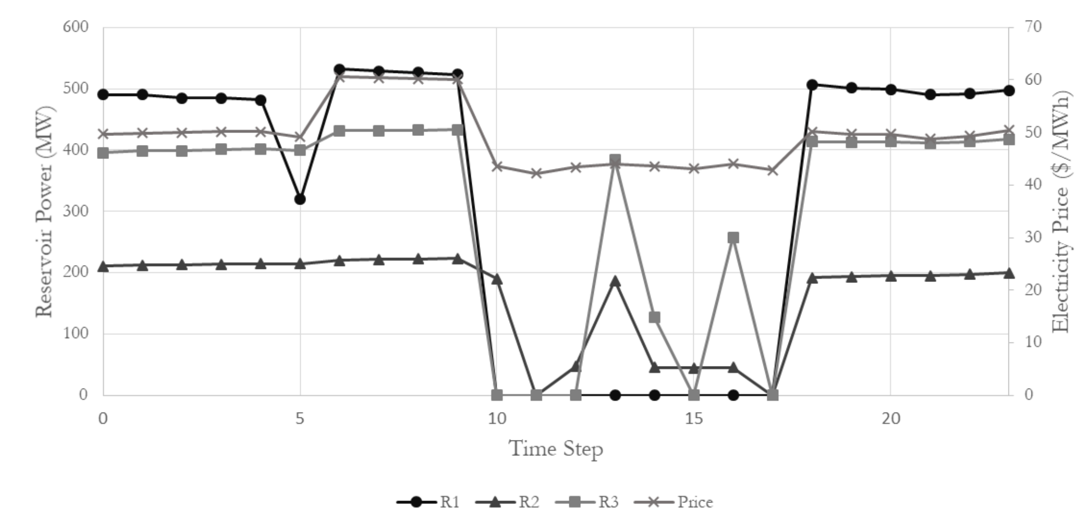

Figure C.6: Total reservoir power outputs for the “true” price profile from the 1% 3 time step stochastic (Sto. 3 TS) case without cost with the electricity price profile.

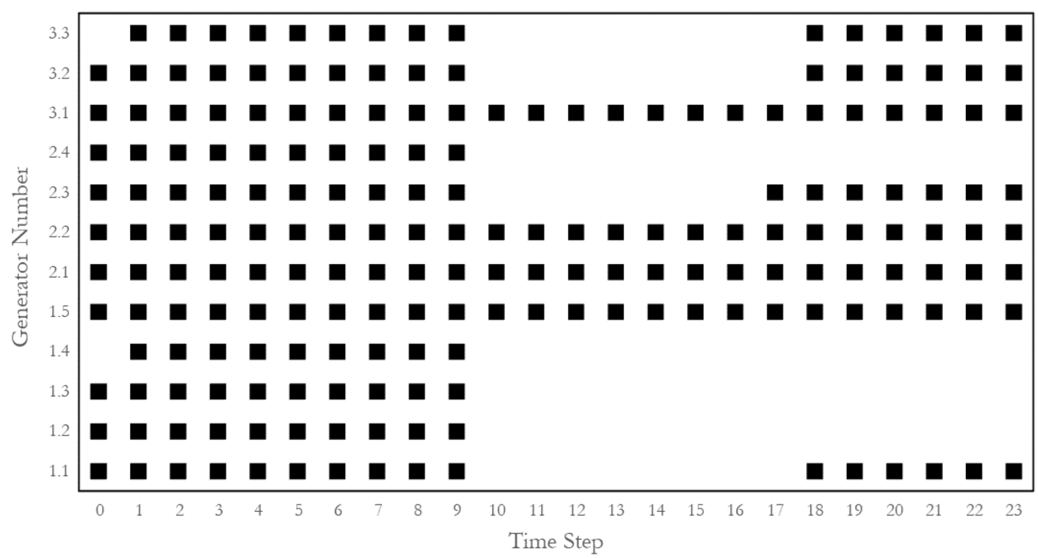

Figure C.7: Generating unit statuses for the “true” price profile from the 1% individual deterministic (Ind. Det.) case with cost.

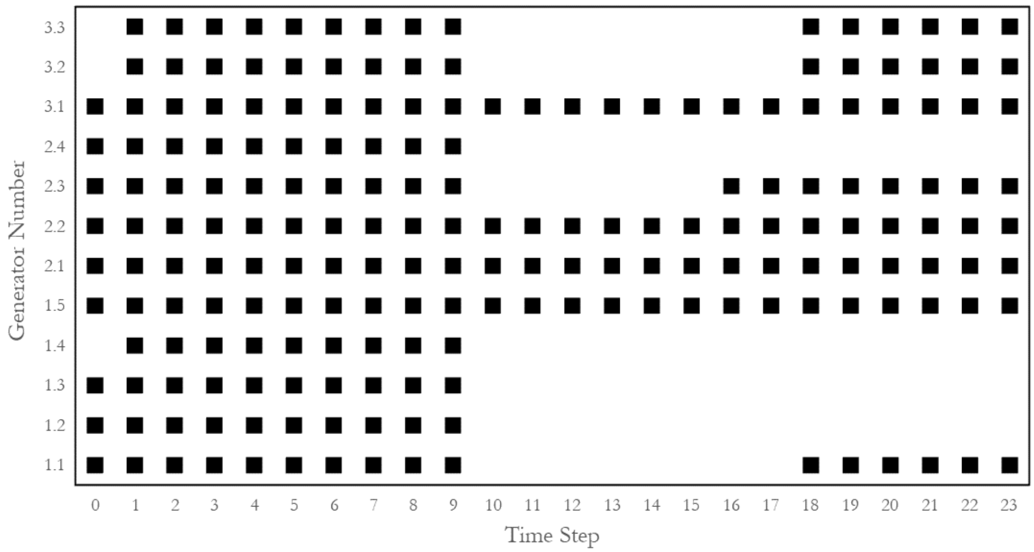

Figure C.8: Generating unit statuses for the "true" price profile from the 1% single deterministic (Sin. Det.) case with cost.

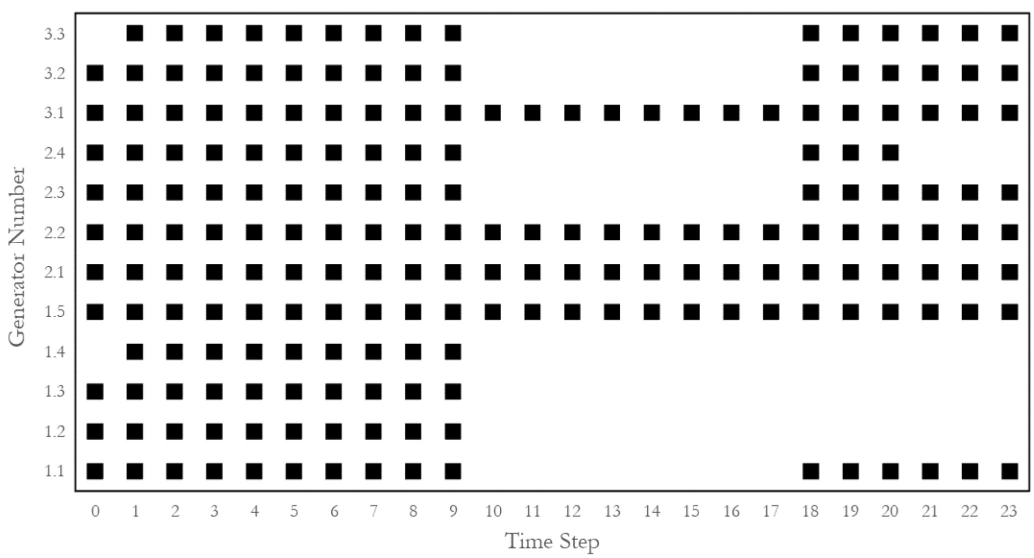

Figure C.9: Generating unit statuses for the "true" price profile from the 1% 3 time step stochastic (Sto. 3 TS) case with cost.

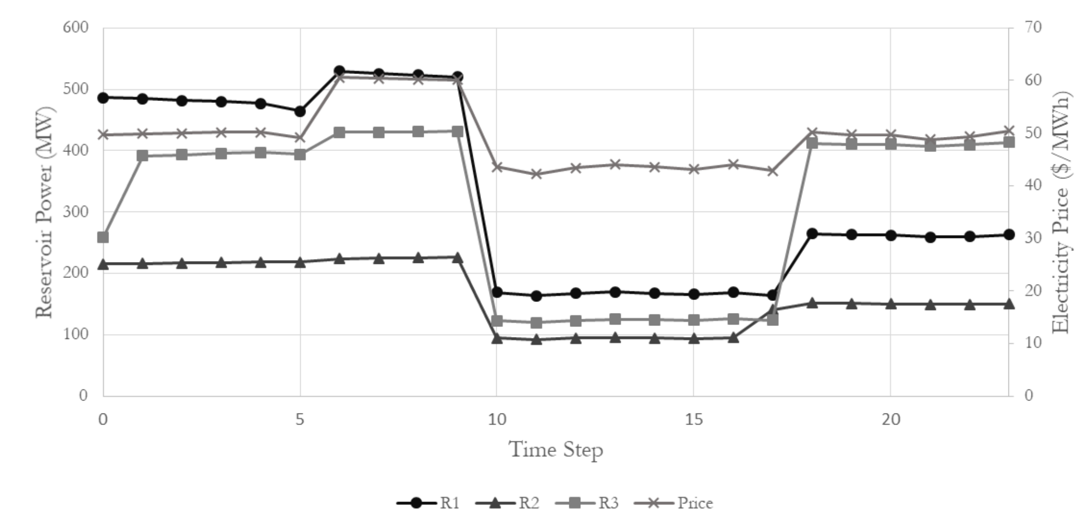

Figure C.10: Total reservoir power outputs for the “true” price profile from the 1% individual deterministic (Ind. Det.) case with cost with the electricity price profile.

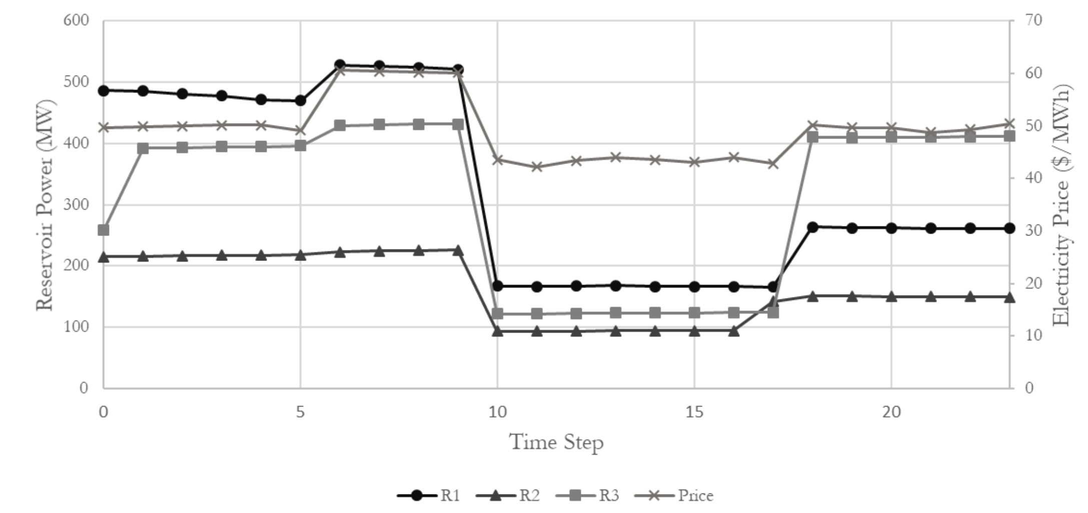

Figure C.11: Total reservoir power outputs for the “true” price profile from the 1% single deterministic (Sin. Det.) case with cost with the electricity price profile.

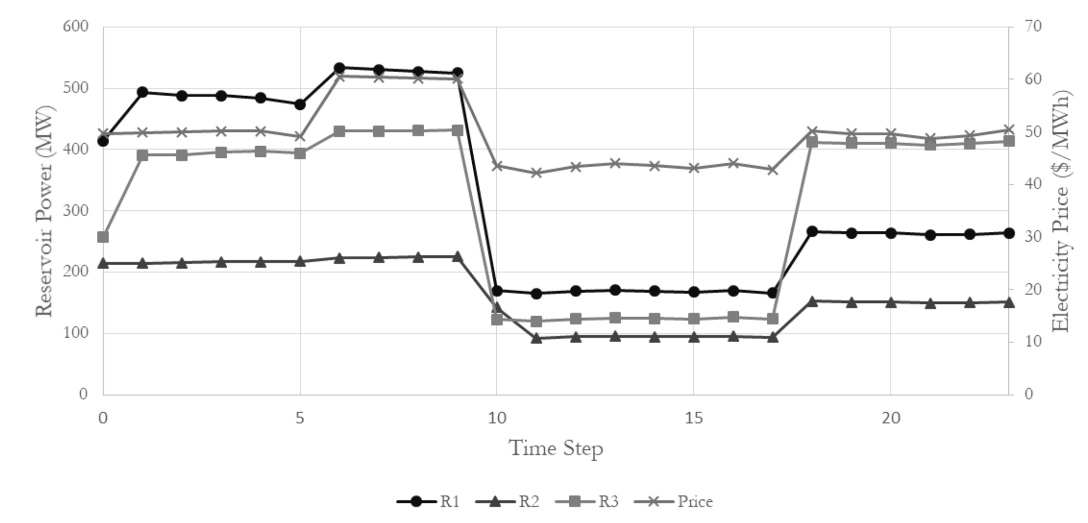

Figure C.12: Total reservoir power outputs for the “true” price profile from the 1% 3 time step stochastic (Sto. 3 TS) case with cost with the electricity price profile.

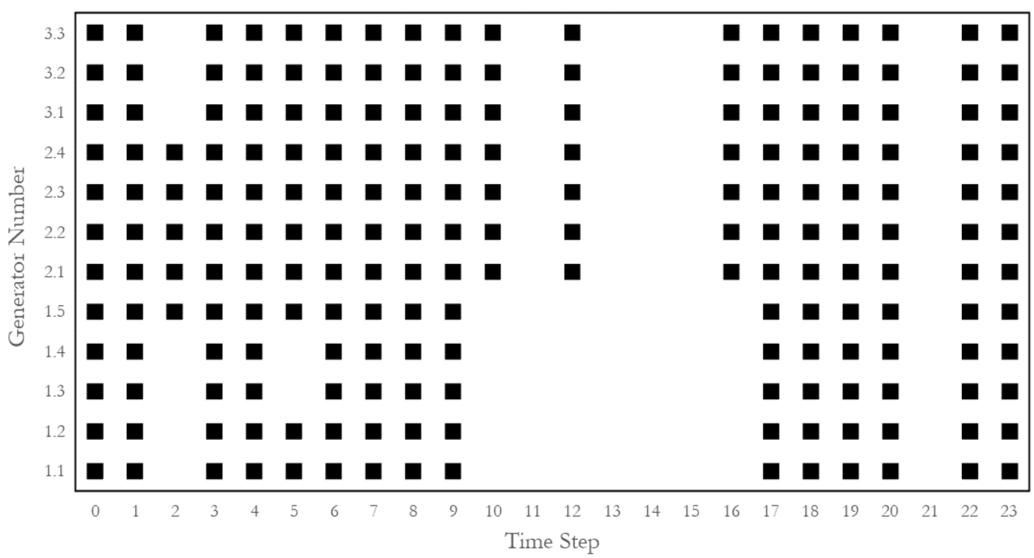

Figure C.13: Generating unit statuses for the “true” price profile from the 5% individual deterministic (Ind. Det.) case without cost.

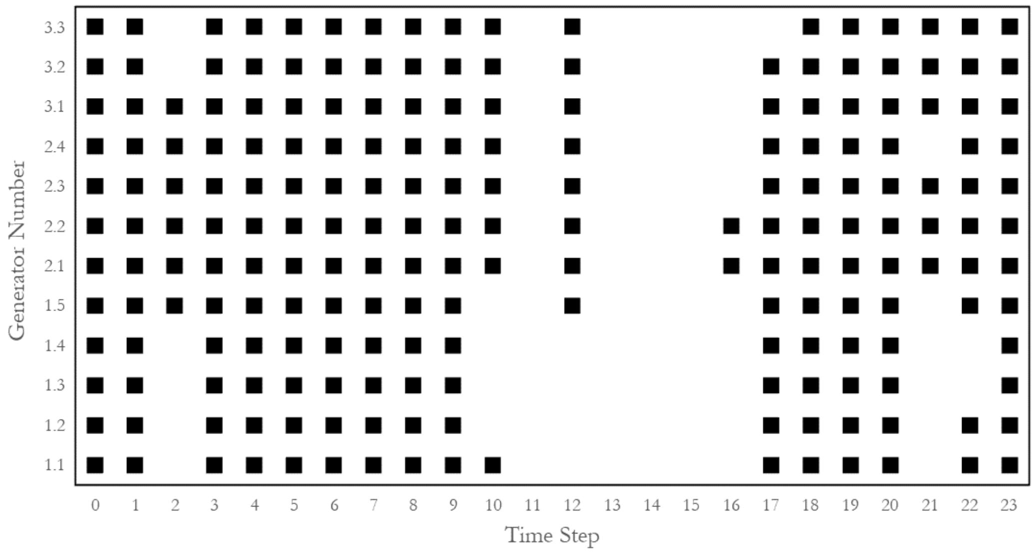

Figure C.14: Generating unit statuses for the "true" price profile from the 5% single deterministic (Sin. Det.) case without cost.

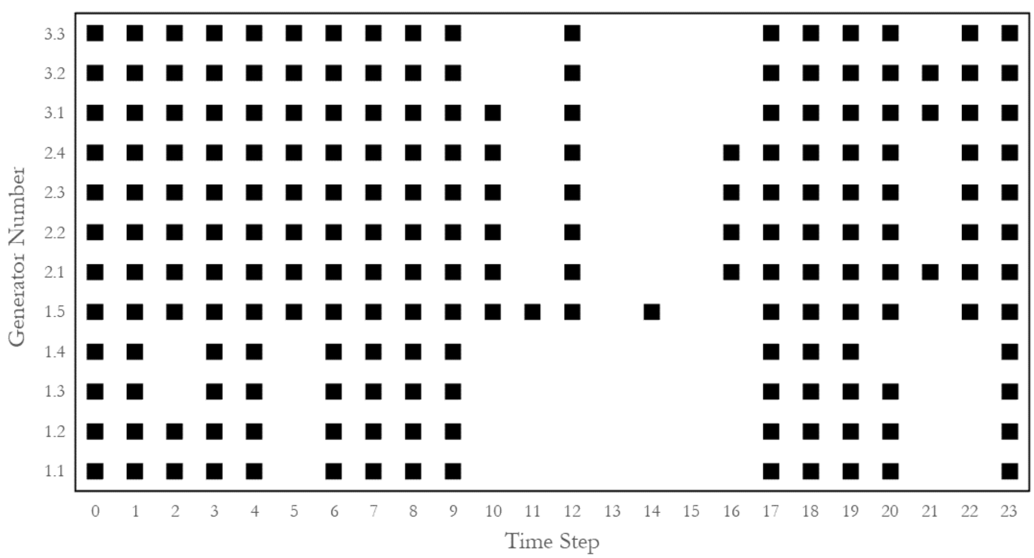

Figure C.15: Generating unit statuses for the "true" price profile from the 5% 3 time step stochastic (Sto. 3 TS) case without cost.

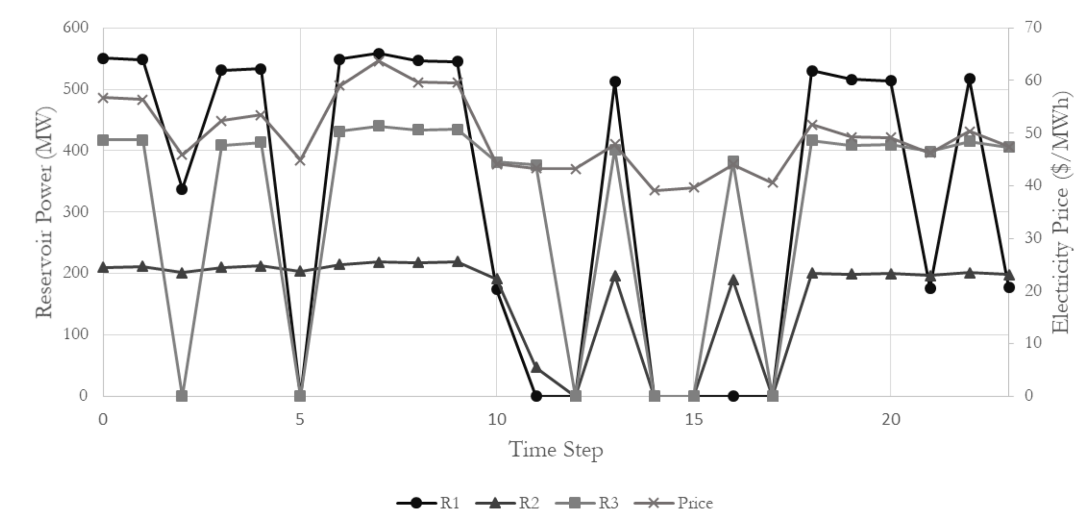

Figure C.16: Total reservoir power outputs for the "true" price profile from the 5% individual deterministic (Ind. Det.) case without cost with the electricity price profile.

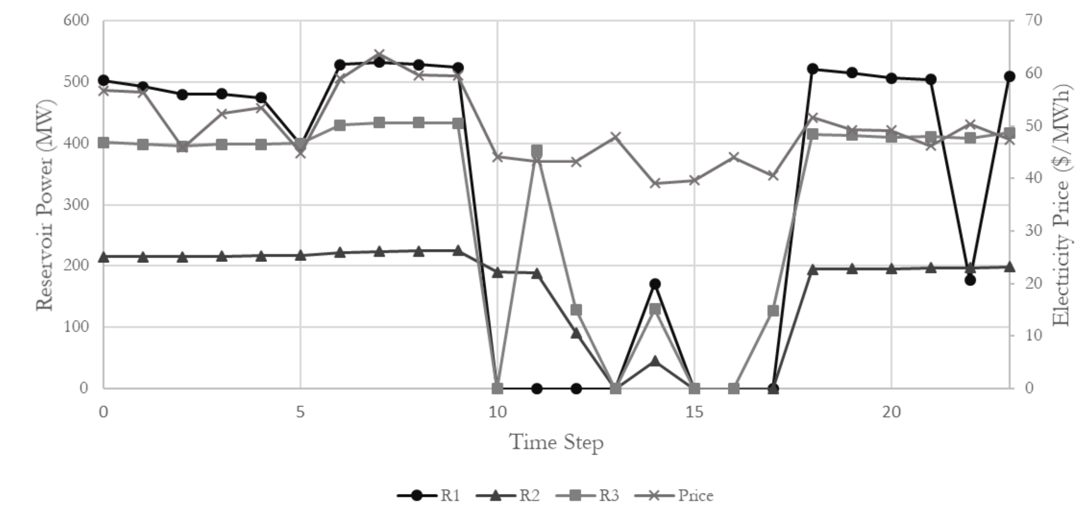

Figure C.17: Total reservoir power outputs for the "true" price profile from the 5% single deterministic (Sin. Det.) case without cost with the electricity price profile.

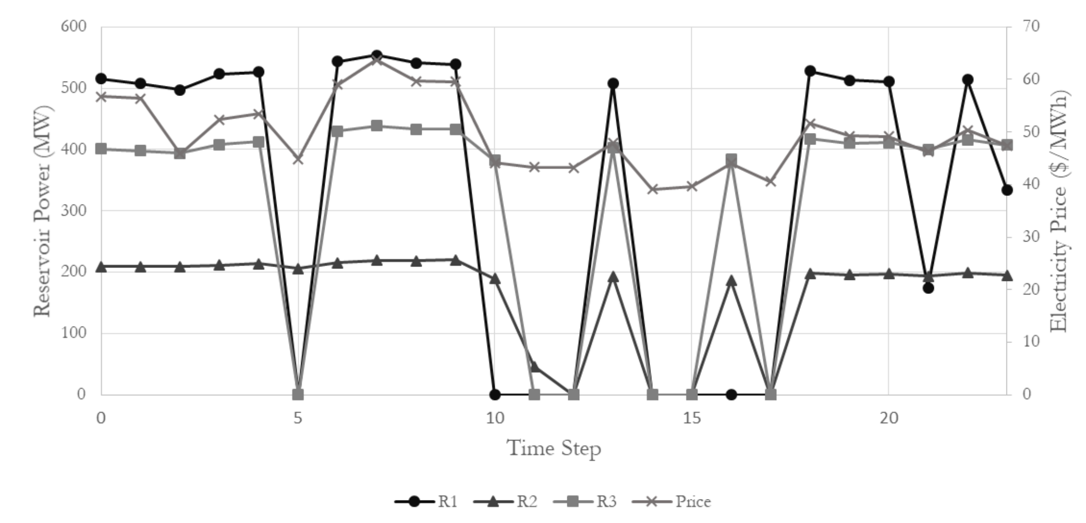

Figure C.18: Total reservoir power outputs for the "true" price profile from the 5% 3 time step stochastic (Sto. 3 TS) case without cost with the electricity price profile.

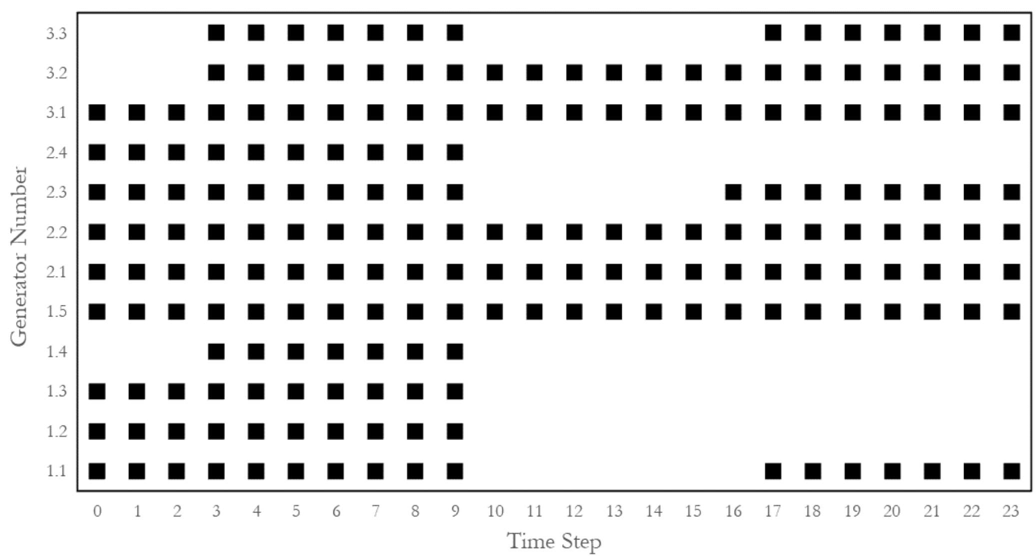

Figure C.19: Generating unit statuses for the "true" price profile from the 5% individual deterministic (Ind. Det.) case with cost.

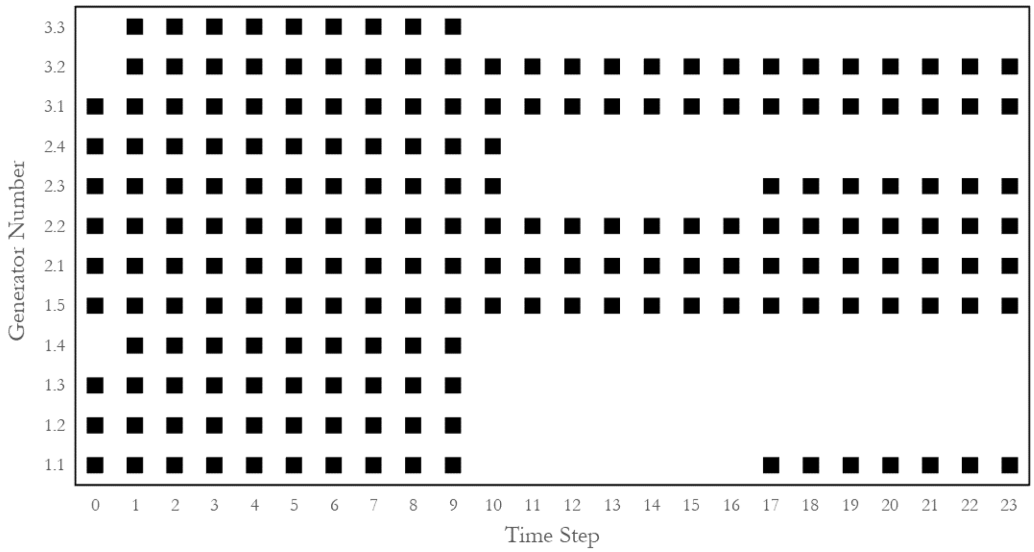

Figure C.20: Generating unit statuses for the “true” price profile from the 5% single deterministic (Sin. Det.) case with cost.

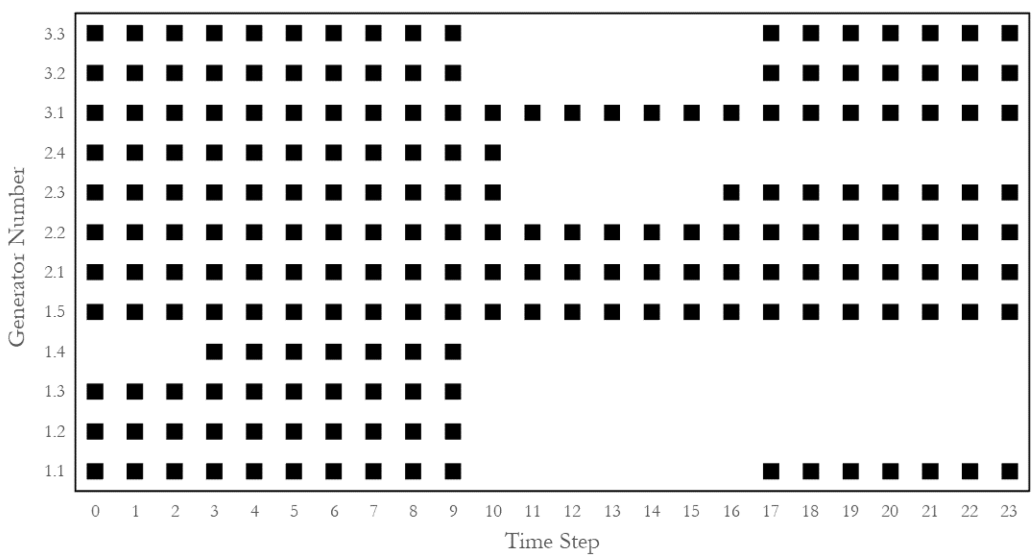

Figure C.21: Generating unit statuses for the “true” price profile from the 5% 3 time step stochastic (Sto. 3 TS) case with cost.

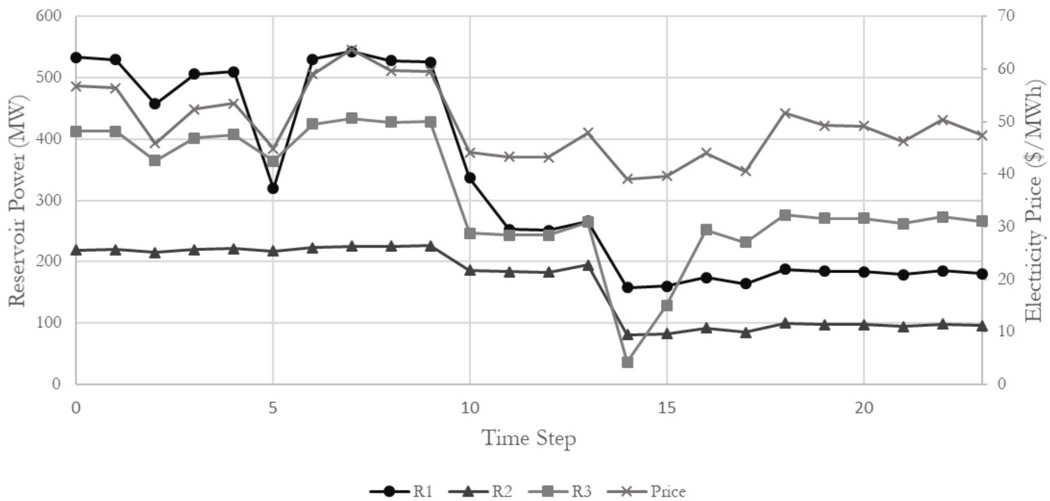

Figure C.22: Total reservoir power outputs for the "true" price profile from the 5% individual deterministic (Ind. Det.) case with cost with the electricity price profile.

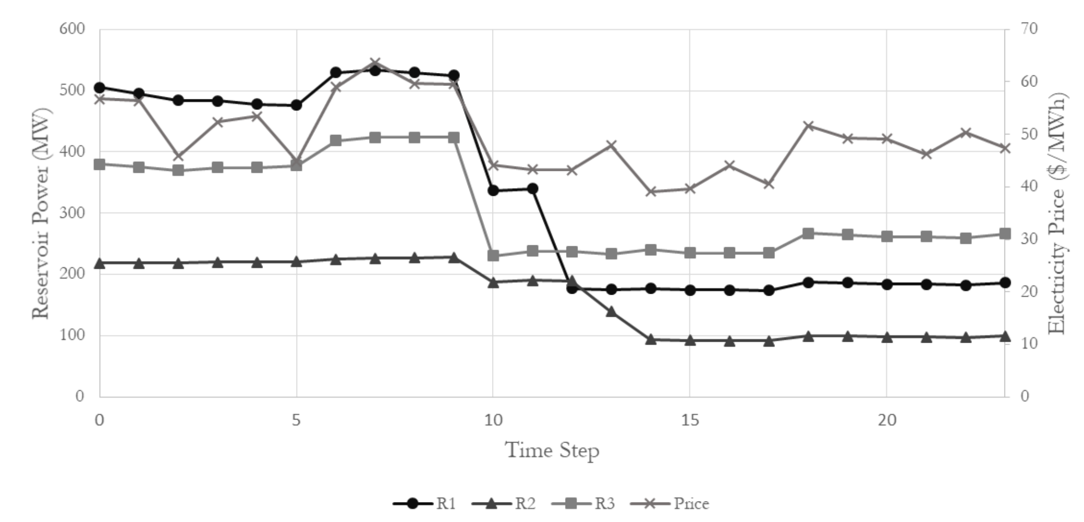

Figure C.23: Total reservoir power outputs for the "true" price profile from the 5% single deterministic (Sin. Det.) case with cost with the electricity price profile.

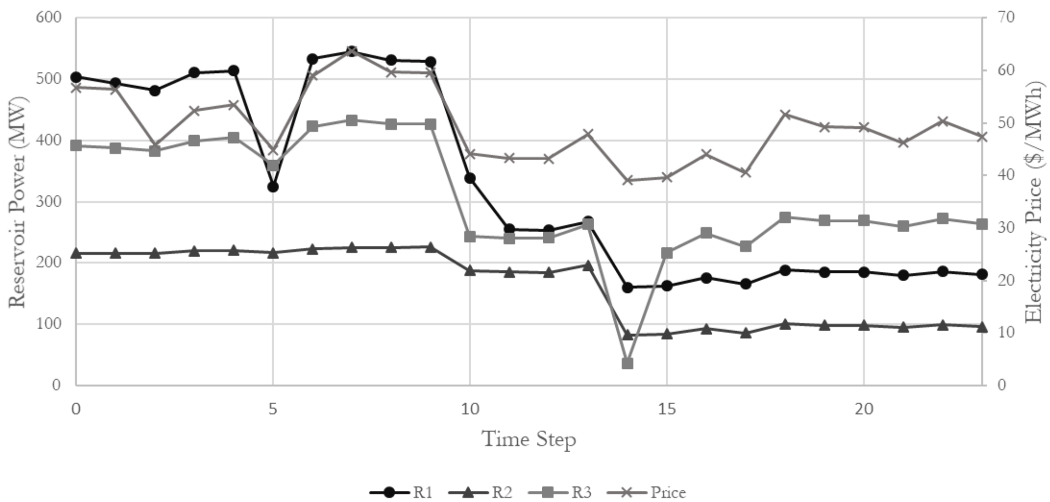

Figure C.24: Total reservoir power outputs for the “true” price profile from the 5% 3 time step stochastic (Sto. 3 TS) case with cost with the electricity price profile.

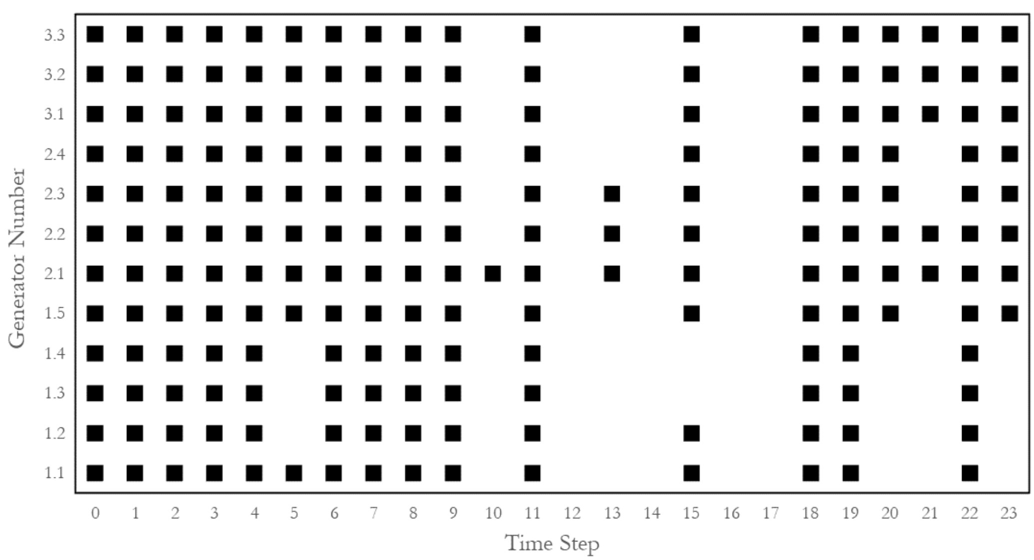

Figure C.25: Generating unit statuses for the “true” price profile from the 10% individual deterministic (Ind. Det.) case without cost.

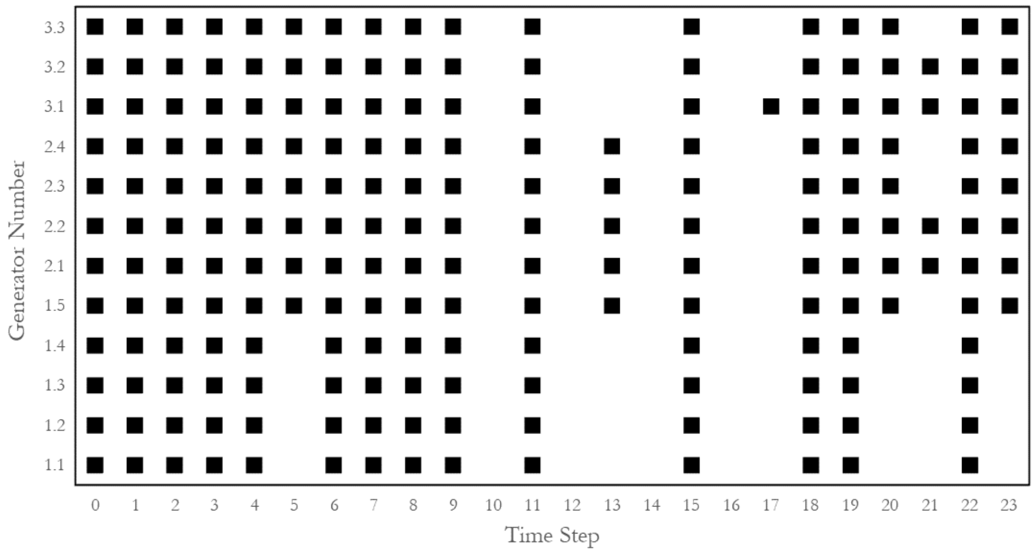

Figure C.26: Generating unit statuses for the "true" price profile from the 10% single deterministic (Sin. Det.) case without cost.

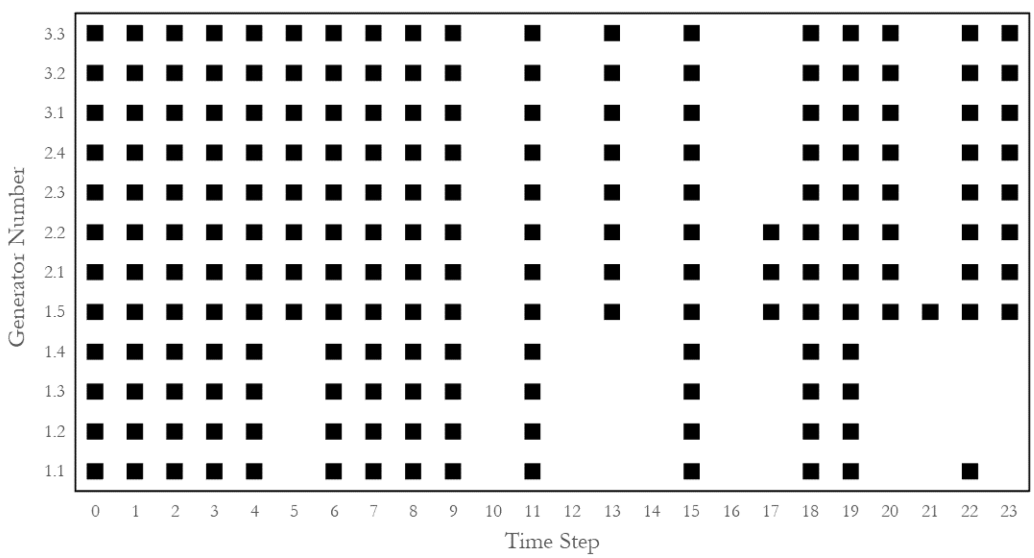

Figure C.27: Generating unit statuses for the "true" price profile from the 10% 3 time step stochastic (Sto. 3 TS) case without cost.

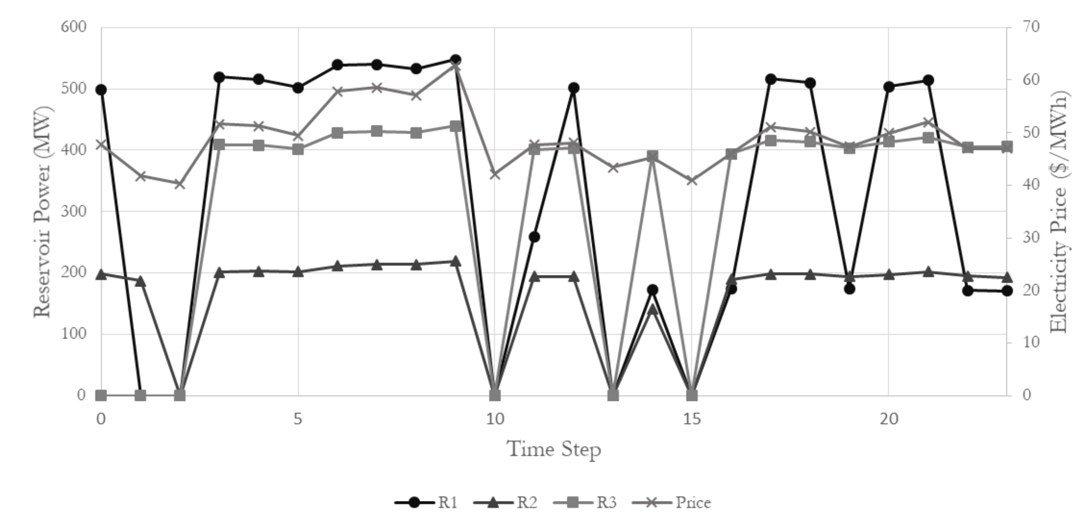

Figure C.28: Total reservoir power outputs for the “true” price profile from the 10% individual deterministic (Ind. Det.) case without cost with the electricity price profile.

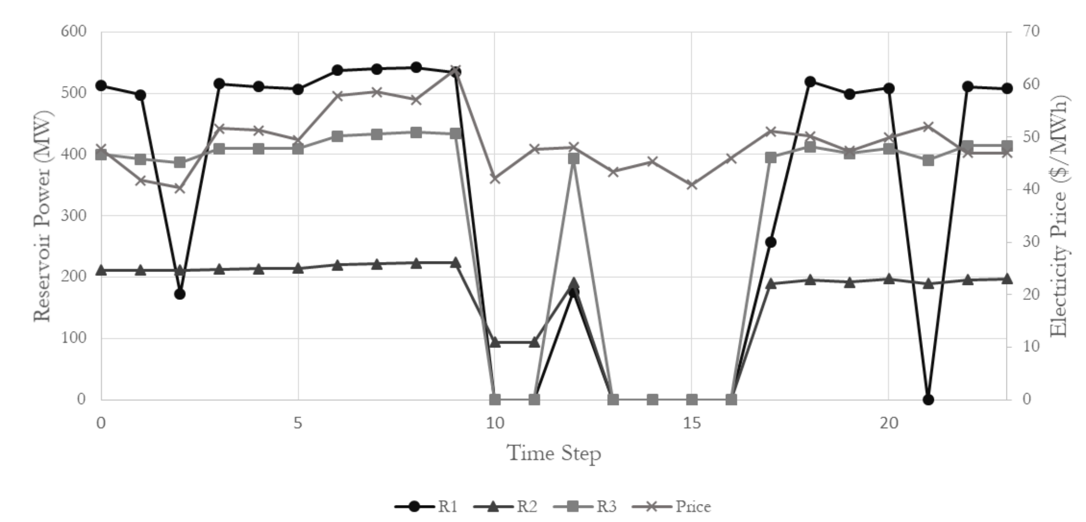

Figure C.29: Total reservoir power outputs for the “true” price profile from the 10% single deterministic (Sin. Det.) case without cost with the electricity price profile.

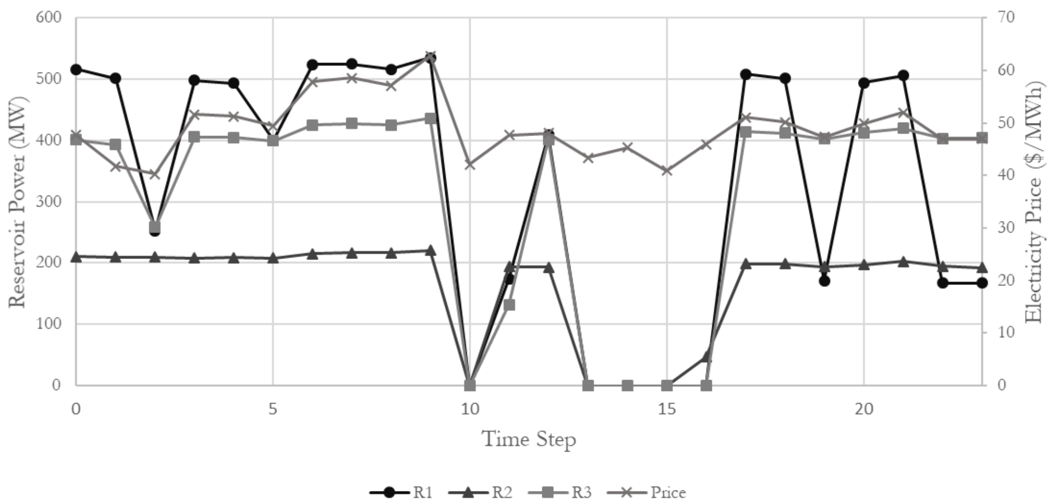

Figure C.30: Total reservoir power outputs for the "true" price profile from the 10% 3 time step stochastic (Sto. 3 TS) case without cost with the electricity price profile.

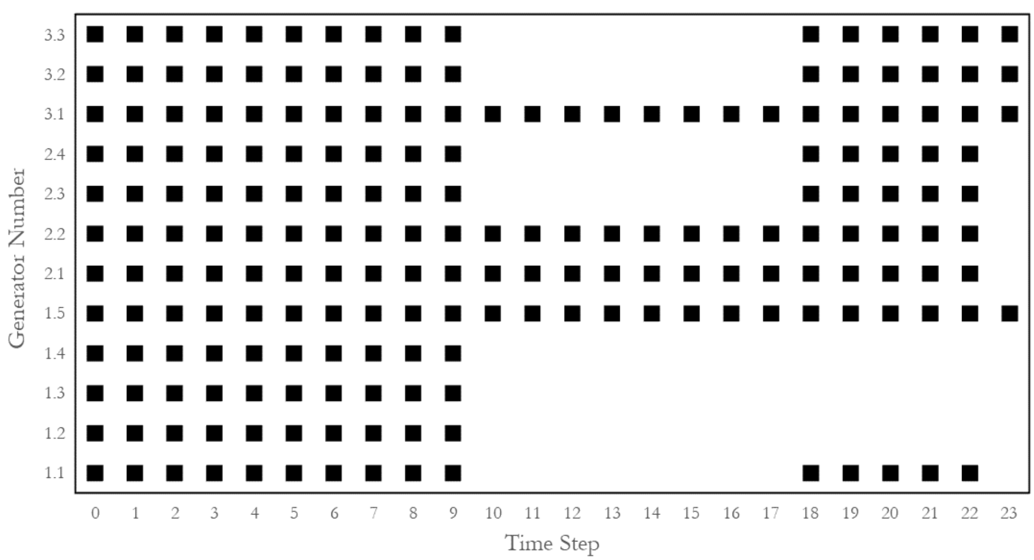

Figure C.31: Generating unit statuses for the "true" price profile from the 10% individual deterministic (Ind. Det.) case with cost.

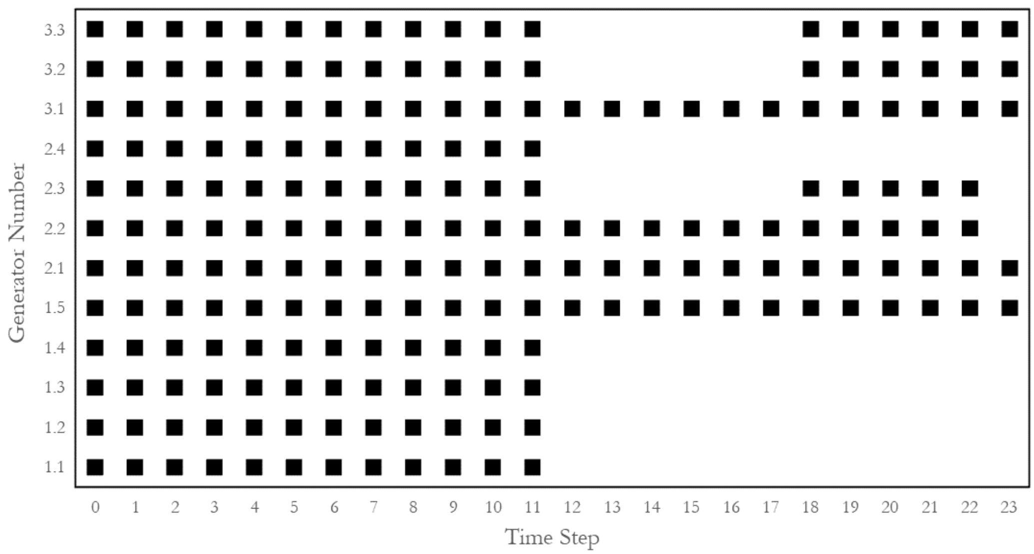

Figure C.32: Generating unit statuses for the "true" price profile from the 10% single deterministic (Sin. Det.) case with cost.

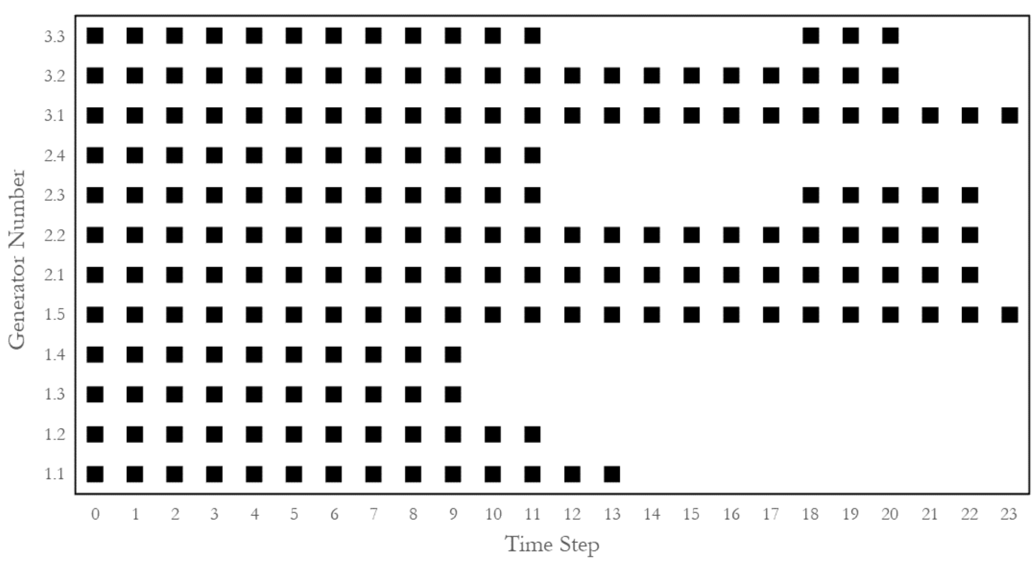

Figure C.33: Generating unit statuses for the "true" price profile from the 10% 3 time step stochastic (Sto. 3 TS) case with cost.

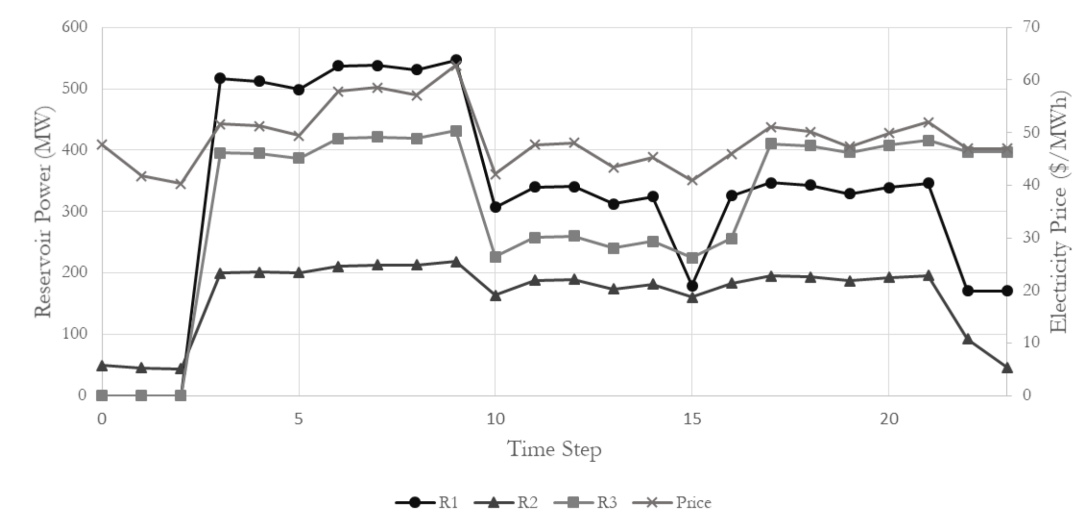

Figure C.34: Total reservoir power outputs for the “true” price profile from the 10% individual deterministic (Ind. Det.) case with cost with the electricity price profile.

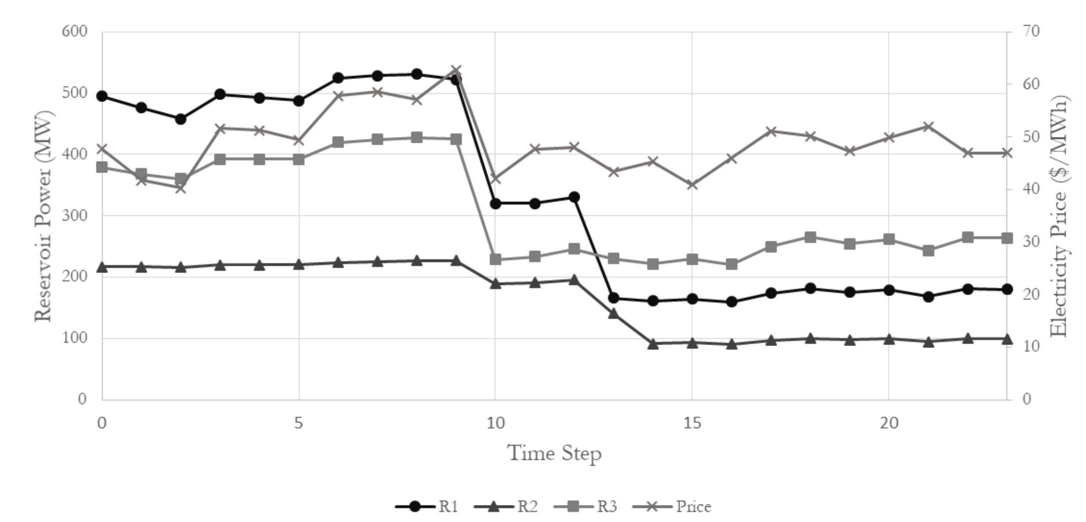

Figure C.35: Total reservoir power outputs for the “true” price profile from the 10% single deterministic (Sin. Det.) case with cost with the electricity price profile.

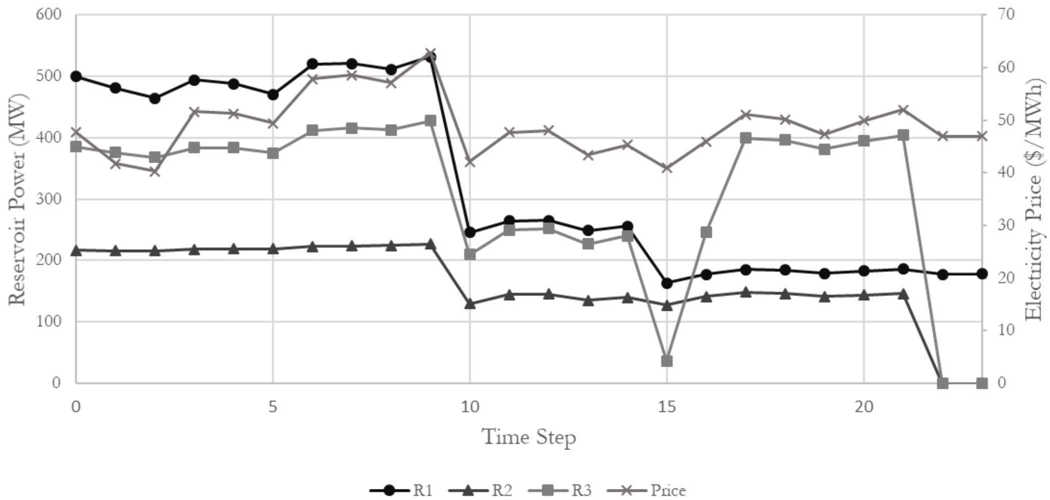

Figure C.36: Total reservoir power outputs for the “true” price profile from the 10% 3 time step stochastic (Sto. 3 TS) case with cost with the electricity price profile.